SJSU SAN JOSÉ STATE UNIVERSITY

MTI MINETA TRANSPORTATION INSTITUTE

Performance Testing of Asphalt Binder Modified with Amine-Impregnated Zeolite and Plastic in Hot Mix Asphalt to Reduce Carbon Footprint

Shadi Saadeh, PhD   Mohammad Javad Kazemi   Roger Khoudessian
Unmona Aditi   Elham Fini, PhD

CSUTC **California State University** Transportation Consortium

CALIFORNIA STATE UNIVERSITY **LONG BEACH**

MINETA TRANSPORTATION INSTITUTE

Founded in 1991, the Mineta Transportation Institute (MTI), an organized research and training unit in partnership with the Lucas College and Graduate School of Business at San José State University (SJSU), increases mobility for all by improving the safety, efficiency, accessibility, and convenience of our nation's transportation system. Through research, education, workforce development, and technology transfer, we help create a connected world. MTI leads the Mineta Consortium for Equitable, Efficient, and Sustainable Transportation (MCEEST) funded by the U.S. Department of Transportation, the California State University Transportation Consortium (CSUTC) funded by the State of California through Senate Bill 1 and the Climate Change and Extreme Events Training and Research (CCEETR) Program funded by the Federal Railroad Administration. MTI focuses on three primary responsibilities:

Research

MTI conducts multi-disciplinary research focused on surface transportation that contributes to effective decision making. Research areas include: active transportation; planning and policy; security and counterterrorism; sustainable transportation and land use; transit and passenger rail; transportation engineering; transportation finance; transportation technology; and workforce and labor. MTI research publications undergo expert peer review to ensure the quality of the research.

Education and Workforce Development

To ensure the efficient movement of people and products, we must prepare a new cohort of transportation professionals who are ready to lead a more diverse, inclusive, and equitable transportation industry. To help achieve this, MTI sponsors a suite of workforce development and education opportunities. The Institute supports educational programs offered by the Lucas Graduate School of Business: a Master of Science in Transportation Management, plus graduate certificates that include High-Speed and Intercity Rail Management and Transportation Security Management. These flexible programs offer live online classes so that working transportation professionals can pursue an advanced degree regardless of their location.

Information and Technology Transfer

MTI utilizes a diverse array of dissemination methods and media to ensure research results reach those responsible for managing change. These methods include publication, seminars, workshops, websites, social media, webinars, and other technology transfer mechanisms. Additionally, MTI promotes the availability of completed research to professional organizations and works to integrate the research findings into the graduate education program. MTI's extensive collection of transportation-related publications is integrated into San José State University's world-class Martin Luther King, Jr. Library.

Performance Testing of Asphalt Binder Modified with Amine-Impregnated Zeolite and Plastic in Hot Mix Asphalt to Reduce Carbon Footprint

Shadi Saadeh, PhD

Unmona Aditi

MohammadJavad Kazemi

Elham Fini, PhD

Roger Khoudessian

March 2025

TECHNICAL REPORT DOCUMENTATION PAGE

1. Report No. 24-38	2. Government Accession No.	3. Recipient's Catalog No.
4. Title and Subtitle Performance Testing of Asphalt Binder Modified with Amine-Impregnated Zeolite and Plastic in Hot Mix Asphalt to Reduce Carbon Footprint		**5. Report Date** March 2025
		6. Performing Organization Code
7. Authors Shadi Saadeh, PhD Unmona Aditi Mohammad Javad Kazemi Elham Fini, PhD Roger Khoudessian		**8. Performing Organization Report** CA-MTI-2323
9. Performing Organization Name and Address Mineta Transportation Institute College of Business San José State University San José, CA 95192-0219		**10. Work Unit No.**
		11. Contract or Grant No. ZSB12017-SJAUX
12. Sponsoring Agency Name and Address State of California SB1 2017/2018 Trustees of the California State University Sponsored Programs Administration 401 Golden Shore, 5th Floor Long Beach, CA 90802		**13. Type of Report and Period Covered**
		14. Sponsoring Agency Code
15. Supplemental Notes 10.31979/mti.2025.2323		

16. Abstract

The rise in global temperatures, driven in part by significant transportation carbon emissions, necessitate sustainable solutions for infrastructure. Traditional asphalt binders and lime additives significantly contribute to carbon emissions, and conventional liquid amine-based antistrip agents, which are used to reduce moisture damage, lose efficacy over time. This study evaluates the performance of PG 64-16 Low Carbon binder, incorporating 10% post-consumer plastic and amine-impregnated zeolite (AIMZ) as a protective carrier for liquid amines. Researchers compare this low-carbon binder to conventional PG 64-16 binder and evaluate AIMZ against amine and zeolite separately (AZ) and a commercial liquid antistrip (LAS). The study tests three aging levels (3, 5, and 7 days), simulating 4, 8, and 10 years, respectively, of field aging in Southern California. The evaluation of moisture-induced damage uses the Tensile Strength Ratio (TSR), while the Hamburg Wheel Tracking (HWT) test assesses rutting resistance (the wear from tires and loads that occurs on roads). The IDEAL Cracking Test measures cracking resistance, and the Moisture-Induced Shear-Thinning Index (MISTI) and Multiple-Stress Creep Recovery (MSCR) tests analyze moisture susceptibility and rheological properties, all of which are important factors to consider in long-term efficacy. AIMZ demonstrated higher TSR values compared to those with AZ and LAS at both 5 days and 7 days of aging levels for both binders. Rutting resistance is comparable between binders, and low-carbon binder mixtures show improved cracking resistance over time. MISTI values suggest lower moisture susceptibility for the low-carbon binder, though MSCR results suggest it is best suited for low-traffic volumes. This study indicates that AIMZ effectively prolongs liquid amine efficacy and that low-carbon binders, despite some limitations, offer environmental and performance benefits. These findings support the potential for incorporating post-consumer plastics in asphalt pavements, promoting sustainability in infrastructure.

17. Key Words Asphalt concrete pavement, moisture damage, antistrip additives, plastics, sustainable development.	**18. Distribution Statement** No restrictions. This document is available to the public through The National Technical Information Service, Springfield, VA 22161.		
19. Security Classif. (of this report) Unclassified	**20. Security Classif. (of this page)** Unclassified	**21. No. of Pages** 129	**22. Price**

Form DOT F 1700.7 (8-72)

ACKNOWLEDGMENTS

CONTENTS

LIST OF FIGURES

LIST OF TABLES

Executive Summary

Global temperatures are rising continuously which poses an existential crisis. Carbon dioxide emissions are largely responsible for this temperature rising, so to eliminate the threat, we face the challenge of determining how to lower carbon emissions. Asphalt paving materials require an extremely high temperature, contributing to carbon emissions. In addition, asphalt paving often uses lime or liquid amine as an additive to reduce moisture damage. Lime production is another contributor to a significant amount of carbon emissions. Liquid amines lose their long-term efficacy of pavement service life due to weathering and UV radiation. In order to prolong the efficacy of amines, zeolite can be used as a protector. In this study, the performance of PG 64-16 Low Carbon asphalt binder is compared to conventional PG 64-16 asphalt binder. In addition, we investigated the effect of amine-impregnated zeolite (AIMZ) on asphalt mixture performance. PG 64-16 Low Carbon is made with 10% post-consumer plastic which reduces CO_2 emission from liquid asphalt by approximately 5%. AIMZ was used to investigate the use of zeolite as a carrier, which can protect the liquid amines from weathering effects and release them gradually over the years. Ethylene diamine and 90% to 92% clinoptilolite zeolite were used in this study. The performance of AIMZ is compared to that of amine and zeolite separately (AZ) and a commercial amine-based liquid antistrip (LAS) named LOF 65-00.

Mixes were prepared with three different aging levels—3 days, 5 days, and 7 days—representing roughly 4 years, 8 years, and 10 years, respectively, of field aging in the weather of Southern California, according to NCHRP Research Report 973. The Tensile Strength Ratio (TSR) was used to evaluate the resistance to moisture-induced damage. The Hamburg Wheel Tracking (HWT) test was used to examine the rutting resistance. The IDEAL Cracking Test was used to evaluate the cracking resistance. The susceptibility to moisture-induced damage and the rheological properties of both types of binder were investigated using the Moisture-Induced Shear-Thinning Index (MISTI) and the Multiple-Stress Creep Recovery (MSCR) test. The results showed that the dry tensile strength of PG 64-16 Low Carbon binder was 30% to 40% lower than the conventional binder for all additives at every aging level. Similarly, the wet tensile strength of the low-carbon binder was also significantly lower than the conventional binder. Mixtures incorporating AIMZ demonstrated higher TSR values compared to those with AZ and LAS at both 5 days and 7 days of aging levels for both binders. The rutting resistance of specimens with a low-carbon binder was similar to a conventional binder. There were no significant differences in rutting resistance among different additives. For cracking resistance, by the 3 days aging mark, mixtures with PG 64-16 LC demonstrated comparable results to those with conventional PG 64-16. At both 5 and 7 days of aging, mixtures utilizing low-carbon binder showcased higher CT_{index} values than those employing a conventional binder. This suggests that a low-carbon binder offers improved resistance to cracking over extended period. MISTI values suggest that the conventional binder is more susceptible to moisture compared to the low-carbon binder. However, MSCR test results show that low-carbon binders are suitable only for low-volume-traffic loads. Although further investigation is needed, this study is one step forward in evaluating amine-impregnated

zeolite as an antistrip that can be environmentally friendly and effective in long-term pavement service life. Additionally, these findings contribute to the ongoing efforts aimed at incorporating post-consumer plastics into asphalt pavement.

1. Introduction

Road construction and maintenance exert a significant environmental impact due to the substantial number of resources involved (Sollazzo et al., 2020). In the United States (US), pavement construction, preservation, and rehabilitation activities contribute to approximately 75 million metric tons of CO_2 equivalent greenhouse gas emissions annually, constituting about 5% of the total emissions from the US transportation sector (J et al., 2015). Recognizing the urgency of climate action, the National Asphalt Pavement Association (NAPA) has pledged to achieve net zero carbon emissions by 2050. To achieve this goal, it is crucial to understand the primary factors driving emissions in the asphalt industry. Innovative strategies are imperative to reduce the CO_2 emissions from road construction while ensuring durable asphalt pavement structures.

The durability of asphalt mixtures is influenced not only by traffic loads, but also by environmental factors (İskender et al., 2012). Moisture-induced damage in asphalt mixtures, commonly referred to as stripping, is a major issue in pavement engineering. It leads to the loss of adhesion between aggregate and binder within asphalt mixtures, resulting in premature pavement deterioration (Park et al., 2017). Caro et al. (2008) classified the moisture damage process in two steps: first, the transportation of water in liquid or vapor form to the aggregate-binder interface, and second, alterations in the internal structure of the pavement due to water presence, resulting in decreased bearing capacity. Various micro- and macro-scale mechanisms can describe this process of water-induced damage. For instance, the presence of acidic aggregates in pavement can lead to moisture susceptibility. This occurs because the silanol group renders the aggregate surface hydrophilic, creating a repulsive force between aggregate and asphalt binder. Therefore, silica-rich materials such as granite are not recommended for use in flexible pavement (Hamedi and Tahami, 2018).

Research has demonstrated that lime serves as an effective additive in mitigating deformations attributed to water damage (Şengül et al., 2022). The use of lime as a filler material in asphalt pavement is widespread in the US. However, lime production generates CO_2 as a byproduct. Approximately 1.2 tons of CO_2 emissions are attributed to producing 1 ton of lime (Ojuri et al., 2022). Despite this, the natural carbonation process of lime can only reabsorb 23% to 33% of CO_2 produced during calcination (Pietro Campo et al., 2021).

A viable substitute for lime in asphalt pavement could be an amine-based antistripping agent. The primary objective of such an agent is to enhance the physicochemical bond between the asphalt binder and aggregate (İskender et al., 2012). These amines typically comprise two compounds: a long-chain hydrocarbon exhibiting hydrophobic properties and a hydrophilic amine group. The amine group reacts with the aggregate surface, while the hydrocarbon portion interacts with the binder. Consequently, the amine-based additives serve as a bridging element between the hydrophilic aggregate and hydrophobic bitumen surfaces (Tarrer and Wagh, 1991). However, the long-term effectiveness of liquid amines raises concerns. When a binder treated with amine-based

liquid antistripping agents is subjected to prolonged heating, the lighter amine compounds tend to evaporate, and the remaining heavier compounds lose their antistripping effect (Hesami & Mehdizadeh, 2017). Both short-term aging, which occurs during asphalt pavement mixing and placement, and long-term in-service aging of asphalt binder, induced by Rolling Thin Film Oven (RTFO) and Pressure Aging Vessel (PAV) tests per AASHTO T 240 and AASHTO R 28, have proven to cause thermal degradation of amine-based liquid antistrips (Wasiuddin et al., 2007).

Additionally, long-term aging associated with UV radiation can significantly reduce the effectiveness of amines (Mousavi et al., 2022b). In summary, amine-based additives can lose their efficacy throughout production, application, and pavement service life. Developing a heat-resistant barrier around amine molecules could potentially mitigate the thermal degradation of amines.

Plastic pollution stands as a pressing crisis in today's world. Incorporating recycled plastic waste into asphalt pavement could yield substantial environmental benefits, given the extensive use of asphalt pavement. Even adding a small percentage of plastic waste in asphalt mixtures can significantly reduce plastic waste overall, especially when scaled up to match total asphalt mixture production (Hao et al., 2024).

This study investigates using zeolite as a protective agent to enhance the long-term efficacy of liquid amines against weathering in asphalt pavements. It compares the benefits of incorporating amine-impregnated zeolite (AIMZ) as an additive in asphalt mixtures with the use of commercial liquid amine-based antistripping agents and the separate use of amine and zeolite in the asphalt mixtures. The porous structure of zeolite suggests that it may shield amines from heat and UV radiation while gradually releasing them over the pavement's service life.

Additionally, the study examines the performance of PG 64-16 Low Carbon (LC), which contains 10% post-consumer plastic. Our aim is to reduce CO_2 emissions from liquid asphalt by 5% and significantly address global plastic pollution. The evaluation of PG 64-16 LC performance is compared to that of conventional binder grade PG 64-16. The long-term aging of 3 days, 5 days, and 7 days simulate field aging equivalent to 4 years, 8 years, and 10 years, respectively, in the South Coast of California, following road paving guidelines outlined in NCHRP Research Report 973 (Kim et al., 2021). The mechanical properties of mixtures at different long-term aging levels are compared to that of non-aged mixtures to understand how mechanical properties change over a long duration. The rutting resistance, moisture susceptibility, and fatigue cracking resistance of different mixtures at different aging levels are evaluated using Hamburg Wheel Tracking (HWT), Tensile Strength Ratio (TSR), and the IDEAL Cracking Test (CT). This study also compared two properties of low-carbon binders versus conventional binders: the vulnerability of an asphalt-stone interface to moisture-induced damage, as measured by the Moisture-Induced Shear-Thinning Index (MISTI) and the rheological properties of low-carbon binders and conventional binders when they are subjected to repeated loading and rest cycles at intermediate temperatures, as measured by the Multiple-Stress Creep Recovery (MSCR) Test. Based on the study's findings, conclusions are drawn regarding whether the use of amine-

impregnated zeolite is effective in reducing moisture damage over the long term. The conclusions also indicate whether incorporating plastics into an asphalt binder can enhance the long-term performance of pavement.

2. Literature Review

Amine-modified zeolite has gained attention as a Carbon Capture and Storage (CSS) technology. While using amine-impregnated zeolite in asphalt mixtures is a novel concept, numerous studies have explored the use of amine-based additives and zeolites in asphalt mixtures. Numerous ongoing research projects investigate the effectiveness of integrating waste plastics into asphalt mixtures. The literature review is structured into sections that provide a concise overview of existing literature on amine-modified zeolite in carbon capture technology and the utilization of amine-based additives, zeolites, and plastics in asphalt mixtures.

2.1 Use of Amine Modified Zeolite in Carbon Capturing

Addressing carbon dioxide emissions is paramount in today's world as our planet struggles with the effects of climate change. Carbon dioxide, a major contributor to this issue, is produced largely from industrial processes including cement production and the burning of fossil fuels. These emissions exacerbate problems such as glacier melting, rising sea levels, and overall global warming (Pérez-Botella et al., 2020). Alhwaige et al. (2013) reported that CO_2 contributes to approximately 60% of global warming. Over the past five decades, atmospheric CO_2 levels have surged by over 100 parts per million by volume (ppmv), as noted by Murge et al., (2019). Various methods exist for capturing CO_2 with the use of amines for adsorption being a prominent approach. This process requires two amine groups to fully capture one molecule of CO_2 (Santos et al., 2015).

$$RNH_2 + CO_2 \rightarrow RNH_2^+COO^-$$

$$RNH_2^+COO^- + RNH_2 \rightarrow RNHCOO^- + RNH_3^+$$
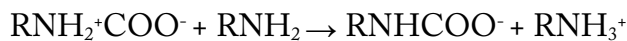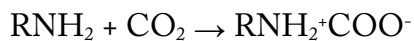
However, this procedure has disadvantages, such as high energy consumption, inefficient regeneration, and toxicity. As an alternative, solid-based adsorption systems have gained popularity due to their various advantages, including high CO_2 adsorption capacity, low energy consumption, and resistance to moisture (Choi et al., 2009). Numerous experiments have assessed the effectiveness of solid-based adsorption systems for CO_2 capture. Due to their porous structure, large surface area, low cost, and widespread availability, zeolite materials have been extensively used as CO_2 adsorbents. Additionally, zeolites offer the advantage of customizable surface area, porosity, and acidity through laboratory synthesis (Murge et al., 2019). Zeolites can be categorized into two types based on their porous structure: microporous, such as ZSM-5, 13X, MER type, Y type, and Beta; and mesoporous, including MCM series, KIT series, and SBA series (Yuan et al., 2020). Incorporating amines into zeolites can be achieved through four methods: grafting, impregnation, in-situ polymerization, and amine double functionalization (Lin et al., 2017).

Panda et al. (2018) chose Zeolite 4A as the solid adsorbent for carbon capture. They employed two methods for amine functionalizing: grafting and impregnation. The amine grafting involved using (3-Aminopropyl) trimethoxy silane (APTMS), while amine impregnation utilized isopropyl

amine (IPA). Prior to amine incorporation, the Zeolite 4A with a granule size of 3–5 mm was ground into powder. The concentration of both IPA and APTMS solutions in ethanol was standardized at 0.3% by weight. Adsorption experiments of CO_2 revealed that impregnated Zeolite 4A exhibited superior CO_2 adsorption capacity compared to grafted Zeolite 4A. The experimental values for adsorption values for impregnated Zeolite 4A were approximately 1.39 mmol g-1 (6.11 wt.%) at 0.15 bar and 2.31 mmol g-1 (10.16 wt.%) at 1 bar, whereas for grafted Zeolite 4A, the values were around 0.1 mmol g-1 (0.44 wt.%) at 0.15 bar and 1.05 mmol g-1 (4.62 wt.%) at 1 bar. The discrepancy was attributed to IPA's low molecular size and density, facilitating its diffusion inside the Zeolite 4A surface and enhancing CO_2 adsorption.

Conversely, the high density of APTMS resulted in pore mouth blockage, leading to low carbon adsorption. However, in terms of thermal stability, grafted Zeolite 4A outperformed impregnated Zeolite 4A. Dindi et al. (2018) obtained comparable results using different zeolite and amine types. They employed cancrinite-type zeolite derived from fly ash (termed FAC). Cancrinite-type zeolite requires minimal water to be synthesized in hydrothermal or molten salt method. For amines, they grafted FAC with 3-Aminopropyl triethoxysilane (APTES) and impregnated FAC with Diethanolamine (DEA) and monoethanolamine (MEA). Both grafting and impregnation involved mixing FAC with 60 wt.% amine solutions at a ratio of 1.21g solution per g of activated fly ash. CO_2 adsorption capacity testing revealed that APTES-grafted FAC exhibited increased adsorption capacity with rising temperatures up to 80°C, with an optimum APTES loading of 30%. Conversely, at lower temperatures, the adsorption values for DEA- and MEA-impregnated FAC surpassed those of APTES-grafted FAC but decreased with increasing temperature due to the evaporation of impregnated amines.

Moreover, cyclic CO_2 adsorption capacities demonstrated stability for APTES grafted FAC but a decreasing trend for impregnated FAC. The researchers emphasized the pivotal role of amine selection. Santos et al. (2015) functionalized ZSM-12/MCM-48, a micro-mesoporous composite material, with APTES and established a correlation between CO_2 adsorption and amine content, pore volume, total surface area, and the mesoporous structure of zeolite.

Quant et al. (2022) employed MCM41 as the zeolite material derived from microalgae ash. MCM41, a mesoporous material, was synthesized using various calcination temperatures to explore its CO2 adsorption capacity. Recognizing its inherent limitations compared to microporous materials in carbon capture, the researchers loaded amine, specifically polyethyleneimine (PEI), into MCM41 via the wet impregnation method. Different loading amounts of PEI (30%, 40%, 50%, and 60%) were investigated, along with CO2 capturing capacities conducted at three different temperatures. Optimal results were observed at the lowest calcination temperature of 450°C, attributed to zeolite's favorable porosity and surface area, as high calcination temperature negatively affected the pore structure. Consequently, PEI was solely loaded into MCM41-450. The highest CO_2 adsorption capacity occurred at 60% PEI loading, with adsorption slightly decreasing at higher temperatures for lower PEI loading, whereas high

PEI loading remained unaffected by temperature variations, suggesting a dominant role of chemical adsorption capacity.

Jia et al. (2020) conducted experiments on photocatalytic CO_2 reduction into hydrocarbon fuels using amine-impregnated Ti-MCM-41 zeolites with a molar ratio (Ti/Si) of 10. They explored the efficacy of tetraethylenepentamine (TEPA) compared to other amines such as ethylenediamine (EDA), triethylenetetramine (TETA), and ethylenediamine (PEI-600). While all amines enhanced the photocatalytic reduction Ti-MCM-41, TEPA demonstrated optimum performance. TEPA's advantages include a high boiling point of 340°C and a composition comprising both primary and secondary amines (Murge et al., 2013).

Yang et al. (2017) investigated TEPA for CO_2 capture using the wet impregnation method on mesoporous ZSM-5 type zeolite, renowned for its homogeneous pore structure, outstanding hydrothermal stability, and hydrophobic properties (Ge et al., 2022). Different amine loadings at various temperatures were studied, revealing various adsorption trends. The impregnated zeolites were designated as ZTx, with "x" representing the mass of TEPA in grams utilized in the process. ZT7 outperformed ZT9 due to reduced accessible amine groups caused by excessive TEPA agglomeration. ZT7 also exhibited high performance over five adsorption-desorption cycles, indicating optimum amine loading.

Ge et al. (2022) combined mesoporous and microporous zeolites to exploit their respective advantages. These benefits encompass the high thermal stability of the microporous ZSM-5 structure and the larger pore sizes inherent in the mesoporous SBA-16 structure. They prepared ZSM-5/SBA-16 composites via an embedding method, incorporating amine bi-functionalization by grafting a fixed number of APTES and impregnating TEPA at different loadings. The findings indicated that while maintaining a constant APTES loading and increasing levels of TEPA impregnation, the CO_2 adsorption capacity initially rose before declining, with 55% TEPA identified as the optimum loading. The subsequent decrease beyond this optimal amine loading was attributed to the blockage of the carrier channels induced by an excess of amine.

Yuan et al. (2020) also delved into the utilization of zeolite composites and amine bi-functionalization. They grafted 3-aminopropyltrimethoxysilane (APTS) and impregnated TEPA on Beta/KIT-6 zeolite composites. The optimal outcome was exhibited at 50% TEPA loading. While chemical adsorption was recognized as the dominant adsorption mechanism, it became apparent that the whole adsorption process involved a synergy between chemical and physical adsorption. However, when employing Y-type zeolite, TEPA impregnation exhibited adverse effects (Murge et al., 2013).

In contrast, Lee et al. (2013) observed different outcomes when utilizing Y-type zeolite in an indoor air environment. They employed amine impregnation with three different types of amines. TEPA-modified zeolite demonstrated the highest adsorption capacity compared to MEA and IPA-impregnated zeolite, respectively.

Another promising zeolite, Zeolite 5A, has gained popularity for its ability to separate from other gas mixtures. This popularity stems from the low Si/Al ratio of Zeolite 5A, which facilitates strong polarity, increased surface oxygen charge, and improved interaction with CO_2 (Szostak, 1992). However, the CO_2 adsorption capacity of Zeolite 5A diminishes in the presence of water due to its hydrophilic nature. Similarly, Zeolite 13X experiences a reduction in CO_2 adsorption capacity in the presence of water molecules (Joos et al., 2013). To address this issue, Liu et al. (2016) developed a solution by creating a protective shell around the zeolite particle to obstruct the diffusion of water molecules in the zeolite pores. Subsequently, they modified the Zeolite 5A with PEI by the wet impregnation method. This synthesized zeolite retained its CO_2 adsorption capacity even in humid conditions.

In summary, amine-modified zeolite has demonstrated effectiveness in CO_2 adsorption, offering promising potential for mitigating greenhouse gas emissions.

2.2 Use of Amine-Based Additives in Asphalt Mixtures

Badawy and Rahim (2023) conducted a study to investigate the impact of additives on the moisture resistance capacity of Hot Mix Asphalt (HMA). They compared five types of additives, including two amine-based liquid antistripping agents (HP Plus and LOF 6500), two surface-modified nano clays, and hydrated lime. The wet tensile strength of all mixtures improved compared to the mix without any additives. However, HP Plus did not yield any satisfactory results in terms of dry tensile strength. Despite this, among all the additives tested, the amine-based liquid antistripping agent emerged as the most cost-effective choice.

In a separate study, Xiao et al. (2022) examined the effects of amine-based antistripping agents in various asphalt and aggregate mixtures. The result demonstrated increased Tensile Strength Ratio (TSR) values for all mixtures. The addition of amine increased the polar component, thereby reducing the free energy release of asphalt pavement in the presence of moisture. Although the results also indicated a reduction in cohesive energy in asphalt due to adding amine-based antistripping agents, these effects were deemed negligible.

Park et al. (2017) evaluated the effectiveness of a liquid antistripping agent derived from aliphatic amine, comparing it with the use of limestone powder. Through indirect tensile strength tests, Hamburg Wheel Tracking (HWT) tests, and curve fitting methods, they found that adding amine-based antistripping agents improved rutting and stripping resistance. In contrast, limestone powder did not significantly affect rutting resistance.

In a study by Aksoy et al. (2005), it was demonstrated that the use of 0.2% of Wetfix I and 0.4–0.6% of Lilamin VP 75P, both fatty amines, achieved a minimum acceptable TSR of 0.7. Among these, adding 0.4% of Lilamin VP 75P exhibited the highest TSR of 0.89. Furthermore, Lilamin VP 75P slightly improved Marshall stability compared to the control mix.

However, caution is advised when using amine-based antistripping agents in binders modified with other materials, such as crumb rubber. Singh et al. (2020) found that amine-based antistripping agents could significantly reduce the fatigue life of a crumb rubber-modified binder, although only minor effects were observed regarding low-temperature cracking performance.

In real-world asphalt production, mixtures are often stored at or near production temperature for several hours before they are laid and compacted in the field. Hesami and Mehdizadeh (2017) sought to replicate this plant production scenario in their study. Their findings revealed that the effectiveness of liquid amines under plant production conditions is considerably lower than under laboratory conditions.

Similarly, Tayebali et al. (2008) investigated the impact of prolonged heating on the bond strength between aggregate and asphalt containing LOF 6500. Their TSR results indicated an increase in moisture susceptibility with longer heating durations. These findings underscore the importance of insuring that asphalt mixtures used in roadway construction meet the agency's minimum requirements for moisture sensitivity at the time of placement in the field (i.e., on plant-produced material) rather than solely during the formulating of the job mix formula (JMF) (i.e., on laboratory-produced material).

2.3 Use of Zeolite in Asphalt Mixtures

HMA production necessitates high mixing temperatures, leading to significant greenhouse gas emissions and increased fuel costs (Al-Hadidy et al., 2023 and Xu et al., 2017). In response, Warm Mix Asphalt (WMA) technologies have emerged to mitigate emissions and enhance safety for construction personnel. The pioneering effort by Csanyi and Ladis in 1956, which attempted to foam the bitumen by injecting water, marked the inception of WMA development (Csanyi, 1957). Since then, various strategies have been explored to reduce bitumen viscosity, with zeolite application being one such method.

Both natural zeolites like clinoptilolite and synthetic variants such as Aspha-min and Advera have been utilized to produce WMA mixtures (Zou et al., 2022). Ahmadzadegan and Sarkar (2022) investigated the mechanical properties of WMA modified with synthetic zeolite in nano and granule forms, with ZSM-5 concentrations of 0.1%, 0.2%, and 0.3%. Their study involved conducting Indirect Tensile Strength (ITS) tests on conditioned and unconditioned specimens. While unconditioned specimens improved performance with increasing zeolite content, conditioned specimens exhibited decreased ITS values with higher zeolite concentrations. Nonetheless, zeolite addition reduced rutting depth in both conditioned and unconditioned specimens, with nanocrystal powder form outperforming granules.

In contrast, Arabani et al. (2021), observed that incorporating zeolite could augment the total surface free energy (SFE) of an asphalt binder, necessitating greater energy to induce cracking, thereby decreasing moisture susceptibility in asphalt mixtures. Furthermore, Al-Hadidy et al.

(2023) demonstrated that opting for natural zeolite over synthetic variants in WMA production proves to be more efficient in terms of time and fuel consumption. Their study highlighted the superior mechanical performance of WMA incorporating natural zeolite, which exhibited better results at lower compaction efforts compared to WMA with synthetic zeolite.

Utilizing zeolite in asphalt applications offers the additional benefit of reducing volatile organic compound (VOC) emissions through physical and chemical adsorption mechanisms (Chang et al., 2023). In a study by Chen et al. (2022), zeolite ceramsite derived from 13X Zeolite and Attapulgite Clay was employed to modify the asphalt binder. The study examined the impact of small (5%) and large (50%) dosages of zeolite ceramsite on the VOC adsorption capacity. Results indicated that a large dosage could achieve a significant volume reduction of up to 45% in VOC emissions, whereas the reduction with a small dosage was less than 10%.

2.4 Use of Plastics in Asphalt Mixtures

Recycling waste plastics, particularly polyethylene terephthalate (PET), has emerged as a focal point in recent times due to its widespread use, constituting approximately 18% of global polymer production (Ji, 2013). In an innovative approach, Mashaan et al. (2022) explored the incorporation of waste PET into asphalt mixture alongside Nano-Silica (NS) as a hybrid additive to improve the mechanical properties of stone mastic asphalt. Their study revealed that a combination of 6% PET with varying percentages of NS yielded optimal results, particularly enhancing rutting resistance and fatigue life. Additionally, this hybrid additive increased indirect tensile strength and TSR values.

Similarly, Li et al. (2021) investigated PET-derived additives for their efficacy as antistripping agents. Through an aminolysis reaction, PET-based additives significantly improved moisture resistance, with even a 1 wt.% addition leading to TSR values exceeding 90%. Molecular Dynamics (MD) simulations further supported PET's role in improving binder-aggregate adhesion.

However, contradictory findings were reported by Ahmadinia et al. (2012), whose study observed a reduction in tensile strength and TSR in stone mastic asphalt with increasing percentages of waste PET compared to the control mix. Nonetheless, all TSR values remained above 70%, meeting acceptable limits, while the addition of waste PET notably improved rutting resistance.

Styrene butadiene styrene (SBS) serves as a conventional polymer additive extensively employed for asphalt mix modification. In a study by Modarres and Hamedi (2014), the fatigue properties of asphalt mixes modified with PET derived from waste plastic bottles were compared with those modified with SBS. Both modifiers demonstrated positive effects on fatigue life, with SBS exhibiting slightly better results, particularly at higher strain levels. However, from both economic and environmental perspectives, PET is more desirable due to its status as a recycled material. In terms of stiffness properties, Movilla-Quesada et al. (2019) found that the inclusion of PET resulted in a more flexible mixture even at low temperatures.

Gürü et al. (2014) introduced two additives derived from PET: Thin Liquid Polyol PET (TLPP) and Viscous Polyol PET (VPP). The effects of these additives were examined at both binder and mixture levels. Bending Beam Rheometer (BBR) tests revealed that both TLPP and VOO had a positive effect on low-temperature cracking resistance. Similarly, Dynamic Shear Rheometer (DSR) tests demonstrated their positive effects on fatigue temperature cracking resistance.

TLPP additives, across all concentrations, notably increased the Marshall stability of mixtures with low asphalt contents (4% to 4.5%). Conversely, low concentrations of VPP increased the Marshall stability over a broader range of asphalt content.

In a study by Moghaddam et al. (2014), static and dynamic creep tests were utilized to evaluate the rutting resistance in PET-modified asphalt mixtures under static and dynamic loads. Results indicated that PET modification negatively affected the rutting resistance under static loading conditions but had a positive effect on pavements experiencing dynamic loadings.

Taherkhani and Arshadi (2017) investigated the effect of waste PET particle size on asphalt mixtures. Two different particle sizes were examined: 1.18-2.36 mm as coarse-graded PET, and 0.297–0.595 mm as fine-graded PET. Mixtures containing 2% PET by weight of the binder exhibited optimal results in indirect tensile strength and moisture resistance for both particle sizes. However, increasing PET content led to a reduction in tensile strength. Moreover, finer PET particles outperformed coarser PET particles.

Esfandabad et al. (2020) explored the utilization of granular PET as a substitute for mineral aggregates in asphalt mixtures. Higher PET content resulted in a reduction in the optimum binder content, attributed to PET's lower superficial porosity compared to natural aggregates. While increasing PET content improved rutting resistance, it also increased susceptibility to fracture failure in the mixtures.

In the case of cost-benefit analysis, the study of Abdalfattah et al. (2022) compared a recycled polyethylene (RPE) modified asphalt mixture to a conventional mixture and found that the most cost-effective pavement over a 30-year period was produced using RPE via the dry process, followed by the wet process. In contrast, the control pavement was the least cost-effective, indicating that RPE-modified pavements offer a higher ROI and greater sustainability compared to conventional pavements. Hao et al. (2024) incorporated three types of waste plastics— low-density polyethylene (LDPE), high-density polyethylene (HDPE), and polypropylene (PP)—into porous asphalt mixtures via the wet process in varying dosages (5%, 10%, and 15%) and did an economic evaluation. The life cycle cost analysis (LCCA) highlights that incorporating plastic waste into porous asphalt mixtures can significantly reduce costs. While the material costs are lowered by replacing expensive polymer-modified asphalt with plastic waste, production costs may increase due to higher mixing and compaction temperatures. Despite this, the improved engineering performance of plastic-modified asphalt, such as enhanced resistance to rutting and stripping, leads to extended service life and reduced maintenance, lowering user costs. Overall, the

incorporation of 10% HDPE/PP offers the most cost-effective solution, balancing agency and user costs for optimal long-term savings.

In conclusion, the integration of waste plastics into pavement materials has garnered significant interest among researchers. This approach addresses environmental concerns linked to plastic pollution while striving to establish sustainable pavement materials.

3. Objectives

The objective of this project was to evaluate the effectiveness of amine-impregnated zeolite additives in enhancing the moisture resistance of HMA, a prevalent issue contributing to pavement distress over the course of its service life. This study compares the performance of three additives: amine-impregnated zeolite, amine and zeolite separately, and a commercial liquid antistrip agent. Additionally, it evaluates the mechanical properties of PG 64-16 Low Carbon (LC) binder compared to conventional PG 64-16 binder at different aging levels to simulate the effects of HMA aging that occurs over a pavement's service life.

The evaluation involves analyzing the performance of asphalt mixtures at three different long-term aging intervals: 3 days, 5 days, and 7 days, representing approximately 4 years, 8 years, and 10 years of field aging, respectively, in the climate conditions of Southern California. These mixtures are compared against non-aged HMA mixtures.

To achieve the objective of this study, the following comparisons were made.

- Comparing the rutting resistance and inflection point of asphalt mixture samples incorporating three types of additives and two types of asphalt binders across four different aging levels.

- Comparing the tensile strength of dry and freeze thaw (one cycle) conditioned specimens among asphalt mixtures incorporating three types of additives and two types of asphalt binders across four different aging levels.

- Comparing the cracking resistance of asphalt mixture samples incorporating three types of additives and two types of asphalt binders across four different aging levels.

Additionally, following comparisons were made between the conventional and low-carbon binder.

- The vulnerability of a bitumen-stone interface to moisture-induced damage.

- The binder's tendency to undergo permanent deformation and the binder's capability to recover its original form after the removal of stress.

Through this comprehensive evaluation, the study aims to provide insight into the efficacy of different additives and asphalt binders in enhancing the long-term performance and durability of HMA under varying aging conditions, contributing to developing more resilient and sustainable pavement materials.

Table **1** shows the factorials used in the study.

Table 1. Test Factorial

Binder	Additives	Aging Levels	Sample Identification Name
PG 64-16	Amine-Impregnated Zeolite (AIMZ)	Without Aging	AIMZ-0
		3 days	AIMZ-3
		5 days	AIMZ-5
		7 days	AIMZ-7
	Amine and Zeolite (AZ)	Without Aging	AZ-0
		3 days	AZ-3
		5 days	AZ-5
		7 days	AZ-7
	Liquid Antistrip (LAS)	Without Aging	LAS-0
		3 days	LAS-3
		5 days	LAS-5
		7 days	LAS-7
PG 64-16 Low Caron (LC)	Amine-Impregnated Zeolite (AIMZ)	Without Aging	LC-AIMZ-0
		3 days	LC-AIMZ-3
		5 days	LC-AIMZ-5
		7 days	LC-AIMZ-7
	Amine and Zeolite (AZ)	Without Aging	LC-AZ-0
		3 days	LC-AZ-3

Binder	Additives	Aging Levels	Sample Identification Name
		5 days	LC-AZ-5
		7 days	LC-AZ-7
	Liquid Antistrip (LAS)	Without Aging	LC-LAS-0
		3 days	LC-LAS-3
		5 days	LC-LAS-5
		7 days	LC-LAS-7

4. Materials

HMA is typically comprised of 95% aggregates and 5% asphalt binders by weight. Aggregates provide stability to the mix, while binders are essential for cohesion and durability. Additional additives are incorporated into the binder to improve the overall properties of the mixture.

4.1 Aggregates

The aggregates for this study were procured from CalPortland's Garey Aggregate Plant in Garey, California. Various aggregate sizes (3/4", 1/2", 3/8", and Rock Dust) were sampled from stockpiles at CalPortland and transported to the laboratory in bulk bags. These aggregates, representing different stockpiles, underwent sieving to separate them into their primary sizes and then blended to achieve the desired target gradation. The nominal maximum aggregate size (NMAS) selected was 1/2". The gradation, plotted on a 0.45 power chart, is illustrated in Figure 1 below.

Figure 1. Aggregate Gradation Curve
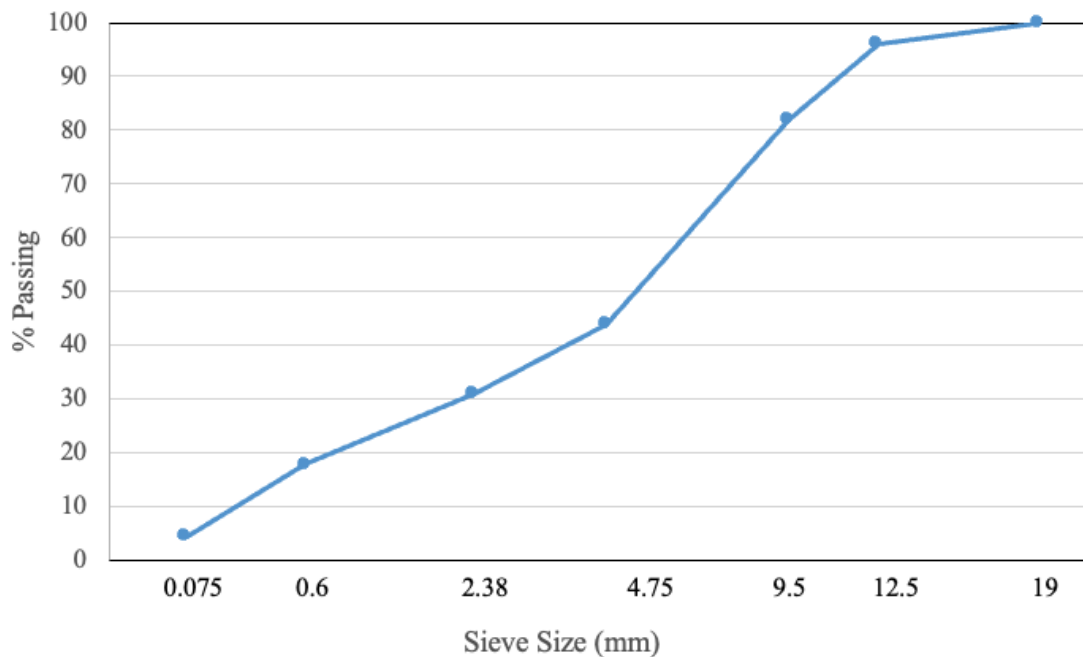
4.2 Binder

This research utilized two types of binders: PG 64-16 and PG 64-16 Low Carbon (LC). Both binders were sourced from Centennial Asphalt Terminal, California. PG 64-16 LC is a binder incorporated with 10% post-consumer plastics, enabling a 5% reduction in CO_2 emissions and facilitating the recycling of plastics from the waste stream. Emissions were calculated utilizing values from the Emerald Eco-Label program by the National Asphalt Pavement Association (NAPA) and average emission values from the Energy Information Administration (EIA). This binder meets the specifications of the Federal Highway Administration, ASTM D6373, and AASHTO M 320. Table 2 provides a comparison of the properties of both binders sourced from the referenced asphalt company.

<p style="text-align:center">Table 2. Asphalt Binder Properties</p>

Property	Test Methods		Results		AASHTO M 320 Specification	
	ASTM	AASHTO	Conventional PG 64-16	PG 64-16 LC	Minimum	Maximum
Test on Original Asphalt						
Dynamic Shear, G*/Sinδ at 64°C (kPa)		T315	1.15	1.45	1	
Viscosity at 135°C, Pa-s	D4402	T316	0.347	0.277		3
Flash Point (°C)	D92	T48	304	310	230	
Test on Residue from Rolling Thin Film Oven (RTFO)	D2872	T240				
Dynamic Shear, G*/Sinδ at 64°C (kPa)		T315	3.46	2.44	2.2	
Mass Loss, %	D2872	T240	-0.655	-0.399		1
Test on Residue from Pressure Aging Vessel (PVA)	D6521	R28				
Dynamic Shear, G*Sinδ at 28°C (kPa)		T315	3,122	1,812		5,000
BBR Stiffness at -6°C (MPa)	D6648	T313	141	73		300
BBR Slope m-value at -6°C	D6648	T313	0.399	0.32	0.3	

4.3 Additives

This study employed three different types of additives: (a) amine-impregnated zeolite, (b) amine and zeolite as separate components, and (c) a commercial amine-based liquid antistripping agent. The amine utilized was Ethylenediamine, at a purity of 99%, sourced from Fisher Scientific. With the chemical formula $C_2H_8N_2$, this strongly basic amine exists as a colorless liquid. The zeolite component utilized was Clinoptilolite Zeolite, at a purity of 90% to 92%, obtained from Heiltropfen®. This ultra-fine micronized powder has a particle size of less than 20 μm. The commercial liquid antistrip, AD-HERE® LOF 65-00, procured from ArrMaz Products Inc., Florida, is a dark brown, viscous liquid at room temperature. The LOF 65-00 dosage applied in this study was 0.5% by weight of the asphalt binder.

5. Methodology

Several steps were undertaken to prepare the compacted specimens to the prescribed specifications. These steps encompassed the application of additives, mixing the materials, the short- and long-term aging of the mixture, compaction, and specimen fabrication. Four different aging levels were implemented to simulate varying degrees of field aging over 4 different pavement service life. In total, 96 specimens were prepared for the Hamburg Wheel Tracking Test, 144 specimens for the Indirect Tensile Strength Test of both dry and conditioned specimens, and 72 specimens for IDEAL Cracking Test. Following these preparation steps, all the tests were conducted as per the experimental protocol.

5.1 Additive Application Method

To prepare the binder with amine-impregnated zeolite (AIMZ), the zeolite underwent an initial drying process at 100°C for 1 hour to eliminate any residual moisture present within the zeolite pores. Subsequently, the zeolite was allowed to cool down to room temperature. The amine to zeolite ratio was carefully chosen at 0.47:1. This ratio was determined by thoroughly mixing the zeolite with amine until it reached a consistency of dry powder, ensuring complete absorption of the amine by the zeolite particles, as illustrated in **Figure 2**. The quantity of AIMZ added to the binder was precisely determined by incorporating 1% amine based on the weight of the asphalt binder. For example, to prepare 100 g of bitumen, 2.13 g of zeolite was mixed with 1 g of amine (at a ratio of 0.47:1), and this amine-impregnated zeolite was subsequently added to the 100 g of binder. Following the preparation of AIMZ, a resting period of 2 hours was observed before adding it to the binder, ensuring the complete absorption of amine molecules within the zeolite pores.

Figure 2. Consistencies at Different Amine to Zeolite Ratios
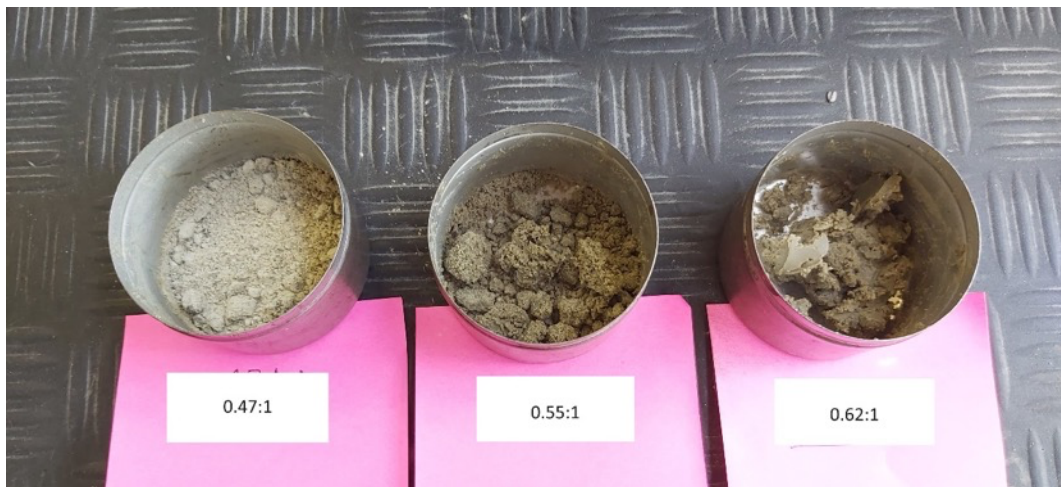
For the binder with amine and zeolite, equivalent quantities of zeolite and amine used in preparing the binder with the amine-impregnated zeolite were added separately into bitumen, ensuring that the amine remained unabsorbed by zeolite powder.

The third additive introduced was the liquid antistrip, LOF 65-00, with a dosage of 0.5% by weight of the asphalt binder.

The binders were heated to 150°C to facilitate the mixing with the additives. Subsequently, all three additives were mixed with the binder using a shear mixer rotating at 750 rpm for 10 minutes, as illustrated in Figure 3.

Figure 3. Shear Mixing of Binder with Additives

5.2 Batching of Aggregates

In compliance with the Asphalt Institute MS-2 manual (Method 3), the aggregate batching and mix sample preparation procedures adhered to protocols aimed at attaining precision and uniformity in outcomes. Initially, each aggregate stockpile underwent a total fractionation over a large rectangular tray-type sieve shaker, where individual coarse and fine aggregate sizes were separated and stored in designated separate pans, as illustrated in **Figure 4**. Later, the aggregates were proportioned in accordance with precise gradation specifications delineated in the mix design to achieve target air voids. Subsequently, individual batch weights were mixed in a mechanical mixer where they underwent a dry-mixing process for a predetermined duration, ensuring the even dispersion of particles throughout the mixture. This meticulous blending process optimizes the

homogeneity and consistency of the resulting aggregate blend, laying the foundation for subsequent asphalt mixture formulation processes.

Figure 4. Individual Aggregate Sizes Following Total Fractionation

5.3 Mixing

As provided by the Centennial Asphalt Company, the mixing temperature range was between 146°C and 151°C for both binders. To ensure uniformity, the aggregates, asphalt binder, mixing bucket, mixer paddle, and spatulas were heated to 151°C for a duration of two hours prior to mixing. The mixing was performed on the same day as the additive application to mitigate the need to reheat the additive-treated binder, which could lead to binder aging and subsequent alterations of additive characteristics. Following this, the individual aggregate sizes were introduced into the tared mixing bucket and weighed on the scale. In succession, 5.75% binder by weight of the total mix was added to the aggregate in the buttered bucket for both conventional and low-carbon binders. As depicted in Figure 5, the mixing process was then initiated using a mobile bucket mixer, with mixing continuing for 2 minutes to ensure 100% uniform coating of all aggregates with asphalt binder. To prevent cross-contamination, separate buckets were employed for each binder type. Subsequently, the HMA mix was transferred to a pan, where it was evenly spread to a thickness ranging between 25 and 50 mm.

Figure 5. Mobile Mixer to Mix Aggregates with Binder

5.4 Aging

For each asphalt mixture, four distinct sets were prepared to evaluate the mechanical performance at four varying aging levels, including (a) without long-term aging, (b) aged for 3 days (simulating 4 years), (c) aged for 5 days (simulating 8 years), and (d) aged for 7 days (simulating 10 years). Each loose mixture was subjected to short-term conditioning per AASHTO R 30 standard to allow for binder absorption during the mix design process and to simulate the plant mixing and construction effects on the mixture. After spreading each mixture evenly in a pan to a thickness of 25 to 50 mm, short-term conditioning occurred in a forced draft oven for 2 hour ± 5 min at a temperature of 135 ± 3ºC. Throughout the conditioning process, mixtures were periodically stirred with a spatula at 60 ± 5 min to ensure uniform conditioning. Once short-term conditioning concluded, one set of samples immediately underwent compaction, while the remaining three underwent long-term conditioning to simulate the aging typical of pavement service life.

Long-term aging of uncompacted HMA followed the procedures outlined in NCHRP Research Report 973; the short-term aged asphalt mixtures were spread onto pans to achieve a loose mix layer approximately equal to the NMAS of 12.5 mm, as shown in Figure 6.

Figure 6. Loose Asphalt Mixture Spread onto a Pan for Long-Term Conditioning

The pans were then placed into the forced draft oven set at 95 ± 3°C, as shown in Figure 7. In this procedure, the required duration of aging to simulate the desired field aging was determined using the following equation:

$$t_{oven} = CAI = \sum_{i=1}^{N} 0.0437 d^{-0.426} e^{\frac{-1601.167}{T_i}}$$

where:

toven = required oven aging duration at 95°C to reflect field aging (days);

CAI = climatic aging index;

d = depth below pavement surface greater than 0.6 cm (cm); and

Ti = pavement temperature obtained from the Enhanced Integrated Climatic Model (EICM) at the depth of interest at the hour of interest, i (kelvin).

NCHRP Research Report 973 provides laboratory aging duration guidelines and maps derived from historical pavement temperature data collected from various locations across the United States via Enhanced Integrated Climatic Model (EICM). These guidelines are tailored to reflect different field ages of 4 years, 8 years, and 16 years. They specify aging durations at depths of 6 mm, 20 mm, and 30 mm, rounded to the nearest day. For our study, these guidelines were utilized to determine the appropriate oven aging durations. We selected 3 days, 5 days, and 7 days of oven aging to correspond to field aging of 4 years, 8 years, and 10 years, respectively, in the southern California region at a depth of 6 mm.

To ensure uniform heat and air flow exposure, the pans were periodically repositioned across different shelves at four evenly spaced intervals during the long-term conditioning process. Once the prescribed aging duration elapsed, the mixtures were removed from the oven and allowed to cool to room temperature before subsequent testing and compaction procedures commenced.

Figure 7. Placement of Pans in the Oven for Long Term Conditioning

5.5 Compaction and Fabrication

The specimens required for this study were prepared according to the Table 1 of Chapter 3. Each HWT test necessitated 4 specimens, each Indirect Tensile Strength Test for TSR required 6 specimens, and each IDEAL-CT required 3 specimens, totaling 312 specimens across all testing conditions. The HWT compacted specimens measured 60.8 mm in height, TSR specimens stood at 95 mm, and IDEAL-CT specimens were 62 mm tall, all with a diameter of 150 mm. Subsequently, four primary standard tests were conducted, as listed below.

- AASHTO T 209: Standard Method of Test for Theoretical Maximum Specific Gravity (G_{mm})

- AASHTO T 312: Preparing and Determining the Density of Asphalt Mixture Specimens by Means of the Superpave Gyratory Compactor

- AASHTO T 166: Standard Method of Test for Bulk Specific Gravity (G_{mb}) of Compacted Hot Mix Asphalt using the Saturated Surface-Dry Method

- AASHTO T 269: Standard Method of Test for Percent Air Voids in Compacted Dense and Open Asphalt Mixtures

Following aging, the initial test conducted was the AASHTO T 209 to determine the loose sample's theoretical maximum specific gravity (Gmm). The theoretical maximum specific gravity, Gmm, is crucial to determine the percentage of air voids in the compacted asphalt mixture. After cooling the mixes to room temperature, loose long-term aged specimens were placed in a metal standardized pycnometer, and sufficient water was added at approximately 25ºC to cover the specimen completely. A high-vacuum pump was then engaged for 15 minutes to remove entrapped air as shown in Figure 8, while maintaining the residual pressure of the vacuum pump at 27.5 ± 2.5 mm Hg. Mechanical agitation was applied to facilitate the removal of air. At the end of the vacuum period, the vacuum was released by increasing the pressure. Once the vacuum process concluded, the container was filled with water until overflow. After waiting 10 minutes for temperature stabilization, the masses of the container filled with specimen and water and of the container filled with water only were determined. Upon completion of the test, the theoretical maximum specific gravity, Gmm, was determined using the following equation:

$$G_{mm} = \frac{A}{A + D - E}$$

where:

A = mass of the oven dry specimen in air, (g);

D = mass of container filled with water at 25˚C, (g); and

E = mass of container filled with specimen and water at 25˚C, (g).

Figure 8. Vacuum Saturation of Conditioned Loose Asphalt Mixture

The calculated Gmm are presented in Table 3.

Table 3. Theoretical Maximum Specific Gravity of Mixtures at Different Aging Levels

	G_{mm}	
	HMA with PG 64-16	HMA with PG 64-16 LC
Without Aging	2.411	2.409
3-Day Aging	2.415	2.414
5-Day Aging	2.419	2.416
7-Day Aging	2.423	2.421

The compaction process followed the AASHTO T 312 standard, employing a Pine Gyratory Compactor, as illustrated in Figure 9. Upon obtaining the Gmm values, samples were prepared for compaction. The compaction temperature range, provided by Centennial Asphalt Company, ranged from 136°C to 140°C for both binders. HMA mixtures and the compaction mold were placed in the forced draft oven until reaching 140ºC. Upon reaching the compaction temperature, the mixtures were introduced into the compaction mold and compacted per the AASHTO T 312 standard. A pressure of 600 kPa with an internal angle of 1.16° was applied, and the number of gyrations was recorded for each specimen. To mitigate the rebound effect inherent in a viscous asphalt binder, a squaring time of 4 min was implemented, allowing the samples to become stable and prevent errors in sample's height or air void percentage calculations.

Figure 9. Superpave Gyratory Compactor for Specimen Compaction

Once compaction and squaring of the samples were completed, the compacted specimen was extruded and allowed to cool to room temperature as illustrated in Figure 10. Each specimen was appropriately labeled for identification. Subsequently, after reaching room temperature, the bulk specific gravity (Gmb) of each specimen was determined.

Figure 10. Compacted Specimens Kept for Cooling Down

The procedure outlined in AASHTO T 166 Method A standard was followed for determining the bulk volume of the compacted HMA mix. It involved measuring the mass of the dry sample and its mass underwater after suspension for 4 minutes, as illustrated in Figure 11. Another crucial measurement required for this test was the Saturated Surface Dry (SSD) mass. Achieving the SSD condition accurately was paramount to account for the surface voids of the compacted HMA specimen. After removing the specimen from the water bath, it was damp-dried by blotting it with a damp towel. The SSD mass was recorded within 15 seconds after the sample was removed from the water bath. The following equation was then employed to determine the Gmb:

$$G_{mb} = \frac{A}{B - C}$$

where:

G_{mb} = bulk specific gravity;

A = mass of specimen in air, (g);

B = mass of surface-dry specimen in air, (g); and

C = mass of sample in water at 25°C, (g).

Figure 11. Determination of Bulk Specific Gravity: (a) Dry Mass of Specimen in Air and
(b) Mass of Specimen Underwater

(a)   (b)

Once the G_{mm} and the G_{mb} were determined, the AASHTO T 269 test method was employed to calculate the air voids (V_a) in the compacted HMA samples using the formula:

$$V_a = 100 \left[1 - \frac{G_{mb}}{G_{mm}} \right]$$

A target air void of 7% ± 0.5% was required for each test, necessitating a trial-and-error approach to achieve this percentage. Multiple trials were conducted, adjusting the loose sample mass until the desired air void was attained. Specimens deviating from the allowed air voids' range were discarded.

Once the sample achieved the target air void, it was ready for the TSR and the IDEAL-CT tests. However, for the HWT test, the compacted samples needed to be cut according to the procedure outlined in AASHTO T 324. Marked specimens were prepared for cutting according to the mold dimensions and sent for saw cutting, as shown in Figure 12.

Figure 12. Saw Cut Specimens for HWT Test

5.6 Testing

This study investigates the rutting resistance, resistance to moisture-induced damage, and fatigue cracking resistance of asphalt mixtures incorporating conventional and low-carbon binders, along with three different types of additives, at four different aging levels. The methods employed to analyze the compacted samples are outlined below:

- AASHTO T 324: Standard Method of Test for Hamburg Wheel-Track Testing of Compacted Asphalt Mixtures.

- AASHTO T 283: Standard Method of Test for Resistance of Compacted Asphalt Mixtures to Moisture-Induced Damage.

- ASTM D8225: Standard Test Method for Determination of Cracking Tolerance Index of Asphalt Mixture Using the Indirect Tensile Cracking Test at Intermediate Temperature.

The study also investigates the vulnerability of a bitumen-stone interface of conventional and low-carbon binders to moisture-induced damage and the rheological properties of conventional and low-carbon binders when they are subjected to repeated loading and rest cycles under intermediate-temperature. The methods employed to analyze the binders are outlined below:

- Moisture-Induced Shear-Thinning Index (MISTI)

- Multiple Stress Creep Recovery (MSCR) Test

5.6.1 Hamburg Wheel Tracking Test

To evaluate rutting resistance, AASHTO T 324: Standard Method of Test for Hamburg Wheel-Track (HWT) Testing of Compacted Asphalt Mixtures was conducted. This method involves evaluating the rutting and moisture susceptibility of submerged, compacted HMA

samples using a reciprocating rolling wheel device. The Superpave Gyratory Compactor (SGC), submerged in a temperature-controlled water bath, was repetitively loaded using a reciprocating steel wheel, and the resultant deformation of the samples caused by the wheel loading was recorded. The Cox Hamburg Wheel Tracker Machine, an electrically powered machine, was used to conduct this test. The diameter and width of the two steel wheels are 8" and 1.85", respectively.

The load on each wheel is 705 N. It reciprocates at a rate of 52 passes per minute. To start the test, the testing machine and software were turned on. The tank was filled with water, and the temperature was set to 50℃. The test temperature is based on the PG grade of the binder and HMA. The saw-cut SGC-compacted sample was placed in the molds and secured rigidly in the mounting tray. For each test, we arranged four SGC specimens into two pairs. This test set up is shown in Figure 13. The software was configured with a maximum of 20,000 passes and a maximum rut depth of 20 mm. Testing stopped upon reaching the maximum number of passes or the maximum impression depth. Once all conditions were met, the test was automatically initiated, operating at the rate of 52 passes per minute. The software monitored and plotted rut depth versus the number of passes for each wheel, and recorded the Stripping Inflection Point (SIP). SIP represents the point at which asphalt binder stripping from the aggregate starts due to moisture. Rut depths were determined by averaging the deepest rut depth of both pairs of samples.

Figure 13. Hamburg Wheel Track Test Setup
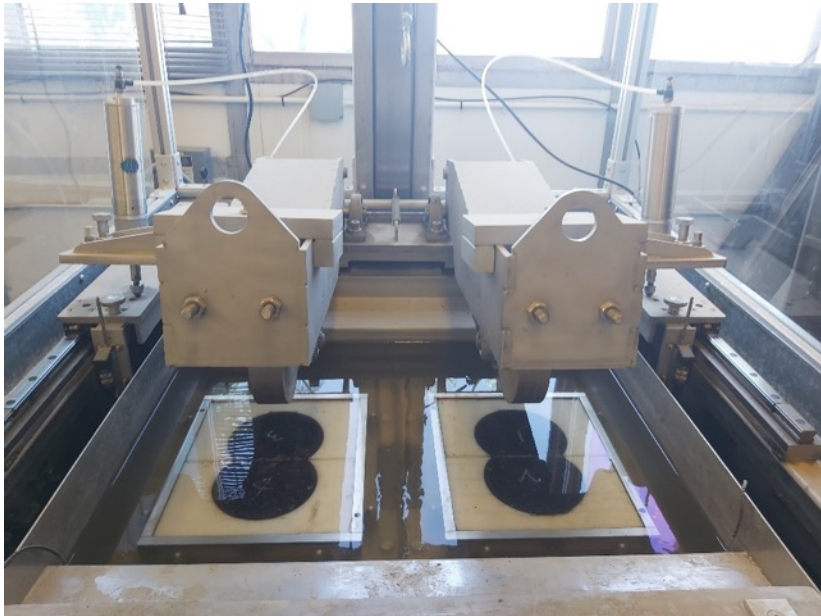
5.6.2 Indirect Tensile Strength Test of Dry- and Moisture-Conditioned Specimens

The moisture resistance evaluation in compacted asphalt mixtures followed the guidelines outlined in AASHTO T 283-22. For each test iteration, six specimens were required for each set. These specimens were divided into dry and conditioned subsets, ensuring that the average air voids of both subsets were approximately equal. The conditioned specimen underwent one cycle of freeze and thaw. The dry specimens were securely sealed in leak-proof plastic bags and immersed in a water bath maintained at 25 ± 0.5ºC for a duration of 2 hours ± 10 minutes prior to testing. On the other hand, the conditioned subsets underwent vacuum saturation level of 70 to 80%, achieved by subjecting each specimen to partial vacuum pressure of approximately 26 in.Hg for a period of 5 minutes. The degree of saturation (S′) was calculated using the following equations:

$$Va = PaE / 100$$

$$J' = B' - A$$

$$S' = 100J' / Va$$

where:

Va = volume of air voids (cm3);

Pa = percent of air voids;

E = volume of the specimen (cm3);

J′ = volume of absorbed water (cm3);

B′ = mass of the saturated surface-dry specimen after partial vacuum saturation (g);

A = mass of the dry specimen in air; and

S′ = degree of saturation (%).

If the degree of saturation fell within the range of 70 to 80%, each specimen was wrapped tightly with a plastic film, ensuring a snug fit, before being placed in a plastic bag along with 10 mL of water. The bags were sealed and subjected to freezing conditions for a minimum duration of 16 hours at a temperature maintained at -18 ± 3ºC. Subsequently, the conditioned specimens were placed in a water bath set at 60 ± 1°C for a duration of 24 hours, following which the plastic films and bags were removed. The specimens were then transferred to a bath maintained at 25 ± 0.5°C for a period of 2 hours ± 10 minutes as shown in Figure 14.

Figure 14. T283 Conditioned Specimens in Water Bath
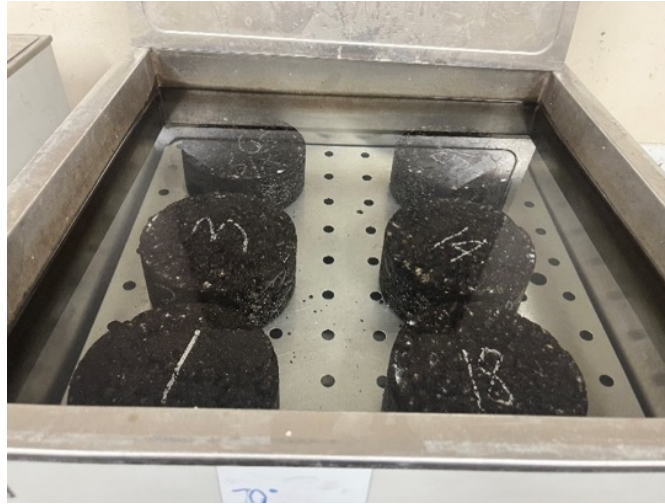
Following conditioning, the thickness of the specimens was determined by measuring at four distinct points around each specimen and subsequently computing the average of the four measurements. For specimens from the dry subset, the final height achieved during compaction using the Superpave Gyratory Compactor was utilized. Subsequently, the specimens were immediately placed between the two Lottman breaking heads in the testing machine, where the load was applied at a constant rate of 50 mm per minute, as shown in Figure 15. The maximum compressive load was recorded, and loading continued until a vertical crack appeared.

Figure 15. ITS Specimen Mounted Between Two Breaking Heads on the Testing Machine

The indirect tensile strength (ITS) for each specimen was calculated using the following equation:

$$S_t = 2P / (\pi t D)$$

Where:

S_t = tensile strength (psi);

P = maximum force placed on specimen during loading (lbs);

t = specimen thickness (in); and

D = specimen diameter (in).

The tensile strength ratio (TSR) serves as a numerical index of the HMA's resilience against detrimental moisture-induced damage, representing the ratio of the strength retained post freeze-thaw conditioning to the strength of the unconditioned specimens. The following equation determines this ratio:

$$TSR = S_2 / S_1$$

where:

S1 = average tensile strength of the dry subset (psi); and

S2 = average tensile strength of the conditioned subset (psi).

5.6.3 IDEAL Cracking Test

ASTM D8225-19, known as the Standard Test Method for Determination of Cracking Tolerance Index of Asphalt Mixture Using the Indirect Tensile Cracking Test at Intermediate Temperature (IDEAL CT), was employed to evaluate the cracking resistance of HMA. Utilizing the Dynamic Testing System (DTS) by Pavetest, equipped with an indirect tensile loading frame, the test apparatus includes components such as an axial loading device, a load cell, loading strips, a sample deformation measurement device, a temperature-controlled chamber, and a data control and acquisitions system. Each test necessitated three SGC compacted specimens, with loading strips sized to be 19.05 mm wide and longer than the sample's thickness for a 150 mm diameter specimen. The IDEAL CT measures cracking resistance based on the fracture-mechanics-derived parameter known as the Cracking Tolerance Index (CT_{index}), derived from factors such as failure energy, the post-peak slope of the load-displacement curve, and the deformation tolerance at 75% of peak load. The IDEAL CT was performed at a target intermediate test temperature of 28ºC, determined by the following equation:

$$PG\ IT = \frac{PG\ HT + PG\ LT}{2} + 4$$

where:

PG IT = intermediate performance grade temperature (°C);

PG HT = climatic high-performance grade temperature (°C); and

PG LT = climatic low-performance grade temperature (°C).

The test specimens were preconditioned in the environmental chamber at the target intermediate test temperature of 28°C for a duration of 2 h ± 10 minutes. Prior to testing, meticulous cleaning of the contact surface of the indirect tensile frame was carried out to ensure the absence of any debris, as its presence could lead to inaccurate measurements. Subsequently, the samples were positioned within an indirect tensile loading frame, aligned to ensure uniform contact with the support, as shown in Figure 16. Input parameters, including a loading rate of 50 mm/minute and a termination load of 0.1 kN, were configured into the software. The test was initiated following setup, with the software capturing and recording displacements alongside corresponding loads for each test. Testing stopped upon detection of sample failure, defined by displacement under a load

of less than 0.1 kN. Graphical representation was then generated, plotting the relationship between load and displacements.

Figure 16. Specimen Prepared for IDEAL CT Testing

Once the load versus displacement graph was generated, the work of failure (W_f) was determined by calculating the area under the load versus displacement curve using the quadrangle rule, as shown in the equation below:

$$W_f = \sum_{i=1}^{n-1} [(l_{i+1} - l_i) \times P_i + \frac{1}{2} \times (l_{i+1} - l_i) \times (P_{i+1} - P_i)]$$

where:

Wf = work of failure (Joules);

Pi = applied load (kN) at the i load step application;

Pi+1 = applied load (kN) at the i + 1 load step application;

li = LLD (mm) at the i step; and

li+1 = LLD (mm) at the i + 1 step.

The failure energy (Gf) was calculated by dividing the work of failure, Wf by the cross-sectional area of the specimen as shown in the following equation:

$$G_f = \frac{W_f}{D \times t} \times 10^6$$

where:

G_f = failure energy (Joules/m²);

W_f = work of failure (Joules);

D = specimen diameter (mm); and

t = specimen thickness (mm).

The post-peak slope ($|m75|$) represents the slope of the tangential zone around the 75% peak load point after the peak, calculated by the following equation.

$$|m_{75}| = |\frac{P_{85} - P_{65}}{l_{85} - l_{65}}|$$

where:

P_{85} = 85% of the peak load (kN) at the post-peak stage;

P_{65} = 65% of the peak load (kN) at the post-peak stage;

l_{85} = displacement (mm) corresponding to the 85% percent of the peak load at the post-peak stage; and

l_{65} = displacement (mm) corresponding to the 85% percent of the peak load at the post-peak stage.

The cracking tolerance index (CT_{index}) was calculated from the parameters obtained from the load-displacement curve, as shown in the following equation:

$$CT_{index} = \frac{t}{62} \times \frac{l_{75}}{D} \times \frac{G_f}{|m_{75}|} \times 10^6$$

where:

CT_{index} = cracking tolerance index;

G_f = failure energy (Joules/m²);

$|m_{75}|$ = absolute value of the post-peak slope m_{75} (N/m);

l_{75} = displacement at 75% the peak load after the peak (mm);

D = specimen diameter (mm); and

t = specimen thickness (mm).

5.6.4 Moisture-Induced Shear-Thinning Index

The Moisture-Induced Shear-Thinning Index (MISTI) is a new test that assesses the vulnerability of a bitumen-stone interface to moisture-induced damage. To produce a reliable and reproducible test that considers the essential material properties that drive moisture damage at the interface, 100-micron glass beads were added to bitumen at a weight ratio of 1:2 (glass beads to bitumen).

To carry out the test, four specimens (0.3 grams each) were prepared using 8 mm silicon molds. Two samples were exposed to normal room conditions, while the other two were subjected to water conditioning at a temperature of 60°C for 24 hours. After drying their surface, each specimen was subjected to a shear rate sweep test with a shear rate range of 0.1 to 100 per sec. The temperature was set at a specific temperature where the sample experienced zero shear thinning zone at low shear rates. Finally, the viscosity-versus-shear rate plot was used to calculate the shear-thinning value, which measures the extent of viscosity change concerning the shear rate.

The MISTI is the ratio of the degree of shear-thinning under wet conditions to that under dry conditions, expressed by Equation 1. The MISTI value is a reliable gauge of moisture-induced deterioration in the binder. A MISTI value of 1 implies no observable changes at the interface after water conditioning. Any value other than 1 indicates that exposure to water has altered the interface. The extent of the change is directly linked to the probability of moisture damage, where a higher MISTI value indicates a more significant modification at the interface.

$$MISTI = \frac{\text{Average Slope (Viscosity vs Shear rate) of Wet Specimen}}{\text{Average Slope (Viscosity vs Shear rate) of Dry Specimen}}$$

5.6.5 Multiple Stress Creep Recovery Test

The Multiple Stress Creep Recovery (MSCR) test is a procedure that evaluates the rheological properties of asphalt binders when they are subjected to repeated loading and rest cycles under intermediate-temperature conditions (40°C). The test is conducted using an Anton Paar dynamic shear rheometer with an 8 mm spindle.

The MSCR test involves applying stress levels of 0.1 and 3.2 KPa to the asphalt binder sample in succession. Each stress level undergoes ten creep and recovery cycles, where each cycle consists of

a 1-second creep (load application) period followed by a 9-second recovery (load removal) period. The total test duration is 200 seconds for the 20 cycles conducted across both stress levels.

The MSCR test derives two critical parameters: Non-recoverable Creep Compliance (Jnr), which indicates the asphalt binder's tendency to undergo permanent deformation, and Percent Recovery, which reflects the material's capability to recover its original form after the removal of stress. These parameters, obtained under controlled stress levels and cycle conditions, offer invaluable insights into the asphalt binder's resistance to rutting and its elastic recovery properties.

6. Results and Analysis

6.1 Hamburg Wheel Tracking Test

Based on the Standard Specification of Caltrans, the minimum number of passes at 12.5 mm rut depth for PG64 is 15,000. In other words, HWT samples are considered to have failed if they exhibit a rut depth of 12.5 mm or more at or before 15,000 passes. In the findings presented here, none of the samples exceeded the 12.5 mm rut depth threshold, thus warranting a comparison based on the rut depth achieved at 15,000 passes rather than the number of passes to failure. Each HWT test involved two wheels, left and right, with rut depth recorded by a Linear Variable Differential Transducer (LVDT). Subsequently, the recorded data were analyzed, and the average rut depth at 15,000 passes was computed. The results, delineating the average rut depth for each mixture at every aging level, are summarized in Table 4. Figures 17 and 18 represent the average rut depth at 15,000 passes for both conventional and low-carbon binders across each aging level, respectively.

The results indicate a consistent reduction in the average rut depth as the aging level increases, suggesting that rutting predominantly occurs during the early stages of the pavement service life. As aging progresses, the oxidation of the binder leads to increased stiffness, thereby mitigating susceptibility for rutting. Across all mixtures, the rut depth at the 7-day aging level exhibited a decrease of approximately 40% to 60% compared to the rut depth observed at the without aging level. For example, a noticeable contrast in rutting is evident in LC-AIMZ mixture, where the rut depth after 20,000 passes decreased from 2.85 mm without aging to 1.7 mm after 7 days of aging, as shown in Figure 19. Notably, for conventional asphalt binder PG 64-16, mixtures with AZ consistently demonstrated lower rut depth compared to those with AIMZ and LAS at 3, 5 and 7 days of aging levels. Conversely, for PG 64-16 LC, mixtures with AZ exhibited higher rut depth than those with AIMZ and LAS at without aging, 3 and 5 days of aging level. At 7 days of aging level, the rut depth of mixtures with AZ was lower than both mixtures with AIMZ and LAS. However, the disparities in rut depth between these mixtures were not significant in either case.

Table 4. Hamburg Wheel Rut Depth Results at 15,000 passes

Aging Level	Sample ID	Rut Depth (mm)			Stripping Inflection Point
		Left	Right	Average	
Without Aging	AIMZ-0	2.06	2.78	2.42	N/A
	AZ-0	3.67	1.52	2.60	N/A
	LAS-0	2.65	2.87	2.76	N/A
	LC-AIMZ-0	3.54	1.76	2.65	N/A
	LC-AZ-0	2.45	3.64	3.05	N/A
	LC-LAS-0	1.18	3.83	2.51	N/A
3 Days	AIMZ-3	2.75	2.41	2.58	N/A
	AZ-3	1.03	1.05	1.04	N/A
	LAS-3	1.98	2.04	2.01	N/A
	LC-AIMZ-3	1.43	2.13	1.78	N/A
	LC-AZ-3	2.75	1.51	2.13	N/A
	LC-LAS-3	1.20	2.22	1.71	N/A
5 Days	AIMZ-5	1.05	1.89	1.47	N/A
	AZ-5	1.39	0.95	1.17	N/A
	LAS-5	1.75	1.08	1.42	N/A
	LC-AIMZ-5	1.36	2.39	1.88	N/A
	LC-AZ-5	1.73	2.32	2.03	N/A
	LC-LAS-5	1.65	1.49	1.57	N/A
7 Days	AIMZ-7	1.35	0.92	1.14	N/A
	AZ-7	1.04	0.64	0.84	N/A
	LAS-7	1.17	1.15	1.16	N/A
	LC-AIMZ-7	1.02	1.80	1.41	N/A
	LC-AZ-7	0.67	1.95	1.31	N/A
	LC-LAS-7	1.37	1.93	1.65	N/A

Figure 17. Average Rut Depth at 15,000 Passes for Mixtures with PG 64-16
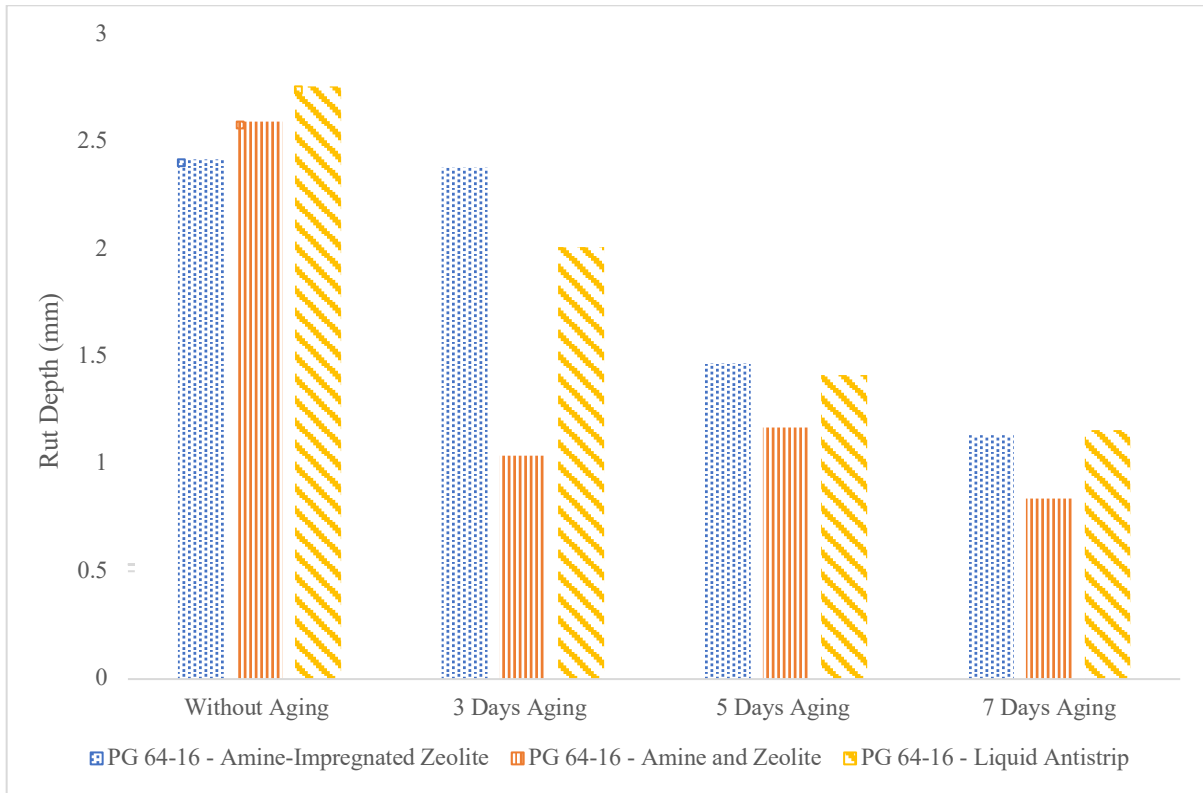
Figure 18. Average Rut Depth at 15,000 Passes for Mixtures with PG 64-16 LC
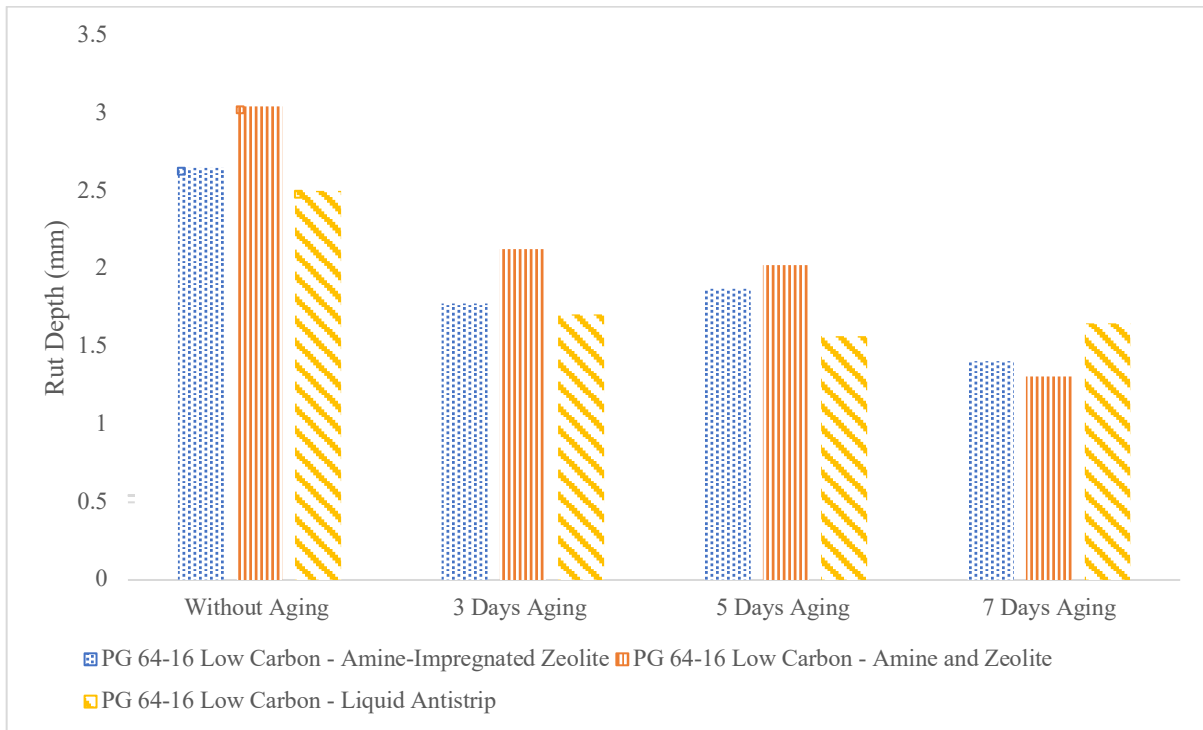
Figure 19. Specimens after HWT Test—(a) LC-AIMZ-0 vs (b) LC-AIMZ-7

Figures 20 to 23 present the average rut depth vs number of passes for mixtures subjected to different aging durations: without aging, 3 days, 5 days, and 7 days, respectively. No discernible trend can be detected among the various mixtures for the without aging and 3 days of aging levels. For 5 and 7 days of aging levels, mixtures with PG 64-16 LC exhibit slightly higher rut depth compared to those with conventional PG 64-16. However, these differences are marginal. No abrupt changes in slope were observed across any of the average rut depth vs. number of passes curve, indicating the absence of any discernible stripping inflection point for any mixture.

Figure 20. Rut Depth vs. No of Passes for Every Mixture at Without Aging
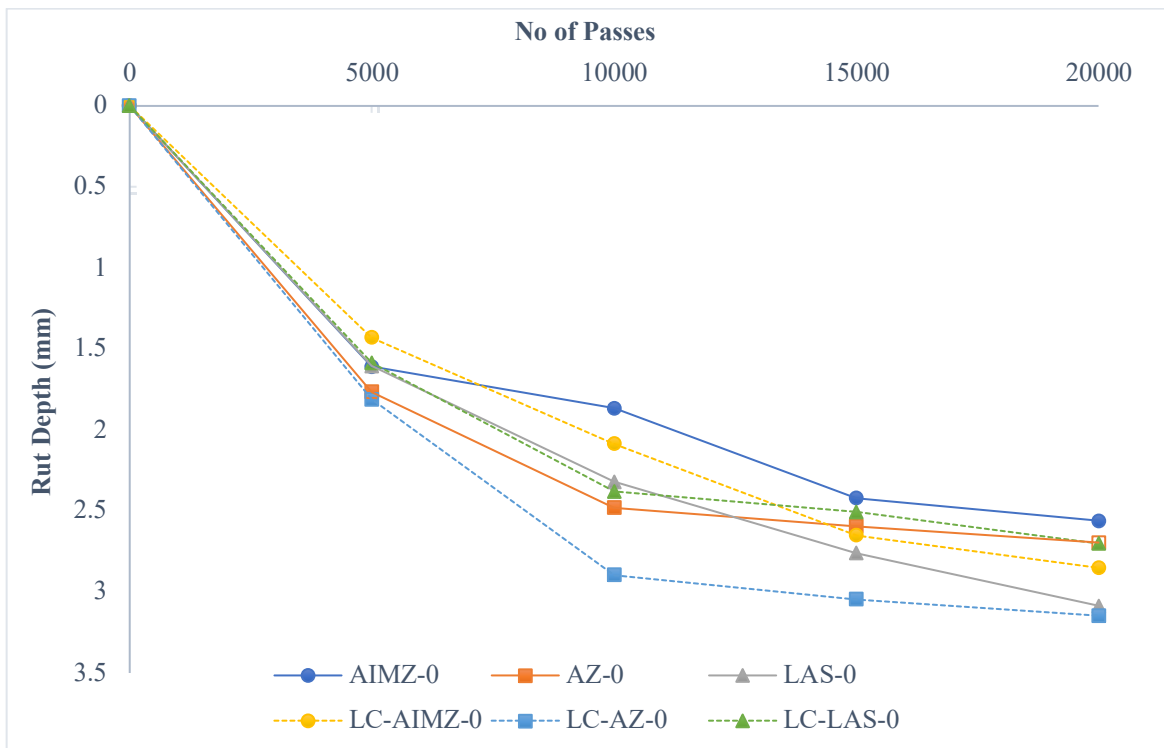
Figure 21. Rut Depth vs. No of Passes for Every Mixture at 3 Days of Aging
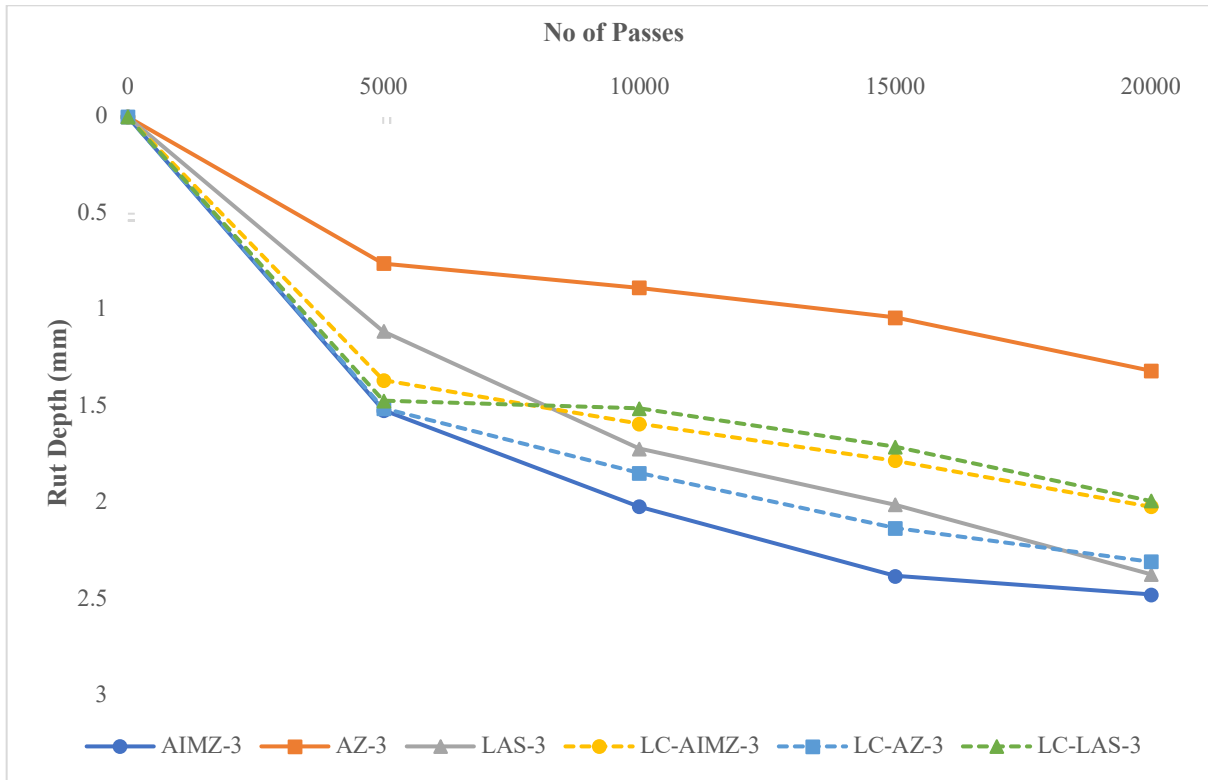
Figure 22. Rut Depth vs. No of Passes for Every Mixture at 5 Days of Aging
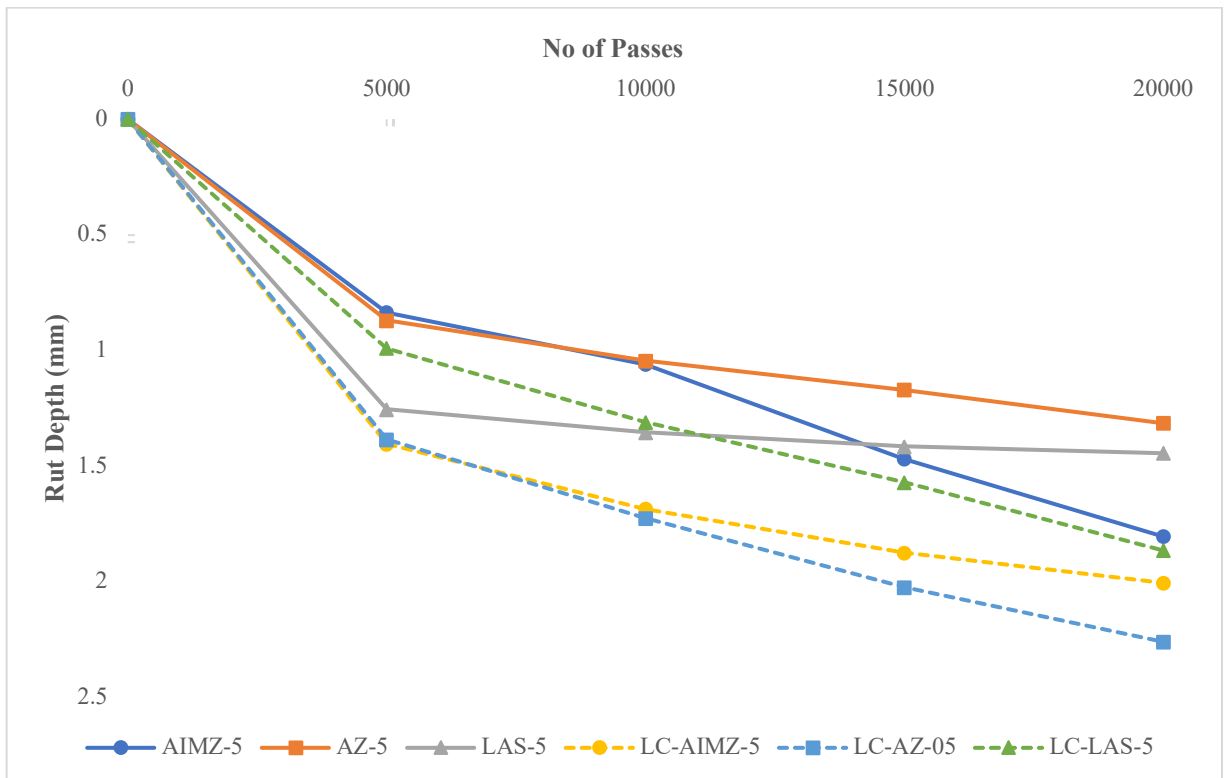
Figure 23. Rut Depth vs. No of Passes for all Mixtures at 7 Days of Aging
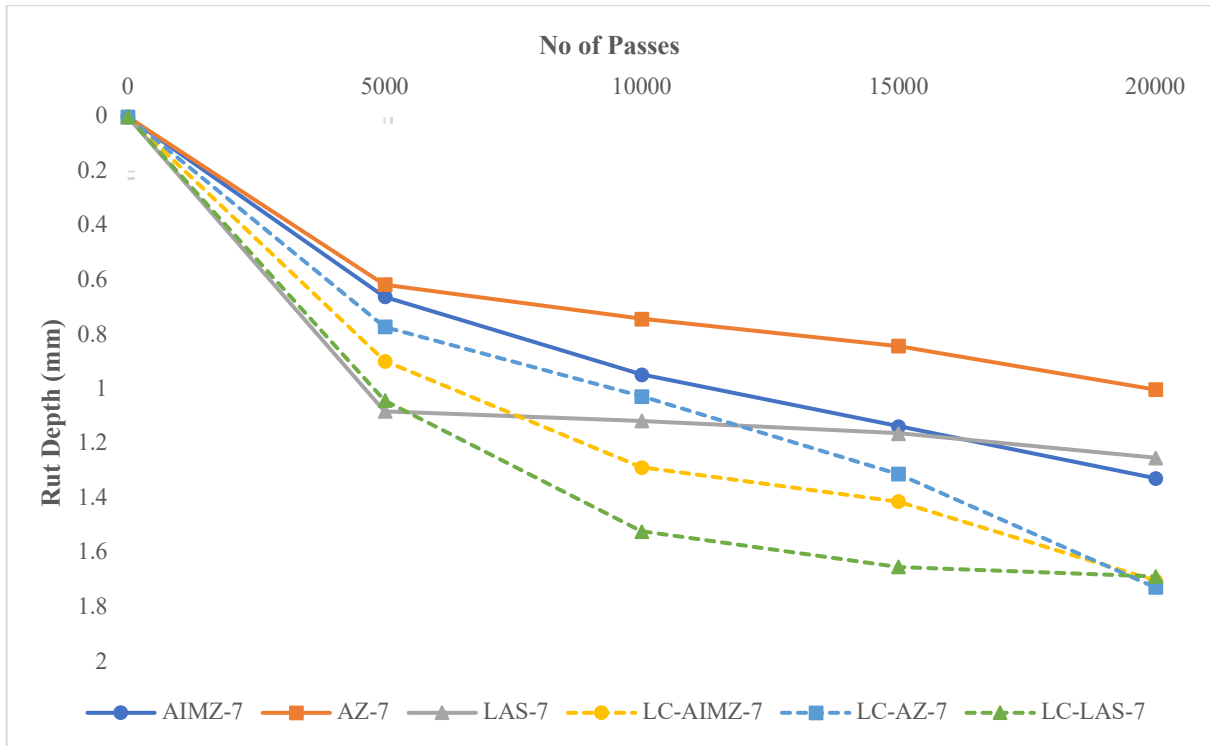
Statistical analysis was carried out using Minitab to compare the results obtained from the experiment. As we have three independent variables, such as binder type, additive, and aging level, and one dependent or response variable (i.e., rut depth), the general linear model was run. The results of the analysis of variance (ANOVA) from the general linear model provide insights into the relationship between the independent variables (binder type, additive, and aging level) and the dependent variable (rut depth). The null hypothesis (Ho) states that there is no significant effect or relationship between the independent variables and the dependent variable, while the alternative hypothesis (Ha) suggests there is a significant effect or relationship. Based on the significance level ($\alpha = 0.05$), if the p-value is less than 0.05, the null hypothesis is rejected. The rejection of the null hypothesis indicates that there is a significant effect of the independent variable on the dependent variable. The results of ANOVA from the general linear model are presented in Table 5. As the p-values for binder and additive are greater than 0.05, it indicates the effect of binder and additive type on the rut depth is insignificant. On the other hand, p-value for aging is less than 0.05, indicating aging has a significant effect on rut depth of the mixtures.

Table 5. Results of ANOVA for Rut Depth of All 24 Mixtures

Source	DF	Adj SS	Adj MS	F-Value	P-Value
Binder	1	0.7829	0.78285	1.92	0.174
Additive	2	0.17	0.08498	0.21	0.813
Aging	3	13.0625	4.35417	10.66	0.000
Error	41	16.7408	0.40831		
Lack-of-Fit	17	3.9047	0.22969	0.43	0.962
Pure Error	24	12.8362	0.53484		
Total	47	30.7561			

A comparative analysis of the additives AIMZ, AZ, and LAS for each binder at every aging level was also conducted. ANOVA was performed to determine if there are differences in the mean values of rut depth among the three mixtures for each binder at each aging level. The null and alternative hypotheses are Ho—the mean values are the same for all mixtures and there is no significant difference among them—and Ha—at least two mean values among the three mixtures differ for individual aging level. At a significance level of α = 0.05, the null hypotheses are rejected if the p-value is less than 0.05. The Tukey pairwise comparison test is used to compare the differences between each pair of means while appropriately adjusting for multiple comparisons. At a significance level of 0.05, the null hypotheses are rejected if their p-values are less than 0.05. This outcome indicates there is sufficient evidence to claim there is a significant difference in pairwise comparisons between the two mixtures.

Tables 6, 7, 8, and 9 tabulate the ANOVA results for rut depth of mixtures with conventional PG 64-16 at the without aging, 3 days, 5 days, and 7 days of aging levels, respectively. At the 3 days of aging level, with a p-value of less than 0.05, the null hypotheses are rejected. This indicates that there is a statistically significant difference between at least two mean values of rut depth among the three mixtures. At the without aging, 5, and 7 days of aging levels, no statistically significant difference is observed among the mean rut depth values for the mixtures containing conventional binder.

Table 6. Results of ANOVA for Rut Depth of Mixtures with Conventional PG 64-16 at the Without Aging Level

Source	DF	Adj SS	Adj MS	F-Value	P-Value
Factor	2	0.1156	0.05782	0.07	0.937
Error	3	2.5947	0.86488		
Total	5	2.7103			

Table 7. Results of ANOVA for Rut Depth of Mixtures with Conventional PG 64-16 at the 3 Days of Aging Level

Source	DF	Adj SS	Adj MS	F-Value	P-Value
Factor	2	2.42493	1.21247	60.83	0.004
Error	3	0.0598	0.01993		
Total	5	2.48473			

Table 8. Results of ANOVA for Rut Depth of Mixtures with Conventional PG 64-16 at the 5 Days of Aging Level

Source	DF	Adj SS	Adj MS	F-Value	P-Value
Factor	2	0.102	0.05102	0.23	0.809
Error	3	0.674	0.22468		
Total	5	0.7761			

Table 9. Results of ANOVA for Rut Depth of Mixtures with Conventional PG 64-16 at the 7 Days of Aging Level

Source	DF	Adj SS	Adj MS	F-Value	P-Value
Factor	2	0.1267	0.06335	1.1	0.438
Error	3	0.1727	0.05755		
Total	5	0.2994			

Tables 10, 11, 12, and 13 show the results derived from Tukey pairwise comparison, illustrating the differences in mean rut depth among the three mixtures with three different additives—AIMZ, AZ, and LAS—at different aging levels: without aging, 3 days, 5 days, and 7 days, respectively for conventional PG 64-16 binder. At the without aging, 5 days, and 7 days of aging levels, no significant difference in mean values is observed.

For the 3-day aging level, a significant difference in mean rut depth is observed between AZ-3 and AIMZ-3 and between LAS-3 and AZ-3. LAS-3 versus AIMZ-3 yielded a p-value greater than 0.05.

Table 10. Results of Tukey Pairwise Comparison for Rut Depth of Mixtures with Conventional PG 64-16 at the Without Aging Level

Difference of Levels	Difference of Means	SE of Difference	95% CI	T-Value	Adjusted P-Value
(AZ-0) - (AIMZ-0)	0.175	0.93	(-3.711, 4.061)	0.19	0.981
(LAS-0) - (AIMZ-0)	0.34	0.93	(-3.546, 4.226)	0.37	0.931
(LAS-0) - (AZ-0)	0.165	0.93	(-3.721, 4.051)	0.18	0.983

*Statistically significant

Table 11. Results of Tukey Pairwise Comparison for Rut Depth of Mixtures with Conventional PG 64-16 at the 3 Days of Aging Level

Difference of Levels	Difference of Means	SE of Difference	95% CI	T-Value	Adjusted P-Value
(AZ-3) - (AIMZ-3)	-1.54	0.141	(-2.130, -0.950)	-10.91	0.003*
(LAS-3) - (AIMZ-3)	-0.57	0.141	(-1.160, 0.020)	-4.04	0.055
(LAS-3) - (AZ-3)	0.97	0.141	(0.380, 1.560)	6.87	0.013*

*Statistically significant

Table 12. Results of Tukey Pairwise Comparison for Rut Depth of Mixtures with Conventional
PG 64-16 at the 5 Days of Aging Level

Difference of Levels	Difference of Means	SE of Difference	95% CI	T-Value	Adjusted P-Value
(AZ-5) - (AIMZ-5)	-0.3	0.474	(-2.281, 1.681)	-0.63	0.814
(LAS-5) - (AIMZ-5)	-0.055	0.474	(-2.036, 1.926)	-0.12	0.993
(LAS-5) - (AZ-5)	0.245	0.474	(-1.736, 2.226)	0.52	0.869

*Statistically significant

Table 13. Results of Tukey Pairwise Comparison for Rut Depth of Mixtures with Conventional
PG 64-16 at 7 Days of Aging Level

Difference of Levels	Difference of Means	SE of Difference	95% CI	T-Value	Adjusted P-Value
(AZ-7) - (AIMZ-7)	-0.295	0.24	(-1.298, 0.708)	-1.23	0.516
(LAS-7) - (AIMZ-7)	0.025	0.24	(-0.978, 1.028)	0.1	0.994
(LAS-7) - (AZ-7)	0.32	0.24	(-0.683, 1.323)	1.33	0.471

*Statistically significant

Tables 14, 15, 16, and 17 tabulate the ANOVA results for rut depth of mixtures with PG 64-16 low carbon at the without aging, 3 days, 5 days and 7 days of aging levels, respectively. At each aging level, the p-value is greater than 0.05. This indicates that no significant difference is observed among the mean rut depth results for the mixtures containing low-carbon binder. Therefore, the three additives have no significant effect on rut depth for mixtures with low-carbon binder.

Table 14. Results of ANOVA for Rut Depth of Mixtures with PG 64-16 LC at the Without
Aging Level

Source	DF	Adj SS	Adj MS	F-Value	P-Value
Factor	2	0.3124	0.1562	0.08	0.924
Error	3	5.8035	1.9345		
Total	5	6.1159			

Table 15. Results of ANOVA for Rut Depth of Mixtures with PG 64-16 LC at the 3 Days of
Aging Level

Source	DF	Adj SS	Adj MS	F-Value	P-Value
Factor	2	0.2025	0.1013	0.2	0.830
Error	3	1.534	0.5113		
Total	5	1.7365			

Table 16. Results of ANOVA for Rut Depth of Mixtures with PG 64-16 LC at the 5 Days of
Aging Level

Source	DF	Adj SS	Adj MS	F-Value	P-Value
Factor	2	0.215	0.1075	0.45	0.675
Error	3	0.7173	0.2391		
Total	5	0.9323			

Table 17. Results of ANOVA for Rut Depth of Mixtures with PG 64-16 LC at the 7 Days of
Aging Level

Source	DF	Adj SS	Adj MS	F-Value	P-Value
Factor	2	0.1221	0.06107	0.14	0.872
Error	3	1.2802	0.42673		
Total	5	1.4023			

Tables 18, 19, 20, and 21 show the results derived from Tukey pairwise comparison, illustrating the differences in mean rut depth among the three mixtures with AIMZ, AZ, and LAS, respectively, at different aging levels: without aging, 3 days, 5 days, and 7 days, respectively, for PG 64-16 LC binder. No significant differences among the different additives are observed while doing pairwise comparison at any aging level for low-carbon binder.

Table 18. Results of Tukey Pairwise Comparison for Rut Depth of Mixtures with PG 64-16 LC at the Without Aging Level

Difference of Levels	Difference of Means	SE of Difference	95% CI	T-Value	Adjusted P-Value
(LC-AZ-0) - (LC-AIMZ-0)	0.4	1.39	(-5.42, 6.21)	0.28	0.957
(LC-LAS-0) - (LC-AIMZ-0)	-0.15	1.39	(-5.96, 5.67)	-0.1	0.994
(LC-LAS-0) - (LC-AZ-0)	-0.54	1.39	(-6.35, 5.27)	-0.39	0.922

*Statistically significant

Table 19. Results of Tukey Pairwise Comparison for Rut Depth of Mixtures with PG 64-16 LC at the 3 Days of Aging Level

Difference of Levels	Difference of Means	SE of Difference	95% CI	T-Value	Adjusted P-Value
(LC-AZ-3) - (LC-AIMZ-3)	0.35	0.715	(-2.638, 3.338)	0.49	0.881
(LC-LAS-3) - (LC-AIMZ-3)	-0.07	0.715	(-3.058, 2.918)	-0.1	0.995
(LC-LAS-3) - (LC-AZ-3)	-0.42	0.715	(-3.408, 2.568)	-0.59	0.836

*Statistically significant

Table 20. Results of Tukey Pairwise Comparison for Rut Depth of Mixtures with PG 64-16 LC at the 5 Days of Aging Level

Difference of Levels	Difference of Means	SE of Difference	95% CI	T-Value	Adjusted P-Value
(LC-AZ-5) - (LC-AIMZ-5)	0.15	0.489	(-1.893, 2.193)	0.31	0.950
(LC-LAS-5) - (LC-AIMZ-5)	-0.305	0.489	(-2.348, 1.738)	-0.62	0.819
(LC-LAS-5) - (LC-AZ-5)	-0.455	0.489	(-2.498, 1.588)	-0.93	0.661

*Statistically significant

Table 21. Results of Tukey Pairwise Comparison for Rut Depth of Mixtures with PG 64-16 LC
at the 7 Days of Aging Level

Difference of Levels	Difference of Means	SE of Difference	95% CI	T-Value	Adjusted P-Value
(LC-AZ-7) - (LC-AIMZ-7)	-0.1	0.653	(-2.830, 2.630)	-0.15	0.987
(LC-LAS-7) - (LC-AIMZ-7)	0.24	0.653	(-2.490, 2.970)	0.37	0.930
(LC-LAS-7) - (LC-AZ-7)	0.34	0.653	(-2.390, 3.070)	0.52	0.867

*Statistically significant

Figures 24 and 25 depict the average number of gyrations required for compacting specimens of each mixture at various aging levels for both conventional and low-carbon binders. The required number of gyrations increased progressively with the aging level for all mixtures, aligning with the increase in binder stiffness. An exception was observed in the gyration number required between LC-AIMZ-5 and LC-AIMZ-7, as well between LC-LAS-5 and LC-LAS-7, which can be attributed to various factors intrinsic to the characteristics of the binder and aggregate, in addition to laboratory environmental condition. For both conventional and low-carbon binder, mixtures containing LAS required a higher number of gyrations compared to those containing AIMZ and AZ at the without aging level.

Another notable observation related to the conventional PG64-16 mixtures is that while the number of gyrations remained relatively consistent at the without aging, 3 days, and 5 days levels, a significant increase in the number of gyrations was observed at the 7-day aging level for all types of mixtures.

Several key observations can be made regarding the mixtures utilizing the PG64-16 LC binder. For the AIMZ samples, the number of gyrations remains steady up to 3 days of aging, with a notable increase observed at 5 days, persisting through 7 days of aging. For the AZ mixtures, the number of gyrations remains consistent up to 5 days of aging, experiencing a significant increase at 7 days. Lastly, for the LAS mixtures, a slight uptick in gyrations occurs at 3 days, followed by a marginal increase at both 5 and 7 days.

Figure 24. Average Number of Gyrations for HWT Specimens with PG 64-16
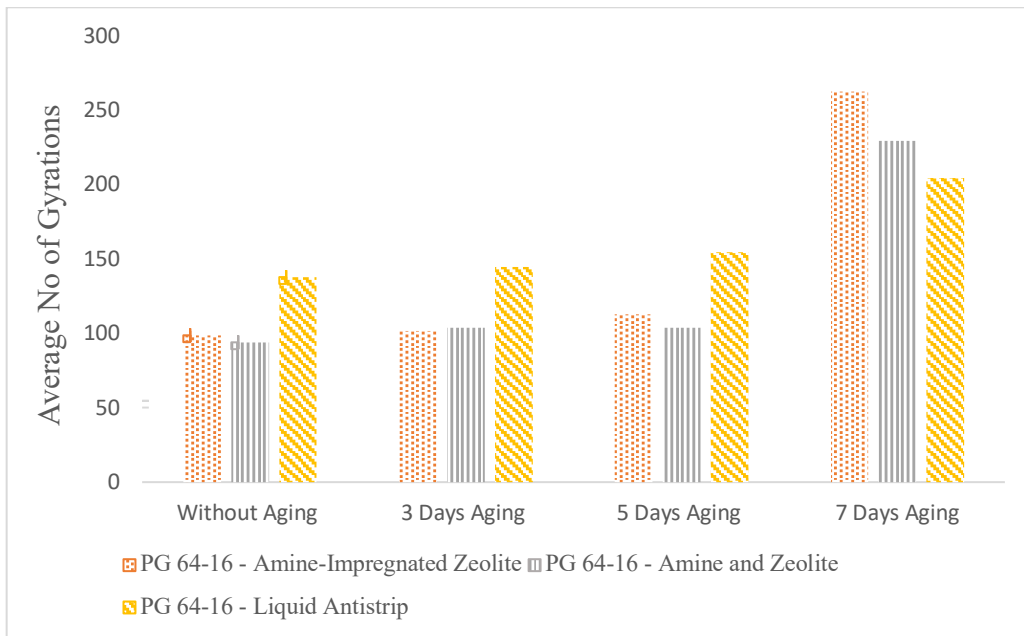
Figure 25. Average Number of Gyrations for HWT Specimens with PG 64-16 LC
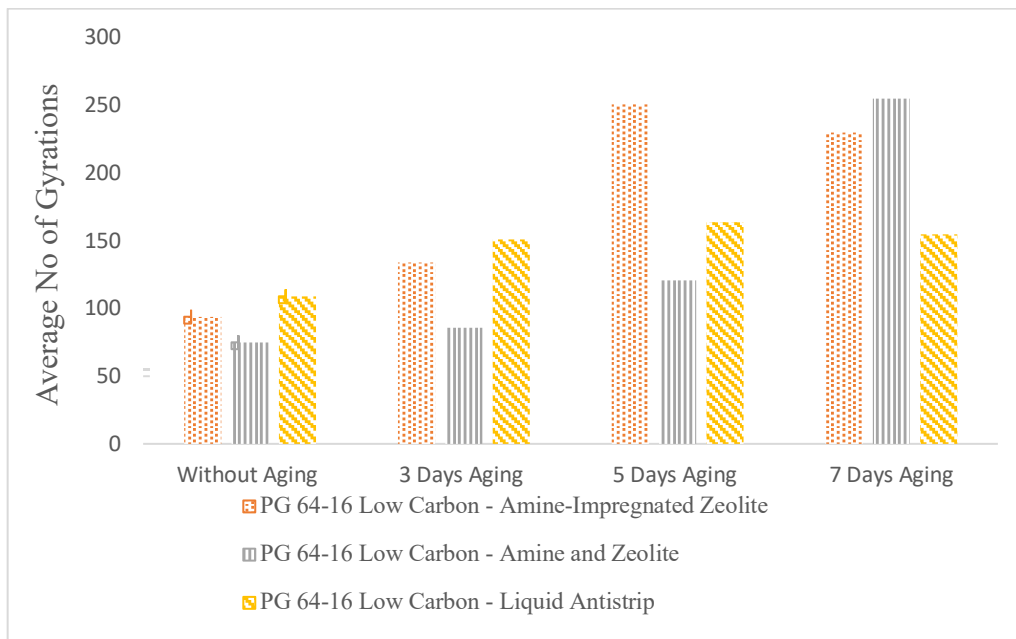
6.2 Indirect Tensile Strength Test of Dry and Moisture Conditioned Specimens

The dry and wet indirect tensile strengths along with the TSR values for each mixture at various aging levels (without aging, 3 days, 5 days, and 7 days), are presented in Tables 22, 23, 24, and 25, respectively.

Table 22. Indirect Tensile Strength and TSR for Each Mixture at Without Aging

	Sample ID	AIMZ-0	AZ-0	LAS-0	LC-AIMZ-0	LC-AZ-0	LC-LAS-0
Indirect Dry Tensile Strength (psi)	Sample 1	217.1	198.4	200.2	121.4	115.3	111.1
	Sample 2	221.4	201.6	181.4	132.6	111.3	130.4
	Sample 3	203.4	198.2	203.7	124.0	134.1	125.2
	Average	**214**	**199.4**	**195.1**	**126**	**120.2**	**122.2**
Indirect Wet Tensile Strength (psi)	Sample 1	176.4	159.7	161.5	99.3	98.7	106.3
	Sample 2	153.9	167.9	165.3	99.5	104.4	109.4
	Sample 3	147.2	172.0	162.2	95.5	115.2	107.3
	Average	**159.2**	**166.5**	**163**	**98.1**	**106.1**	**107.7**
TSR		0.74	0.84	0.84	0.78	0.88	0.88

Table 23. Indirect Tensile Strength and TSR for Each Mixture at 3 Days of Aging

	Sample ID	AIMZ-3	AZ-3	LAS-3	LC-AIMZ-3	LC-AZ-3	LC-LAS-3
Indirect Dry Tensile Strength (psi)	Sample 1	292.7	272.8	228.9	202.5	192.7	159.0
	Sample 2	267.4	261.3	283.2	151.5	171.1	153.4
	Sample 3	234.2	262.5	222.5	183.0	181.0	153.7
	Average	**264.8**	**265.5**	**244.9**	**179**	**181.6**	**155.4**
Indirect Wet Tensile Strength (psi)	Sample 1	219.3	220.6	206.4	144.0	154.3	128.9
	Sample 2	220.0	201.8	190.3	152.1	143.8	132.7
	Sample 3	242.4	210.1	187.4	145.4	160.1	132.7
	Average	**227.2**	**210.8**	**194.7**	**147.2**	**152.7**	**131.4**
TSR		0.86	0.79	0.80	0.82	0.84	0.85

Table 24. Indirect Tensile Strength and TSR for Each Mixture at 5 Days of Aging

	Sample ID	AIMZ-5	AZ-5	LAS-5	LC-AIMZ-5	LC-AZ-5	LC-LAS-5
Indirect Dry Tensile Strength (psi)	Sample 1	289.0	274.0	259.6	201.1	202.8	186.2
	Sample 2	277.6	266.1	263.4	180.3	206.4	187.4
	Sample 3	278.6	253.1	273.8	180.9	164.1	171.7
	Average	**281.7**	**264.4**	**265.6**	**187.4**	**191.1**	**181.8**
Indirect Wet Tensile Strength (psi)	Sample 1	236.7	211.7	220.0	164.9	158.6	158.2
	Sample 2	231.4	210.6	209.9	167.3	173.3	144.6
	Sample 3	243.6	217.9	202.5	174.5	160.9	150.8
	Average	**237.2**	**213.4**	**210.8**	**168.9**	**164.3**	**151.2**
TSR		0.84	0.81	0.79	0.90	0.86	0.83

Table 25. Indirect Tensile Strength and TSR for Each Mixture at 7 Days of Aging

	Sample ID	AIMZ-7	AZ-7	LAS-7	LC-AIMZ-7	LC-AZ-7	LC-LAS-7
Indirect Dry Tensile Strength (psi)	Sample 1	283.3	273.4	273.6	211.5	201.9	192.7
	Sample 2	268.9	282.5	282.3	182.8	178.3	199.3
	Sample 3	291.0	274.3	280.2	187.5	168.4	196.0
	Average	**281.1**	**276.7**	**278.7**	**193.9**	**182.9**	**196**
Indirect Wet Tensile Strength (psi)	Sample 1	239.7	212.2	235.6	170.3	162.9	156.8
	Sample 2	233.6	233.8	217.0	185.6	165.4	166.3
	Sample 3	230.0	220.7	195.0	187.6	150.8	159.6
	Average	**234.4**	**222.2**	**215.9**	**181.2**	**159.7**	**160.9**
TSR		0.83	0.80	0.77	0.93	0.87	0.82

Figures 26 and 27 show the average dry and wet tensile strength with the TSR of each mixture at varying aging levels for conventional PG 64-16 and PG 16-64 LC, respectively. Across both binder types, dry and wet indirect tensile strengths exhibit a gradual increase with aging. Specifically, at the 3-day aging level, each mixture exhibited an increase of approximately 20% to 50% in tensile strength compared to the tensile strengths observed at the without-aging level. Moreover, for wet strength, the AIMZ mixtures demonstrated the highest percentage increase, whereas the LAS mixtures exhibited the lowest percentage increase. Lastly, the highest increase in dry strength was observed in the AZ mixes for both conventional and LC binders, while the highest increase in wet strength occurred in the AIMZ mixtures with both conventional and LC binders.

The increase in tensile strength from 3-day to 5-day aging levels and from 5-day to 7-day aging levels shows a comparatively smaller increase than the jump from the without-aging to 3-day aging levels. Specifically, the dry and wet tensile strengths at the 5-day aging level for each mixture increased approximately 0% to 15% compared to the tensile strengths at the 3-day aging level. Similarly, at the 7-day aging level, the dry and wet strengths for each mixture increased by approximately 0% to 8% compared to the tensile strength at the 5-day aging level.

There is a significant difference in the dry and wet tensile strength between mixtures utilizing conventional PG 64-16 and those utilizing PG 64-16 LC. Specifically, the dry tensile strength for PG 64-16 LC mixtures is approximately 30% to 40% lower than that of conventional PG 64-16 mixtures across all aging levels. Similarly, the wet tensile strength for PG 64-16 LC mixtures is approximately 30% to 40% lower at the without aging and 3-day aging levels, and 20% to 30% lower at the 5-day and 7-day aging levels, compared to conventional PG 64-16 mixtures. The variation in tensile strengths with aging and different binders is visually apparent, as illustrated in **Figure 28**. Mixtures with conventional PG 64-16 show more breakage in aggregate particles after being tested than mixtures with PG 64-16 LC. This indicates that mixtures with higher tensile strength tend to experience more aggregate particle breakage during testing. This trend persists with aging where the number of broken aggregate particles increase at the 7-day aging level compared to the without-aging level.

When comparing different additives, it is observed that at the without aging level, mixtures with AIMZ have lower wet tensile strength compared to mixtures with LAS for both binders, although the difference is not significant. However, this scenario shifts at the 3, 5, and 7 days of aging levels, where mixtures containing AIMZ have higher wet tensile strength than mixtures with LAS.

Figure 26. Average Dry and Wet Indirect Tensile Strength for Mixtures with PG 64-16
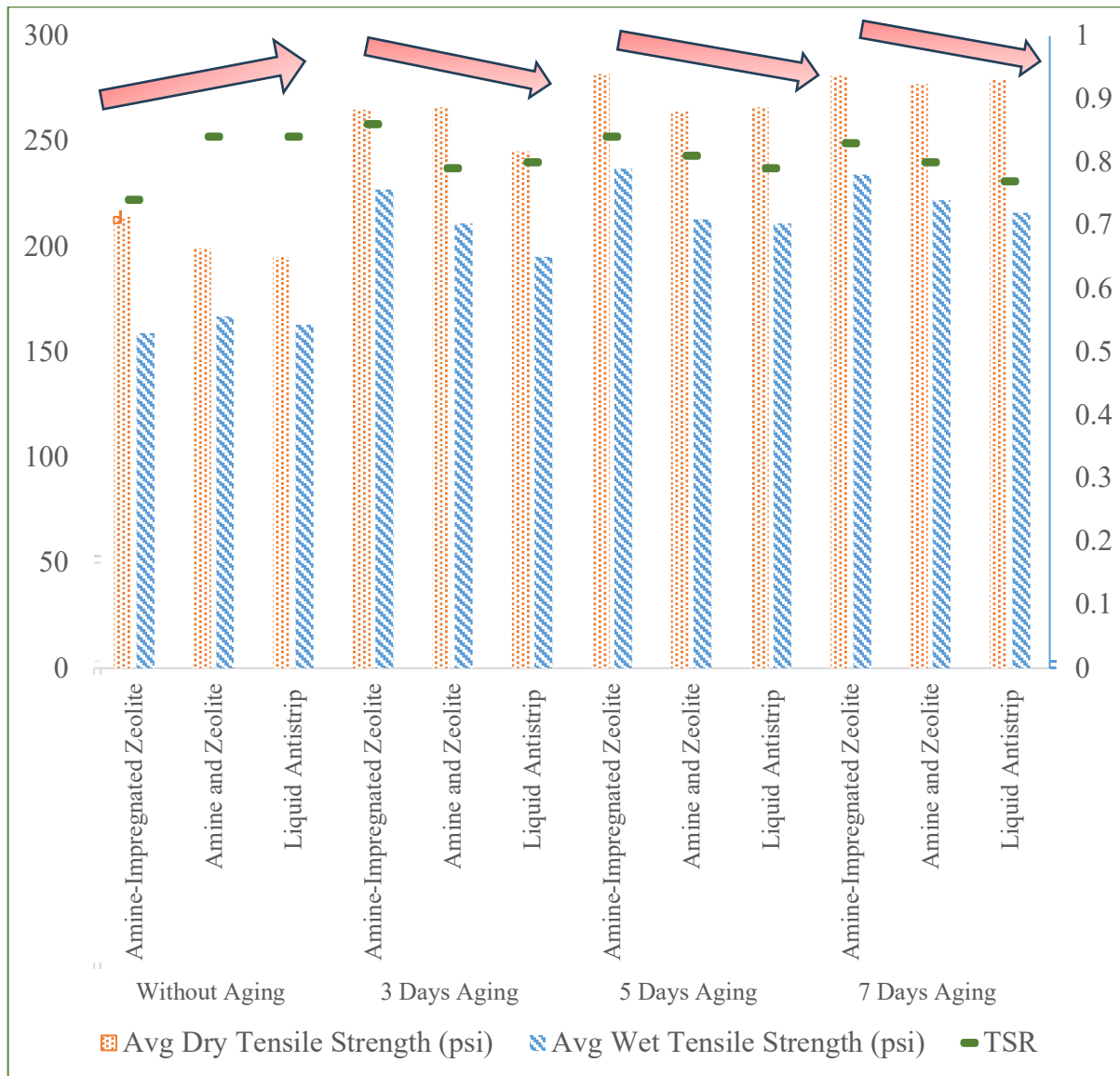
Figure 27. Average Dry and Wet Indirect Tensile Strength for Mixtures with PG 64-16 LC
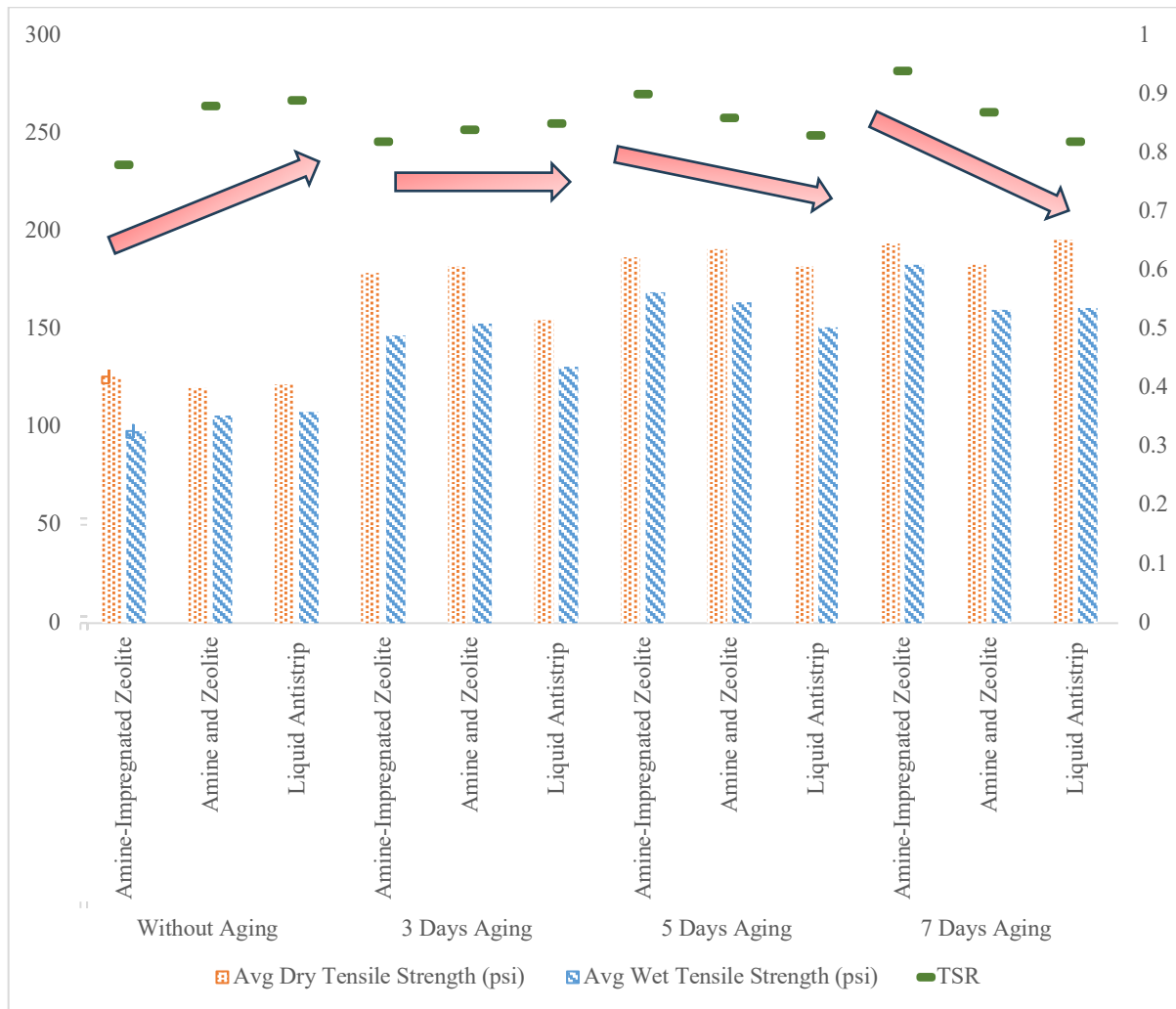
Figure 28. ITS Specimens after Breaking—(a) AIMZ-0, (b) LC-AIMZ-0, (c) AIMZ-7, and (d) LC-AIMZ-7
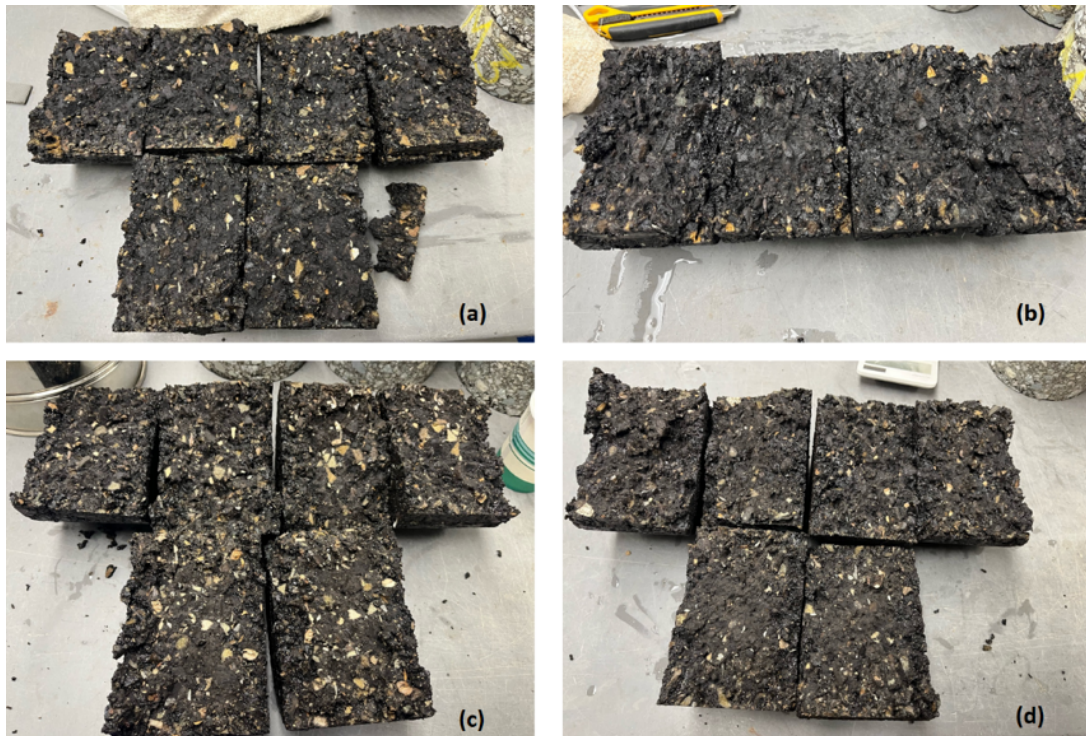
Figures 29 and 30 show the changes of TSR with aging levels for conventional and low-carbon binder, respectively. It's worth noting that the minimum TSR requirement for Superpave mix design stands at 0.80, while for Standard Specifications of Caltrans, the minimum requirement is 0.70.

For mixtures incorporating conventional PG 64-16, at the without-aging level, the TSR for AIMZ-0 measures 0.74, which is below the 0.80 threshold. Conversely, TSR values for AZ-0 and LAS-0 exceed 0.80. Therefore, all mixtures meet the Standard Specification of Caltrans requirement at the without-aging level, but AIMZ-0 fails to meet the Superpave Specifications. The lower TSR for AIMZ-0 can be attributed to the early-stage entrapment of amine molecules within the zeolite pores, restricting their ability to resist moisture damage. However, in the case of AZ-0 and LAS-0, amines are readily available, resulting in a higher TSR.

The dynamics shift at the 3-day aging level. TSR for AIMZ increased from 0.74 to 0.86, while TSR for AZ decreased from 0.84 to 0.79 and TSR for LAS decreased from 0.84 TO 0.80. This decline in TSR is attributable to the thermal degradation of amines. However, as aging progresses, AIMZ is hypothesized to release amines, enhancing its ability to resist moisture damage and resulting in an increase in TSR. For the 5- and 7-day aging levels, the TSR for AIMZ and LAS gradually decreased, whereas the TSR for AZ remained nearly unchanged. The nearly constant TSR for AZ across the aging levels can be attributed to amines sometimes becoming self-impregnated by zeolite when mixed with the binder, shielding some amine molecules from

thermal degradation within zeolite shells. AIMZ consistently demonstrated higher TSR values than both AZ and LAS at 3, 5, and 7 days of aging. At the 7-day aging level, while TSR for LAS dips to 0.77 (below 0.80), TSR for AIMZ remained at 0.83 (above 0.80).

A similar trend emerges for mixtures utilizing PG 64-16 LC. The TSR for LC-AIMZ gradually increased from 0.78 at the without aging level to 0.93 at the 7-day aging level, reflecting the gradual release of amine molecules from zeolite pores during aging. Conversely, The TSR for LC-LAS steadily declined from 0.89 at the without aging level to 0.82 at the 7-day aging level, attributable to the thermal degradation of LAS during aging. Notably, the TSR for LC-AZ remained relatively consistent across all aging levels, a phenomenon possibly linked to the self-impregnation of amine by zeolites. It's worth noting that similar to AIMZ-0, the TSR for LC-AIMZ-0 also failed to meet Superpave design criteria.

Figure 29. TSR vs. Level of Aging for Mixtures with PG 64-16
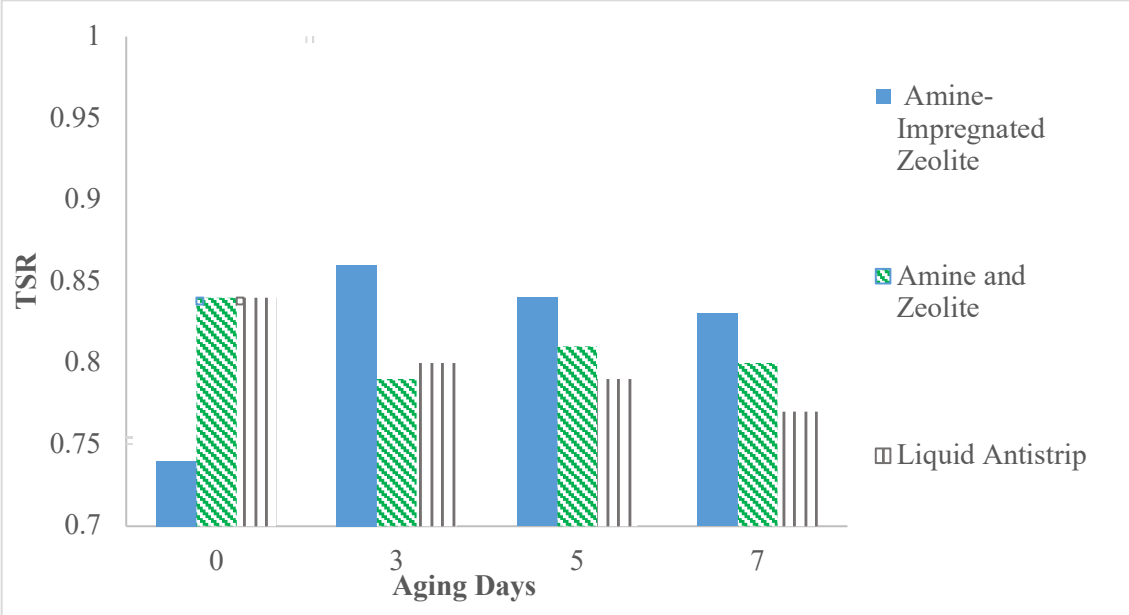
Figure 30. TSR vs. Level of Aging for Mixtures with PG 64-16 LC
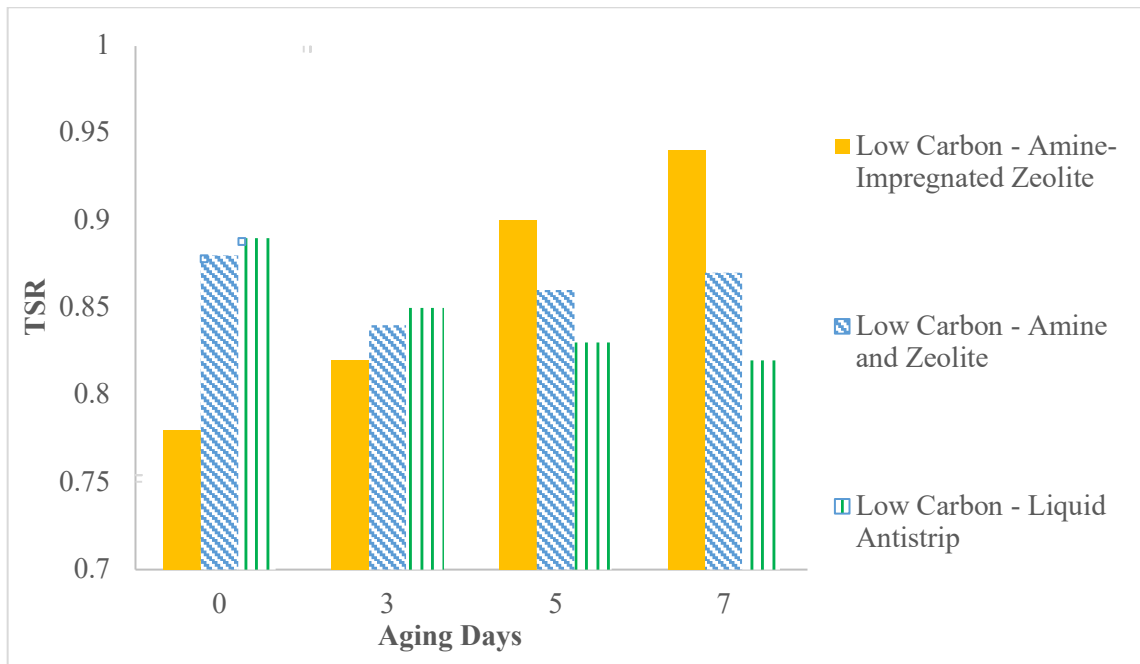
The effect of different factors on the wet tensile strength of the mixtures is an important thing to consider. As we have three independent variables—binder type, additive, and aging level—and one dependent or response variable—wet tensile strength—the general linear model was run which provides insights into the relationship between the independent variables (binder type, additive, and aging level) and the dependent variable (wet tensile strength). The null hypothesis (H0) states that there is no significant effect or relationship between the independent variables (binder type, additive, and aging level) and the dependent variable (wet tensile strength), while the alternative hypothesis (Ha) suggests that there is a significant effect or relationship. The results of ANOVA from the general linear model are presented in Table 26. As the p-values for all the three variables are 0.000; this indicates that binder type, additive, and aging have significant effects on wet tensile strength.

Table 26. Results of ANOVA for Wet Tensile Strength of All 24 Mixtures

Source	DF	Adj SS	Adj MS	F-Value	P-Value
Binder	1	65903	65902.7	609.14	0.000
Additive	2	2604	1301.9	12.03	0.000
Aging	3	43493	14497.7	134	0.000
Error	65	7032	108.2		
Lack-of-Fit	17	3419	201.1	2.67	0.004
Pure Error	48	3614	75.3		
Total	71	119032			

Again, doing a pairwise comparison of the wet tensile strengths among the additives AIMZ, AZ, and LAS, was required for each binder at each aging level. ANOVA was performed to determine if there are differences in the mean values of wet tensile strength among the three mixtures for each binder at each aging level. The null and alternative hypotheses are H0—the mean values are the same for all mixtures—and Ha—at least two mean values among the three mixtures differ for individual aging level. The Tukey pairwise comparison test is used to compare the differences between each pair of means while appropriately adjusting for multiple comparisons.

Tables 27, 28, 29, and 30 tabulate the ANOVA results for wet tensile strength of mixtures with conventional PG 64-16 at the without-aging, 3-day, 5-day, and 7-day aging levels, respectively. At 3 days and 5 days of aging, p-values are less than 0.05. Therefore, the null hypotheses are rejected. This indicates that there is a statistically significant difference between at least two mean values of wet tensile strength among the three mixtures (AIMZ, AZ, and LA). At without aging and 7 days of aging, no statistically significant difference is observed among the mean wet tensile strength values for the mixtures containing conventional binder.

Table 27. Results of ANOVA for Wet Tensile Strength of Mixtures with Conventional PG 64-16 at the Without-Aging Level

Source	DF	Adj SS	Adj MS	F-Value	P-Value
Factor	2	81.45	40.72	0.44	0.663
Error	6	554.55	92.43		
Total	8	636			

Table 28. Results of ANOVA for Wet Tensile Strength of Mixtures with Conventional PG 64-16 at the 3 Days of Aging Level

Source	DF	Adj SS	Adj MS	F-Value	P-Value
Factor	2	1587.7	793.8	6.5	0.031
Error	6	732.4	122.1		
Total	8	2320			

Table 29. Results of ANOVA for Wet Tensile Strength of Mixtures with Conventional PG 64-16 at the 5 Days of Aging Level

Source	DF	Adj SS	Adj MS	F-Value	P-Value
Additive	2	1273.5	636.75	14.68	0.005
Error	6	260.2	43.36		
Total	8	1533.7			

Table 30. Results of ANOVA for Wet Tensile Strength of Mixtures with Conventional PG 64-16 at the 7 Days of Aging Level

Source	DF	Adj SS	Adj MS	F-Value	P-Value
Factor	2	534.1	267	1.44	0.308
Error	6	1111	185.2		
Total	8	1645.1			

Tables 31, 32, 33, and 34 show the results derived from Tukey pairwise comparison, illustrating the differences in mean wet tensile strength among the three mixtures with three different additives at different aging levels: without aging, 3 days, 5 days, and 7 days, respectively, for conventional PG 64-16 binder. At the without aging level and 7 days of aging level, no significant difference in mean values is observed.

For the 3-day aging level, the significant difference in mean wet tensile strength is observed between LAS-3 and AIMZ-3. At the 5 days of aging level, AIMZ-5 shows a significant difference in mean tensile strength when compared to AZ-5 and LAS-5.

Table 31. Results of Tukey Pairwise Comparison for Wet Tensile Strength of Mixtures with Conventional PG 64-16 at the Without Aging Level

Difference of Levels	Difference of Means	SE of Difference	95% CI	T-Value	Adjusted P-Value
(AZ-0) - (AIMZ-0)	7.37	7.85	(-16.72, 31.46)	0.94	0.638
(LAS-0) - (AIMZ-0)	3.83	7.85	(-20.26, 27.92)	0.49	0.879
(LAS-0) - (AZ-0)	-3.53	7.85	(-27.62, 20.56)	-0.45	0.896

*Statistically significant

Table 32. Results of Tukey Pairwise Comparison for Wet Tensile Strength of Mixtures with Conventional PG 64-16 at the 3 Days of Aging Level

Difference of Levels	Difference of Means	SE of Difference	95% CI	T-Value	Adjusted P-Value
(AZ-3) - (AIMZ-3)	-16.4	9.02	(-44.08, 11.28)	-1.82	0.242
(LAS-3) - (AIMZ-3)	-32.53	9.02	(-60.22, -4.85)	-3.61	0.026*
(LAS-3) - (AZ-3)	-16.13	9.02	(-43.82, 11.55)	-1.79	0.251

*Statistically significant

Table 33. Results of Tukey Pairwise Comparison for Wet Tensile Strength of Mixtures with Conventional PG 64-16 at the 5 Days of Aging Level

Difference of Levels	Difference of Means	SE of Difference	95% CI	T-Value	Adjusted P-Value
(AZ-5) - (AIMZ-5)	-23.83	5.38	(-40.33, -7.33)	-4.43	0.01*
(LAS-5) - (AIMZ-5)	-26.43	5.38	(-42.93, -9.93)	-4.92	0.006*
(LAS-5) - (AZ-5)	-2.6	5.38	(-19.10, 13.90)	-0.48	0.881

*Statistically significant

Table 34. Results of Tukey Pairwise Comparison for Wet Tensile Strength of Mixtures with
Conventional PG 64-16 at the 7 Days of Aging Level

Difference of Levels	Difference of Means	SE of Difference	95% CI	T-Value	Adjusted P-Value
(AZ-7) - (AIMZ-7)	-12.2	11.1	(-46.3, 21.9)	-1.1	0.549
(LAS-7) - (AIMZ-7)	-18.6	11.1	(-52.7, 15.5)	-1.67	0.29
(LAS-7) - (AZ-7)	-6.4	11.1	(-40.5, 27.7)	-0.57	0.839

*Statistically significant

Tables 35, 36, 37, and 38 tabulate the ANOVA results for wet tensile strength of mixtures with PG 64-16 low carbon at without aging and 3 days, 5 days, and 7 days of aging levels, respectively. At the without-aging level, the p-value is 0.122, indicating there is no significant difference among the mean wet tensile strength of mixtures with low-carbon binder at without aging level. However, at the 3 days, 5 days, and 7 days of aging levels, there is a significant difference between at least two mean values as the p-values are less than 0.05 at each level.

Table 35. Results of ANOVA for Wet Tensile Strength of Mixtures with PG 64-16 LC at the
Without-Aging Level

Source	DF	Adj SS	Adj MS	F-Value	P-Value
Factor	2	158	78.99	3.05	0.122
Error	6	155.6	25.94		
Total	8	313.6			

Table 36. Results of ANOVA for Wet Tensile Strength of Mixtures with PG 64-16 LC at the
3 Days of Aging Level

Source	DF	Adj SS	Adj MS	F-Value	P-Value
Factor	2	732.2	366.11	11.96	0.008
Error	6	183.6	30.61		
Total	8	915.9			

Table 37. Results of ANOVA for Wet Tensile Strength of Mixtures with PG 64-16 LC at the 5 Days of Aging Level

Source	DF	Adj SS	Adj MS	F-Value	P-Value
Factor	2	505.5	252.75	5.67	0.041
Error	6	267.7	44.61		
Total	8	773.2			

Table 38. Results of ANOVA for Wet Tensile Strength of Mixtures with PG 64-16 LC at the 7 Days of Aging Level

Source	DF	Adj SS	Adj MS	F-Value	P-Value
Factor	2	873	436.5	7.51	0.023
Error	6	348.7	58.12		
Total	8	1221.7			

Tables 39, 40, 41, and 42 show the results derived from Tukey pairwise comparison, illustrating the differences in mean wet tensile strength among the three mixtures with three different additives at different aging levels: without aging, 3 days, 5 days, and 7 days, respectively, for PG 64-16 low carbon binder. No significant difference among AIMZ, AZ, and LAS are observed while doing pairwise comparison at the without aging level for low-carbon binder. At the 3 days of aging level, LC-LAS-3 versus LC-AIMZ-3 and LC-LAS-3 versus LC-AZ-3 indicate a significant difference in mean wet tensile strength. At the 5 days of aging level, a significant difference is observed between LC-LAS-5 and LC-AIMZ-5. At the 7 days of aging level, LC-AIMZ-7 indicates a significant difference in mean when compared with LC-LAS-7 and LC-AZ-7.

Table 39. Results of Tukey Pairwise Comparison for Wet Tensile Strength of Mixtures with PG 64-16 LC at the Without-Aging Level

Difference of Levels	Difference of Means	SE of Difference	95% CI	T-Value	Adjusted P-Value
(LC–AZ-0) - (LC–AIMZ-0)	8	4.16	(-4.76, 20.76)	1.92	0.212
(LC–LAS-0) - (LC–AIMZ-0)	9.57	4.16	(-3.19, 22.33)	2.3	0.132
(LC–LAS-0) - (LC–AZ-0)	1.57	4.16	(-11.19, 14.33)	0.38	0.926

*Statistically significant

Table 40. Results of Tukey Pairwise Comparison for Wet Tensile Strength of Mixtures with PG 64-16 LC at the 3 Days of Aging Level

Difference of Levels	Difference of Means	SE of Difference	95% CI	T-Value	Adjusted P-Value
(LC-AZ-3) - (LC-AIMZ-3)	5.57	4.52	(-8.30, 19.43)	1.23	0.479
(LC-LAS-3) - (LC-AIMZ-3)	-15.73	4.52	(-29.60, -1.87)	-3.48	0.03*
(LC-LAS-3) - (LC-AZ-3)	-21.3	4.52	(-35.16, -7.44)	-4.72	0.008*

*Statistically significant

Table 41. Results of Tukey Pairwise Comparison for Wet Tensile Strength of Mixtures with PG 64-16 LC at the 5 Days of Aging Level

Difference of Levels	Difference of Means	SE of Difference	95% CI	T-Value	Adjusted P-Value
(LC-AZ-5) - (LC-AIMZ-5)	-4.63	5.45	(-21.37, 12.10)	-0.85	0.689
(LC-LAS-5) - (LC-AIMZ-5)	-17.7	5.45	(-34.44, -0.96)	-3.25	0.04*
(LC-LAS-5) - (LC-AZ-5)	-13.07	5.45	(-29.80, 3.67)	-2.4	0.117

*Statistically significant

Table 42. Results of Tukey Pairwise Comparison for Wet Tensile Strength of Mixtures with PG 64-16 LC at the 7 Days of Aging Level

Difference of Levels	Difference of Means	SE of Difference	95% CI	T-Value	Adjusted P-Value
(LC-AZ-7) - (LC-AIMZ-7)	-21.47	6.22	(-40.57, -2.36)	-3.45	0.032*
(LC-LAS-7) - (LC-AIMZ-7)	-20.27	6.22	(-39.37, -1.16)	-3.26	0.04*
(LC-LAS-7) - (LC-AZ-7)	1.2	6.22	(-17.90, 20.30)	0.19	0.98

*Statistically significant

A similar analysis was done for dry tensile strength to check the effect of variables on the dry tensile strength and to do a pairwise comparison among the mixtures at each aging level for each binder. The results of ANOVA from the general linear model for the dry tensile strength of all 24 mixtures is presented in Table 43. As the p-values for all the three variables are less than 0.05, this indicates binder type, additive, and aging have a significant effect on the dry tensile strength.

Table 43. Results of ANOVA for Dry Tensile Strength of All 24 Mixtures

Source	DF	Adj SS	Adj MS	F-Value	P-Value
Binder	1	128609	128609	671.3	0.000
Additive	2	1462	731	3.81	0.027
Aging	3	57958	19319	100.84	0.000
Error	65	12453	192		
Lack-of-Fit	17	2437	143	0.69	0.799
Pure Error	48	10015	209		
Total	71	200481			

Tables 44, 45, 46, and 47 tabulate results from ANOVA for dry tensile strength of mixtures with conventional PG 64-16 at without aging and 3 days, 5 days, and 7 days of aging level, respectively. P-values are greater than 0.05 for each case, indicating there is no effect of different types of additives on mixtures with conventional PG 64-16 at any aging level.

Table 44. Results of ANOVA for Dry Tensile Strength of Mixtures with Conventional PG 64-16 at the Without-Aging Level

Source	DF	Adj SS	Adj MS	F-Value	P-Value
Factor	2	586.6	293.31	3.73	0.089
Error	6	471.7	78.61		
Total	8	1058.3			

Table 45. Results of ANOVA for Dry Tensile Strength of Mixtures with Conventional PG 64-16 at the 3 Days of Aging Level

Source	DF	Adj SS	Adj MS	F-Value	P-Value
Factor	2	823.7	411.9	0.61	0.572
Error	6	4026.1	671		
Total	8	4849.8			

Table 46. Results of ANOVA for Dry Tensile Strength of Mixtures with Conventional PG 64-16 at the 5 Days of Aging Level

Source	DF	Adj SS	Adj MS	F-Value	P-Value
Factor	2	562.2	281.08	4.11	0.075
Error	6	410.5	68.42		
Total	8	972.7			

Table 47. Results of ANOVA for Dry Tensile Strength of Mixtures with Conventional PG 64-16 at the 7 Days of Aging Level

Source	DF	Adj SS	Adj MS	F-Value	P-Value
Factor	2	28.25	14.12	0.25	0.789
Error	6	343.19	57.2		
Total	8	371.44			

Tables 48, 49, 50, and 51 show the result from Tukey pairwise comparisons for dry tensile strength of mixtures with conventional binder at the without aging and 3 days, 5 days, and 7 days of aging levels, respectively. It can be noticed that the p-values for each pairwise comparison at each aging level are greater than 0.05, indicating there are no significant differences among the mean dry tensile strength of mixtures with conventional binder.

Table 48. Results of Tukey Pairwise Comparison for Dry Tensile Strength of Mixtures with Conventional PG 64-16 at the Without-Aging Level

Difference of Levels	Difference of Means	SE of Difference	95% CI	T-Value	Adjusted P-Value
(AZ-0) - (AIMZ-0)	-14.57	7.24	(-36.78, 7.65)	-2.01	0.19
(LAS-0) - (AIMZ-0)	-18.87	7.24	(-41.08, 3.35)	-2.61	0.089
(LAS-0) - (AZ-0)	-4.3	7.24	(-26.52, 17.92)	-0.59	0.828

*Statistically significant

Table 49. Results of Tukey Pairwise Comparison for Dry Tensile Strength of Mixtures with Conventional PG 64-16 at the 3 Days of Aging Level

Difference of Levels	Difference of Means	SE of Difference	95% CI	T-Value	Adjusted P-Value
(AZ-3) - (AIMZ-3)	0.8	21.2	(-64.1, 65.7)	0.04	0.999
(LAS-3) - (AIMZ-3)	-19.9	21.2	(-84.8, 45.0)	-0.94	0.637
(LAS-3) - (AZ-3)	-20.7	21.2	(-85.6, 44.2)	-0.98	0.616

*Statistically significant

Table 50. Results of Tukey Pairwise Comparison for Dry Tensile Strength of Mixtures with Conventional PG 64-16 at the 5 Days of Aging Level

Difference of Levels	Difference of Means	SE of Difference	95% CI	T-Value	Adjusted P-Value
(AZ-5) - (AIMZ-5)	-17.33	6.75	(-38.06, 3.39)	-2.57	0.094
(LAS-5) - (AIMZ-5)	-16.13	6.75	(-36.86, 4.59)	-2.39	0.118
(LAS-5) - (AZ-5)	1.2	6.75	(-19.53, 21.93)	0.18	0.983

*Statistically significant

Table 51. Results of Tukey Pairwise Comparison for Dry Tensile Strength of Mixtures with
Conventional PG 64-16 at the 7 Days of Aging Level

Difference of Levels	Difference of Means	SE of Difference	95% CI	T-Value	Adjusted P-Value
(AZ-7) - (AIMZ-7)	-4.33	6.18	(-23.28, 14.62)	-0.7	0.771
(LAS-7) - (AIMZ-7)	-2.37	6.18	(-21.32, 16.58)	-0.38	0.923
(LAS-7) - (AZ-7)	1.97	6.18	(-16.98, 20.92)	0.32	0.946

*Statistically significant

Tables 51, 52, 53, and 54 present the results of ANOVA, indicating that there is no significant difference among the mean values for dry tensile strength of mixtures with low-carbon binder at aging levels of 0 days, 3 days, 5 days, and 7 days, as the p-value is greater than 0.05.

Table 52. Results of ANOVA for Dry Tensile Strength of Mixtures with PG 64-16 LC at the
Without-Aging Level

Source	DF	Adj SS	Adj MS	F-Value	P-Value
Factor	2	51.44	25.72	0.27	0.77
Error	6	564.59	94.1		
Total	8	616.04			

Table 53. Results of ANOVA for Dry Tensile Strength of Mixtures with PG 64-16 LC at the
3 Days of Aging Level

Source	DF	Adj SS	Adj MS	F-Value	P-Value
Factor	2	1253	626.7	2.38	0.173
Error	6	1578	263		
Total	8	2832			

Table 54. Results of ANOVA for Dry Tensile Strength of Mixtures with PG 64-16 LC at the 5 Days of Aging Level

Source	DF	Adj SS	Adj MS	F-Value	P-Value
Factor	2	132.7	66.33	0.26	0.780
Error	6	1533.1	255.51		
Total	8	1665.7			

Table 55. Results of ANOVA for Dry Tensile Strength of Mixtures with PG 64-16 LC at the 7 Days of Aging Level

Source	DF	Adj SS	Adj MS	F-Value	P-Value
Factor	2	299.2	149.6	0.82	0.482
Error	6	1088.1	181.4		
Total	8	1387.3			

Tables 56, 57, 58, and 59 show the p-values from Tukey pairwise comparison for dry tensile strength of mixtures with low-carbon binder at the without aging and the 3 days, 5 days, and 7 days of aging levels, respectively. As p-value is greater than 0.05 at each case, no significant difference is observed due to the additive types in case of dry tensile strength of mixtures with PG 64-16 LC.

Table 56. Results of Tukey Pairwise Comparison for Dry Tensile Strength of Mixtures with PG 64-16 LC at the Without-Aging Level

Difference of Levels	Difference of Means	SE of Difference	95% CI	T-Value	Adjusted P-Value
(LC–AZ–0) - (LC–AIMZ–0)	-5.77	7.92	(-30.07, 18.54)	-0.73	0.757
(LC–LAS–0) - (LC–AIMZ–0)	-3.77	7.92	(-28.07, 20.54)	-0.48	0.885
(LC–LAS–0) - (LC–AZ–0)	2	7.92	(-22.31, 26.31)	0.25	0.966

*Statistically significant

Table 57. Results of Tukey Pairwise Comparison for Dry Tensile Strength of Mixtures with PG 64-16 LC at the 3 Days of Aging Level

Difference of Levels	Difference of Means	SE of Difference	95% CI	T-Value	Adjusted P-Value
(LC-AZ-3) - (LC-AIMZ-3)	2.6	13.2	(–38.0, 43.2)	0.2	0.979
(LC-LAS-3) - (LC-AIMZ-3)	-23.6	13.2	(–64.3, 17.0)	-1.78	0.252
(LC-LAS-3) - (LC-AZ-3)	-26.2	13.2	(–66.9, 14.4)	-1.98	0.198

*Statistically significant

Table 58. Results of Tukey Pairwise Comparison for Dry Tensile Strength of Mixtures with PG 64-16 LC at the 5 Days of Aging Level

Difference of Levels	Difference of Means	SE of Difference	95% CI	T-Value	Adjusted P-Value
(LC-AZ-5) - (LC-AIMZ-5)	3.7	13.1	(–36.4, 43.7)	0.28	0.958
(LC-LAS-5) - (LC-AIMZ-5)	-5.7	13.1	(–45.7, 34.4)	-0.43	0.903
(LC-LAS-5) - (LC-AZ-5)	-9.3	13.1	(–49.4, 30.7)	-0.72	0.764

*Statistically significant

Table 59. Results of Tukey Pairwise Comparison for Dry Tensile Strength of Mixtures with PG 64-16 LC at the 7 Days of Aging Level

Difference of Levels	Difference of Means	SE of Difference	95% CI	T-Value	Adjusted P-Value
(LC-AZ-7) - (LC-AIMZ-7)	-11.1	11	(–44.8, 22.7)	-1.01	0.600
(LC-LAS-7) - (LC-AIMZ-7)	2.1	11	(–31.7, 35.8)	0.19	0.981
(LC-LAS-7) - (LC-AZ-7)	13.1	11	(–20.6, 46.9)	1.19	0.498

*Statistically significant

Figures 31 and 32 show the required number of gyrations for compacting TSR specimens for conventional and low-carbon binders, respectively. At each aging level, the number of gyrations for TSR specimens ranged between 40 and 60, differing from compacting requirements for HWT specimens. The only exception was observed for AIMZ-0 and AIMZ-7. Notably, the thickness of TSR specimens, at 95 mm, is greater than that of HWT specimens (60.8 mm). So, the required number of gyrations was highly affected for smaller specimens due to aging effects. Conversely, aging did not influence the number of gyrations required for compaction for specimens with greater thickness. Moreover, no significant difference in the number of gyrations was observed among different additives, thus precluding any definitive conclusion regarding workability from compacting TSR specimens.

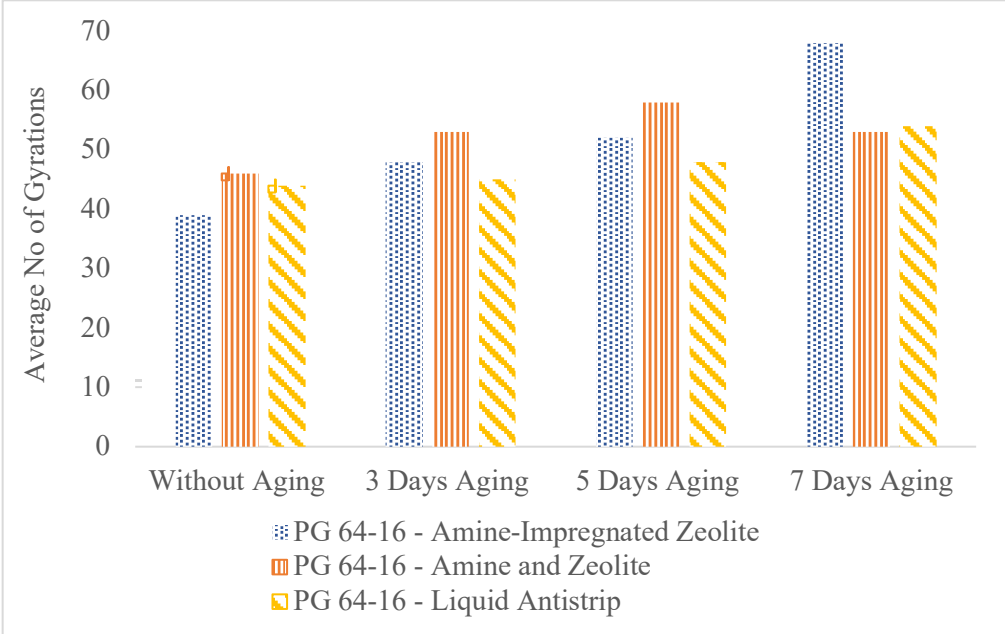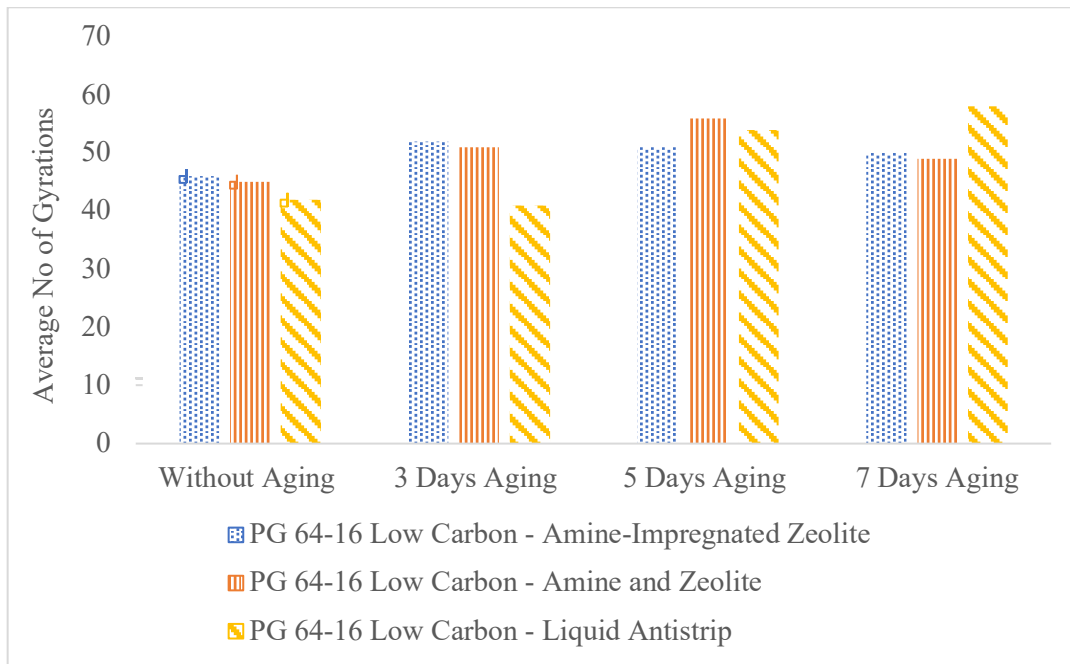Figure 31. Average Number of Gyrations for ITS Specimens with PG 64-16

Figure 32. Average Number of Gyrations for ITS Specimens with PG 64-16 LC

6.3 IDEAL Cracking Test

The CTindex along with other parameters for each mixture at the without aging and the 3 days, 5 days, and 7 days of aging levels are detailed in Tables 60, 61, 62, and 63, respectively. Higher CTindex indicates a better resistance to cracking.

Table 60. IDEAL CT Results for Each Mixture at the Without-Aging Level

Sample ID	Sample	Peak Load (kN)	l_{75} (mm)	$|m_{75}|$ (N/m)	W_f(J)	G_f (J/m²)	CT_{index}
AIMZ-0	1	16.81	6.00	5123124.85	96.22	10346.50	80.78
	2	16.19	5.93	3996479.77	85.68	9212.59	91.11
	3	17.05	5.39	4073047.10	79.44	8541.90	75.36
	Average	**16.68**	**5.77**	**4397550.57**	**87.11**	**9367.00**	**82.42**
AZ-0	1	13.73	7.01	3176227.03	100.43	10798.99	158.97
	2	14.21	5.99	3460833.36	93.11	10011.86	115.60
	3	14.81	6.59	3362894.88	102.25	10994.80	143.53
	Average	**14.25**	**6.53**	**3333318.42**	**98.60**	**10601.89**	**139.37**
LAS-0	1	14.33	5.75	3573394.39	83.18	8943.91	95.91
	2	14.89	7.20	3339035.42	97.41	10473.78	150.46
	3	13.21	7.56	3293193.61	100.41	10796.42	165.17
	Average	**14.14**	**6.83**	**3401874.47**	**93.66**	**10071.37**	**137.18**
LC-AIMZ-0	1	10.47	4.74	3234000.94	54.44	5854.05	57.24
	2	8.52	4.37	2699516.36	39.69	4267.66	46.07
	3	8.45	5.30	2268795.36	43.15	4640.23	72.24
	Average	**9.15**	**4.80**	**2734104.22**	**45.76**	**4920.65**	**58.51**
LC-AZ-0	1	9.27	4.82	2730584.76	45.44	4886.02	57.44
	2	9.54	4.92	3224078.89	48.47	5211.53	52.98
	3	10.52	5.20	3021082.80	51.74	5563.45	63.84
	Average	**9.78**	**4.98**	**2991915.49**	**48.55**	**5220.33**	**58.09**
LC-LAS-0	1	10.00	4.91	3641714.21	44.10	4741.91	42.66
	2	8.84	4.87	2429467.02	46.55	5005.16	66.84
	3	9.53	4.47	2591688.09	46.53	5003.59	57.56
	Average	**9.46**	**4.75**	**2887623.11**	**45.73**	**4916.89**	**55.68**

Table 61. IDEAL CT Results for Each Mixture at the 3 Days of Aging Level

Sample ID	Sample	Peak Load (kN)	l_{75} (mm)	$\|m_{75}\|$ (N/m)	W_f(J)	G_f (J/m²)	CT_{index}
AIMZ-3	1	21.57	10.70	14952431.75	87.30	9387.44	44.79
	2	22.16	6.34	9287015.79	115.13	12379.52	56.30
	3	22.64	4.42	7633788.60	80.62	8669.11	33.48
	Average	**22.12**	**7.15**	**10624412.05**	**94.35**	**10145.36**	**44.86**
AZ-3	1	23.17	4.28	11434084.31	81.86	8802.15	21.96
	2	21.92	4.58	12684885.28	89.59	9632.97	23.20
	3	22.68	4.14	12353414.05	85.43	9186.14	20.52
	Average	**22.59**	**4.33**	**12157461.21**	**85.63**	**9207.09**	**21.89**
LAS-3	1	22.46	5.04	11865623.05	102.77	11050.55	31.29
	2	20.00	5.03	11130387.43	94.71	10183.98	30.68
	3	22.14	4.83	16137566.05	102.82	11055.49	22.04
	Average	**21.53**	**4.97**	**13044525.51**	**100.10**	**10763.34**	**28.00**
LC-AIMZ-3	1	12.39	3.44	5250660.89	43.12	4636.07	20.26
	2	12.80	4.18	5298674.61	46.43	4992.96	26.25
	3	13.45	4.60	5752893.50	60.72	6528.59	34.77
	Average	**12.88**	**4.07**	**5434076.33**	**50.09**	**5385.87**	**27.09**
LC-AZ-3	1	11.81	3.96	4278284.15	46.99	5052.16	31.20
	2	12.61	4.12	6491346.69	51.41	5527.59	23.39
	3	12.34	4.07	5186598.13	50.02	5378.13	28.16
	Average	**12.25**	**4.05**	**5318742.99**	**49.47**	**5319.29**	**27.58**
LC-LAS-3	1	13.36	4.27	5116957.50	51.59	5547.58	30.84
	2	12.35	4.09	7086750.65	48.71	5237.33	20.14
	3	13.39	4.47	6343550.35	66.33	7132.75	33.51
	Average	**13.03**	**4.27**	**6182419.50**	**55.54**	**5972.55**	**28.16**

Table 62. IDEAL CT Results for Each Mixture at the 5 Days of Aging Level

Sample ID	Sample	Peak Load (kN)	l_{75} (mm)	$|m_{75}|$ (N/m)	W_f(J)	G_f (J/m²)	CT_{index}
AIMZ-5	1	19.88	5.10	14989797.43	66.63	7164.04	16.26
	2	19.23	3.97	14319936.51	70.39	7568.64	13.98
	3	20.70	4.70	14223441.79	78.62	8453.36	18.62
	Average	**19.94**	**4.59**	**14511058.58**	**71.88**	**7728.68**	**16.29**
AZ-5	1	20.39	4.13	22262069.04	70.35	7564.92	9.35
	2	20.50	4.50	19824790.81	59.80	6430.07	9.73
	3	17.79	4.80	22598498.79	79.60	8559.09	12.13
	Average	**19.56**	**4.48**	**21561786.22**	**69.92**	**7518.03**	**10.40**
LAS-5	1	21.68	4.55	18942734.84	79.04	8498.44	13.62
	2	23.60	4.31	20430318.23	80.56	8662.59	12.20
	3	21.54	4.67	19086417.29	85.42	9184.74	14.98
	Average	**22.27**	**4.51**	**19486490.12**	**81.67**	**8781.92**	**13.60**
LC-AIMZ-5	1	18.49	3.25	5393258.02	49.80	5354.48	21.53
	2	15.30	5.83	13064108.78	91.64	9853.28	29.33
	3	18.10	7.83	11718133.36	48.85	5253.22	23.42
	Average	**17.30**	**5.64**	**10058500.06**	**63.43**	**6820.32**	**24.76**
LC-AZ-5	1	18.27	4.62	11562154.02	69.29	7450.03	19.84
	2	13.90	4.45	9191582.69	57.35	6166.78	19.89
	3	17.04	4.19	8886567.58	63.74	6853.87	21.57
	Average	**16.40**	**4.42**	**9880101.43**	**63.46**	**6823.56**	**20.43**
LC-LAS-5	1	16.93	4.97	11849052.27	74.83	8046.62	22.49
	2	17.43	4.60	10534694.68	67.47	7254.75	21.13
	3	17.75	3.94	8869558.22	72.07	7749.45	22.93
	Average	**17.37**	**4.50**	**10417768.39**	**71.46**	**7683.61**	**22.19**

Table 63. IDEAL CT Results for Each Mixture at the 7 Days of Aging Level

Sample ID	Sample	Peak Load (kN)	l_{75} (mm)	$|m_{75}|$ (N/m)	W_f(J)	G_f (J/m²)	CT_{index}
AIMZ-7	1	27.32	4.33	50849913.16	104.29	11213.54	6.36
	2	27.46	3.43	43390819.7	69.28	7449.06	3.92
	3	28.46	3.06	41070336.01	72.08	7750.98	3.85
	Average	**27.75**	**3.60**	**45103689.62**	**81.88**	**8804.52**	**4.71**
AZ-7	1	26.45	3.54	44750234.21	70.53	7583.67	4.00
	2	23.52	4.25	37429256.55	79.21	8517.53	6.45
	3	26.97	3.57	31709850.1	86.25	9273.66	6.96
	Average	**25.65**	**3.79**	**37963113.62**	**78.66**	**8458.28**	**5.80**
LAS-7	1	26.70	3.44	75991015.1	69.90	7516.52	2.27
	2	27.00	5.26	84157906.76	89.19	9590.17	4.00
	3	29.17	4.37	103505560	88.72	9539.30	2.68
	Average	**27.62**	**4.36**	**87884827.3**	**82.60**	**8881.99**	**2.98**
LC-AIMZ-7	1	15.40	4.09	10971725.65	68.20	7333.66	18.22
	2	15.70	4.74	8762310.223	55.85	6005.54	21.67
	3	16.67	3.76	9115747.907	62.51	6721.53	18.47
	Average	**15.92**	**4.20**	**9616594.592**	**62.19**	**6686.91**	**19.45**
LC-AZ-7	1	16.55	4.24	9296970.273	52.19	5611.53	17.04
	2	15.10	4.05	7329942.837	47.24	5079.14	18.73
	3	13.16	3.19	8238209.269	46.55	5005.55	12.91
	Average	**14.94**	**3.83**	**8288374.126**	**48.66**	**5232.07**	**16.23**
LC-LAS-7	1	17.10	3.53	11777521.45	53.18	5718.75	11.44
	2	16.43	4.85	14165325.26	62.63	6734.25	15.37
	3	16.83	4.38	14115096.71	62.79	6752.02	13.98
	Average	**16.79**	**4.26**	**13352647.81**	**59.54**	**6401.68**	**13.60**

Figures 33 and 34 show the CTindex for different additives at various aging levels for mixtures with conventional PG 64-16 and PG 64-16 LC, respectively. For all mixtures, CTindex gradually decreased with aging, indicating a decrease in cracking resistance. For conventional PG 64-16, there was a sharp decrease of 80% to 85% in CTindex from the without-aging level to the 3 days of aging level for mixtures containing AZ and LAS. Conversely, mixtures containing AIMZ showed only a 46% decrease in CTindex from the without-aging level to the 3 days of aging level. From the 3 to 5 days of aging level, mixtures containing AZ and LAS underwent a decrease of approximately 50%, and mixtures containing AIMZ underwent a decrease of 64% in CTindex. From the 5 to 7 days of aging level, mixtures containing AIMZ and LAS decreased approximately 70% to 80%; however, mixtures containing AZ underwent a decrease of 44% only in CTindex. For PG 64-16 LC, from the without-aging level to the 3 days of aging level, the CTindex values decreased about 50% to 55% for all mixtures. From the 3 to 5 days of aging level, LC-IMZ had only a 9% decrease; however, LC-AZ and LC-LAS underwent a nearly 20% to 30% decrease in CTindex. From 5 to 7 days of aging level, both LC-AIMZ and LC-AZ had a 21% decrease, and LC-LAS had a 39% decrease in CTindex.

For mixtures with conventional PG 64-16, at the without-aging level, AIMZ-0 showed a lower CT_{index} compared to AZ-0 and LAS-0. However, at 3 and 5 days of aging, mixtures containing AIMZ exhibited higher cracking resistance than those containing AZ and LAS. At the 7 days of aging level, AIMZ-7 had higher CT_{index} than LAS-7, but lower CT_{index} than AZ-7. Nevertheless, the differences in CT_{index} at 7 days of aging level were negligible. For mixtures with PG 64-16 LC, LC-AIMZ showed higher cracking resistance than LC-AZ and LC-LAS at the without-aging level and the 5 and 7 days of aging levels. However, at the 3 days of aging level, LC-AIMZ had lower CT_{index} than LC-AZ and LC-LAS, though these differences were negligible.

When comparing two binders at the without aging level, mixtures with conventional binder had higher cracking resistance than mixtures with low-carbon binder. At the 3 days of aging level, both binders had nearly similar cracking resistance, with the exception of AIMZ-3. At the 5 and 7 days of aging levels, mixtures containing PG 64-16 LC exhibited better results than mixtures containing conventional binder.

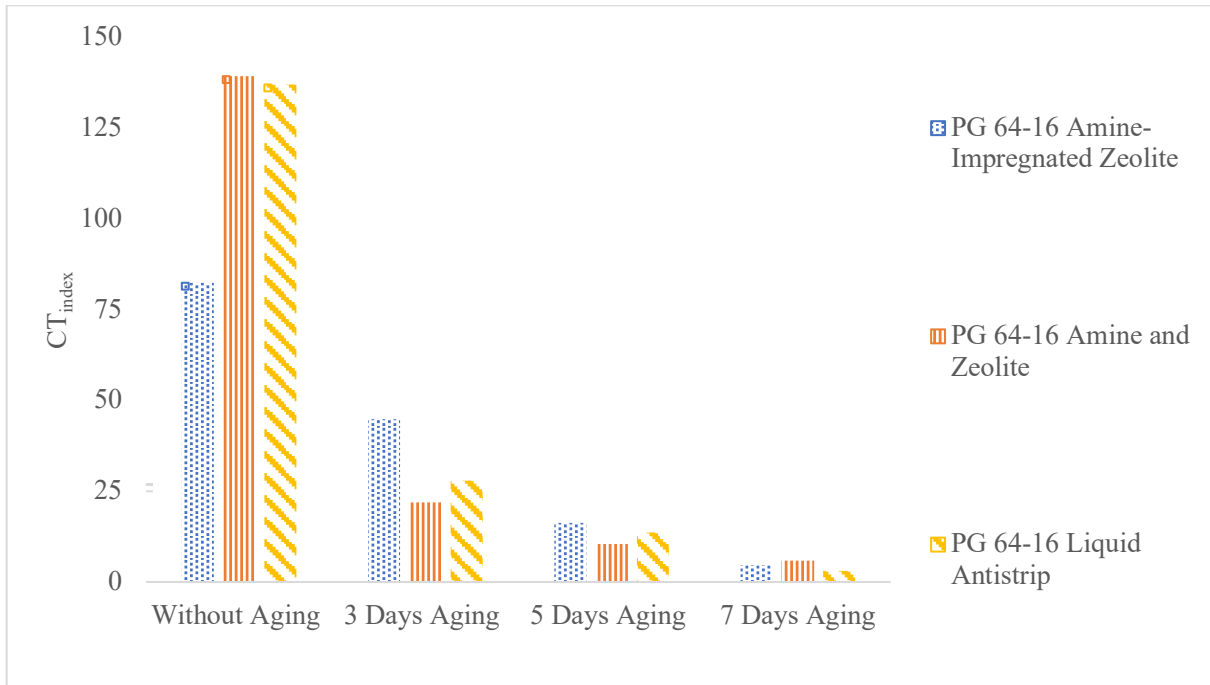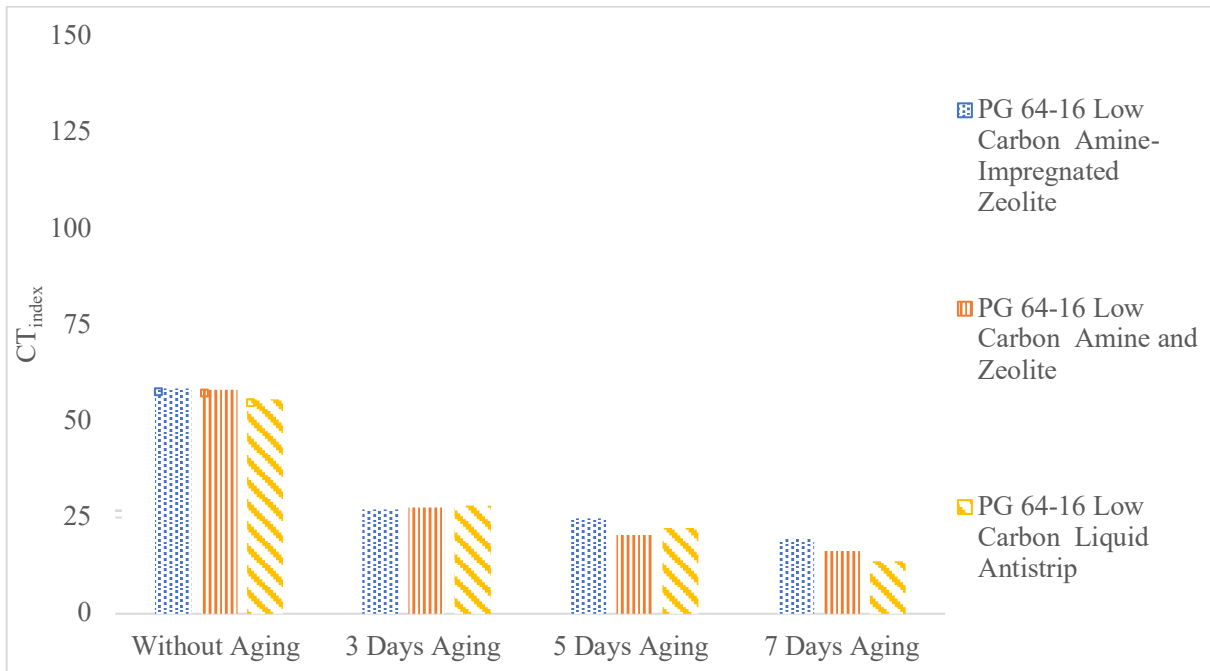Figure 33. CT$_{index}$ for Mixtures with conventional PG 64-16

Figure 34. CT$_{index}$ for Mixtures with PG 64-16 LC

Figures 35, 36, 37, and 38 show the load vs. deformation curves for all mixtures with conventional PG 64-16 at the without-aging level and the 3 days, 5 days, and 7 days of aging levels, respectively. Similarly, Figures 39, 40, 41, and 42 show the load verses deformation curves for all mixtures with PG 64-16 LC at the without-aging level and the 3 days, 5 days, and 7 days of aging levels, respectively. The curve shows that mixtures containing conventional binder gradually became brittle with increasing aging levels as the post-peak slope got steeper with aging. However, mixtures containing the low-carbon binder showed little difference in load verses deformation behavior with aging. The post peak slope is flatter for low-carbon binder than conventional binder at 3 days, 5 days, and 7 days of aging.

Figure 35. Load vs. Deformation Curves for Mixtures with Conventional PG 64-16 at the Without-Aging Level

Figure 36. Load vs. Deformation Curves for Mixtures with Conventional PG 64-16
at the 3 Days of Aging Level

Figure 37. Load vs. Deformation Curves for Mixtures with Conventional PG 64-16
at the 5 Days of Aging Level

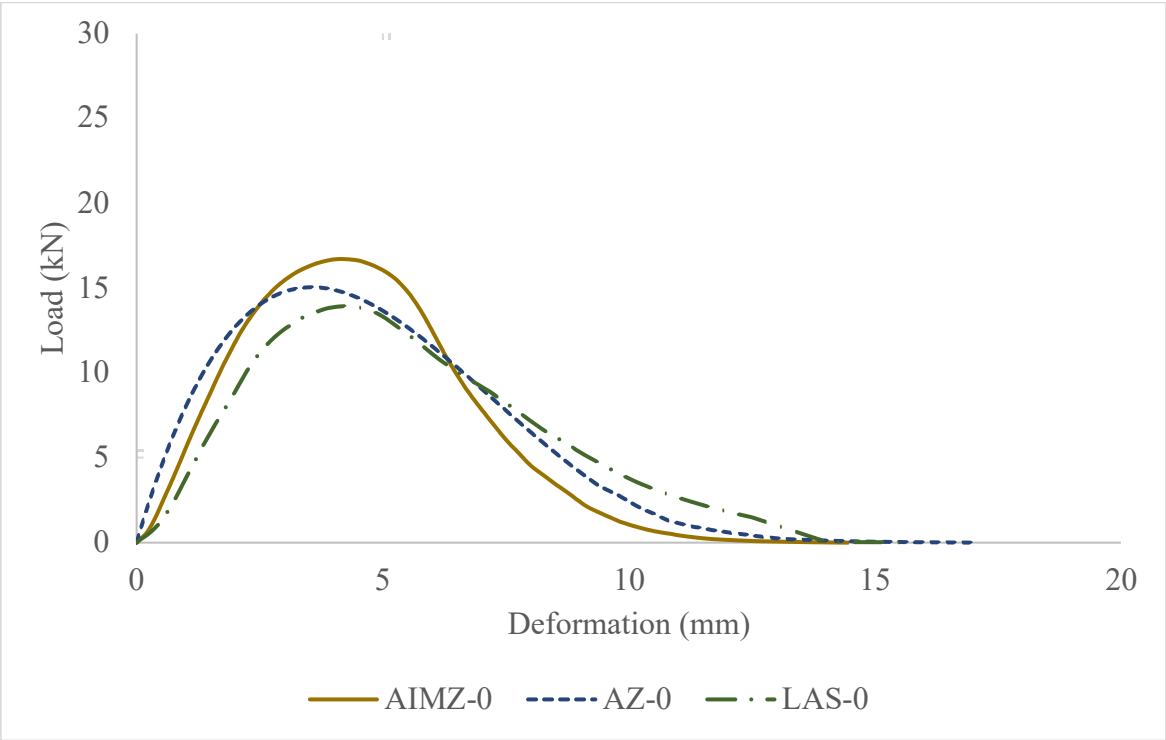Figure 38. Load vs. Deformation Curves for Mixtures with Conventional PG 64-16 at the 7
Days of Aging Level

Figure 39. Load vs. Deformation Curves for Mixtures with PG 64-16 LC
at the Without-Aging Level
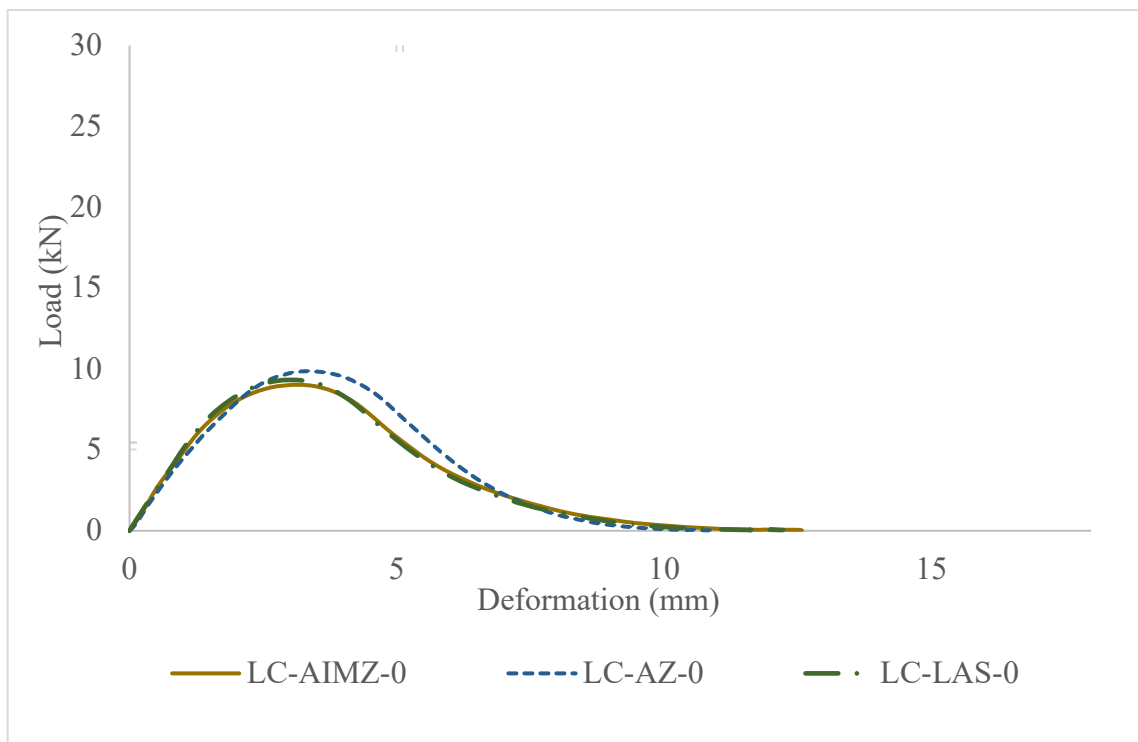
Figure 40. Load vs. Deformation Curves for Mixtures with PG 64-16 LC at the
3 Days of Aging Level

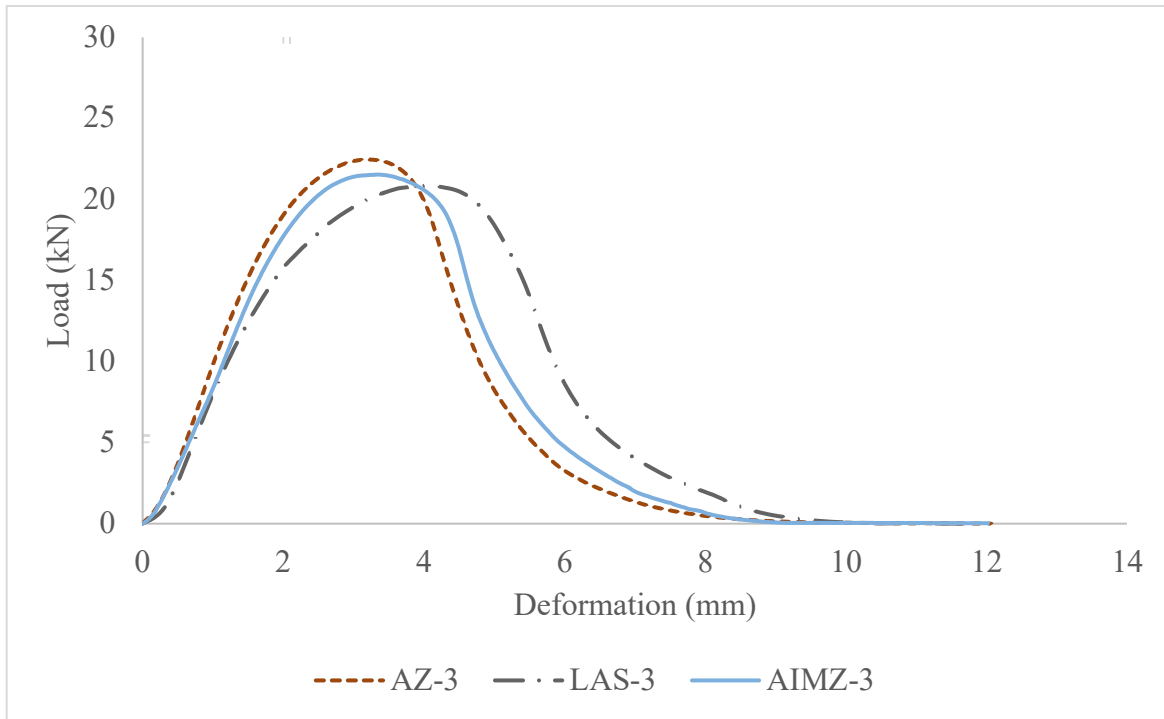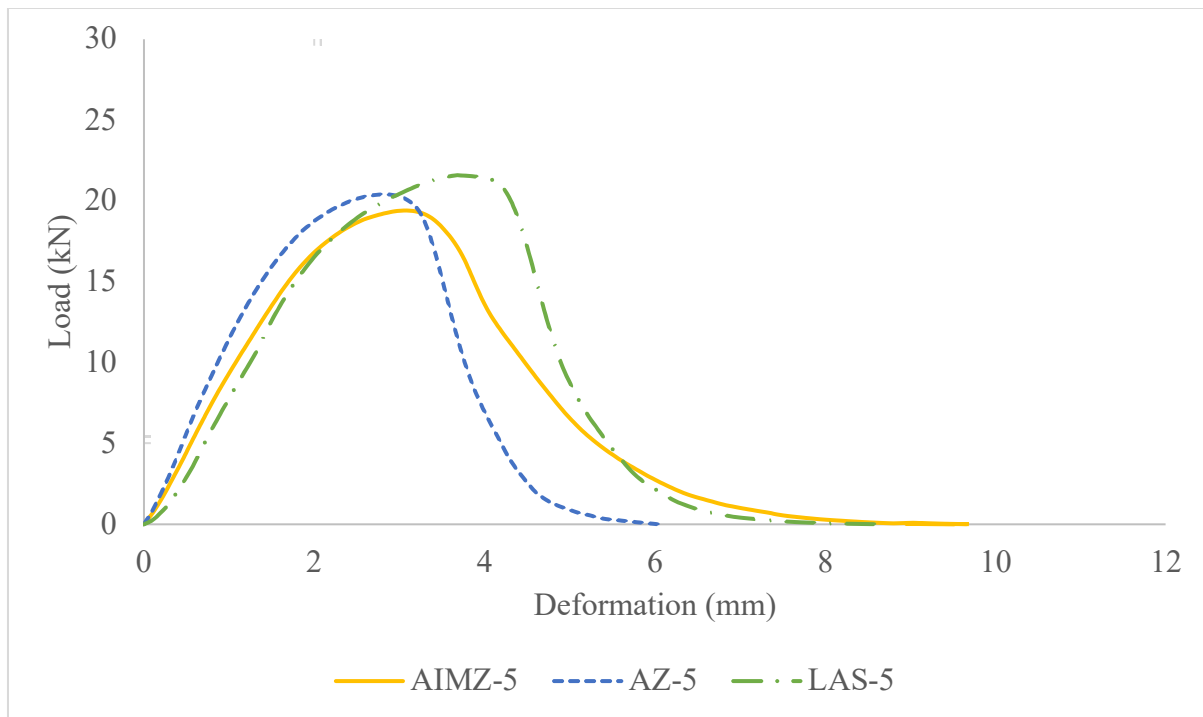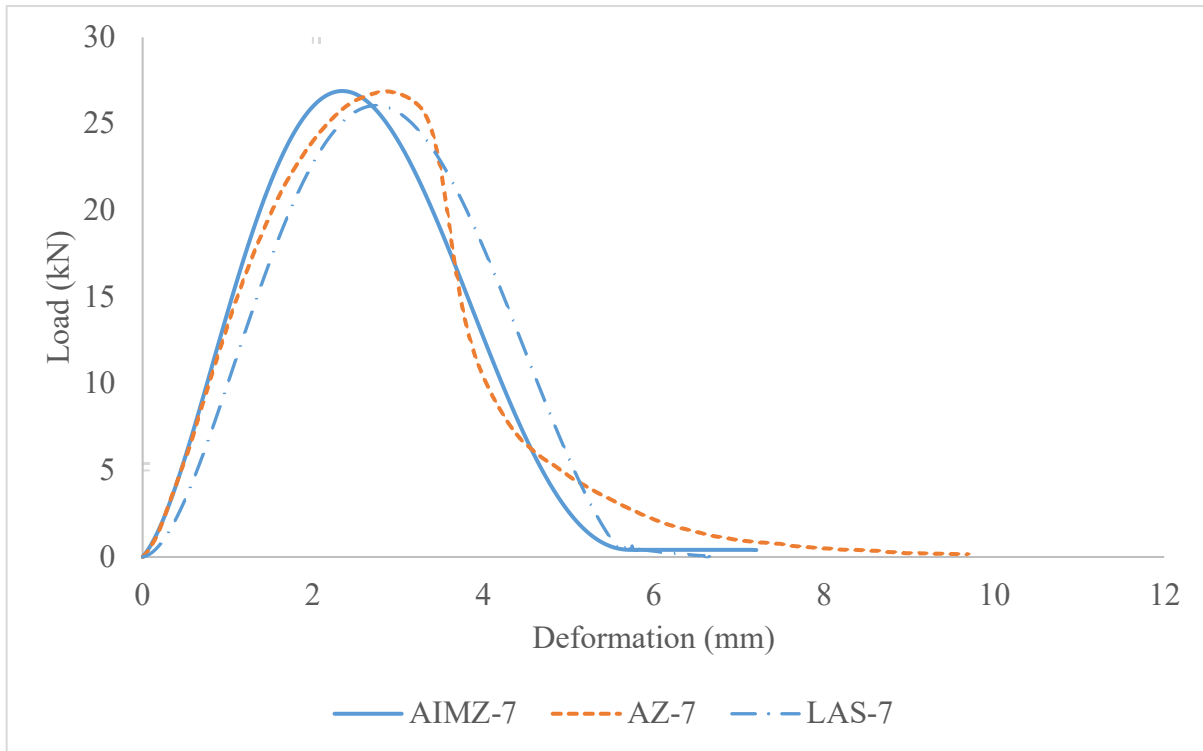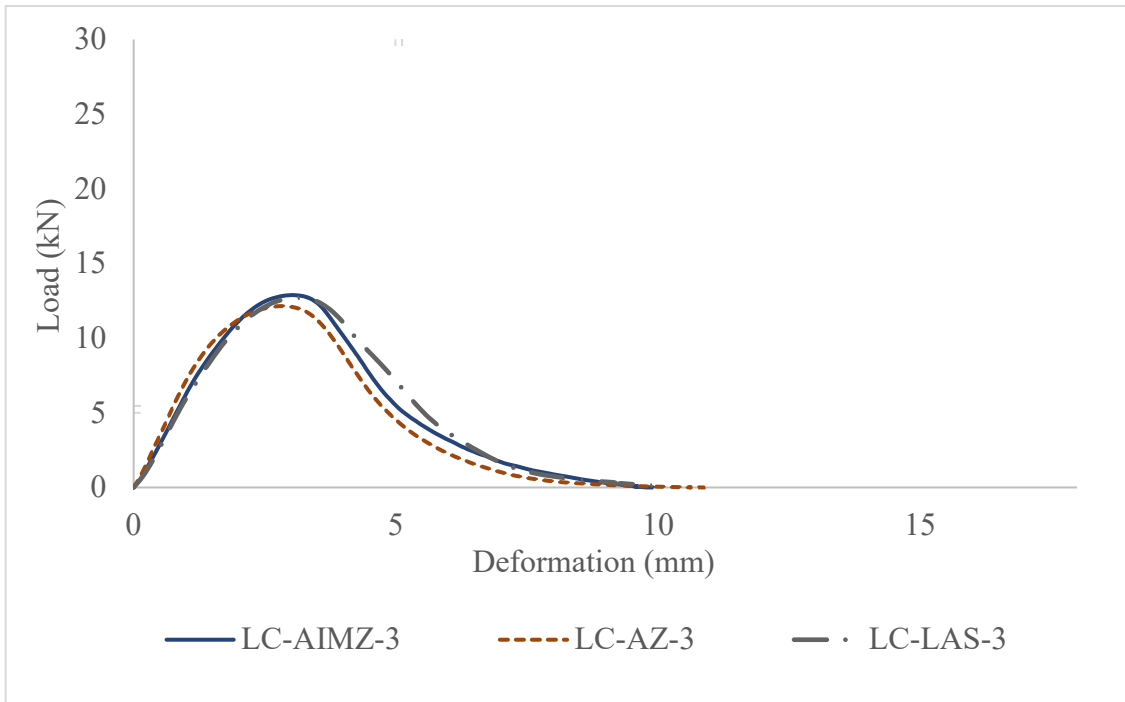Figure 41. Load vs. Deformation Curves for Mixtures with PG 64-16 LC at the 5
Days of Aging Level
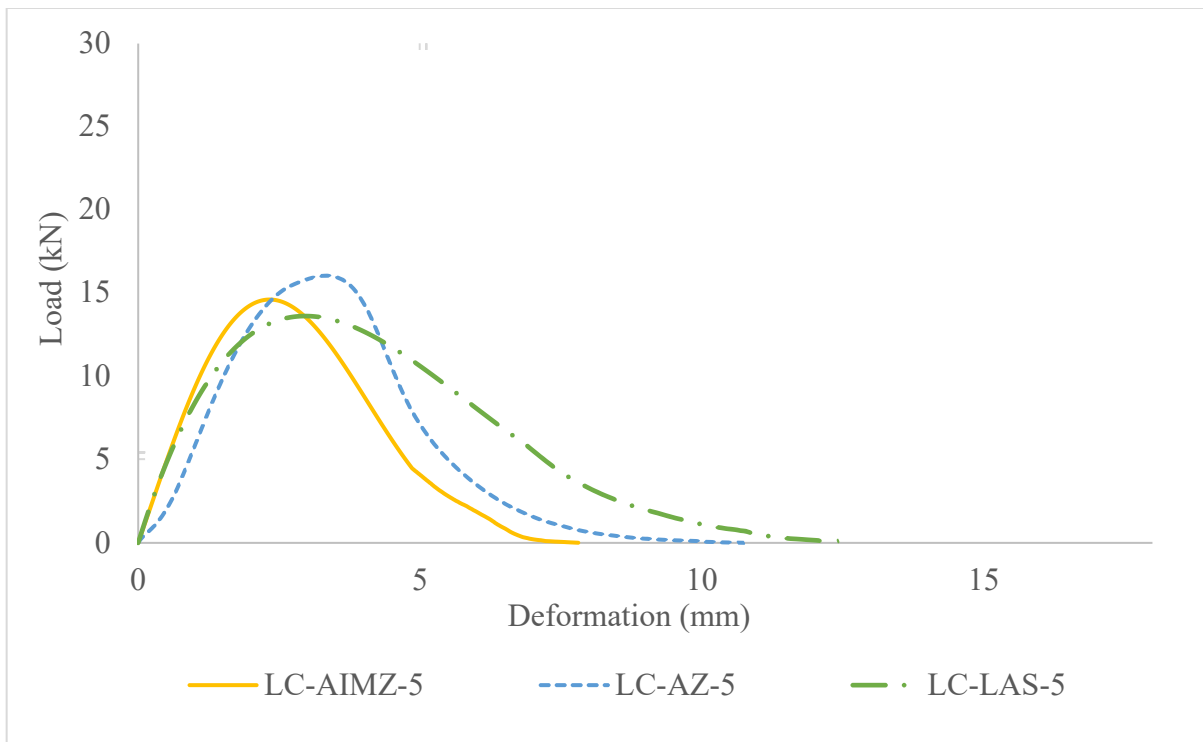
Figure 42. Load vs. Deformation Curves for Mixtures with PG 64-16 LC at the 7 Days of
Aging Level
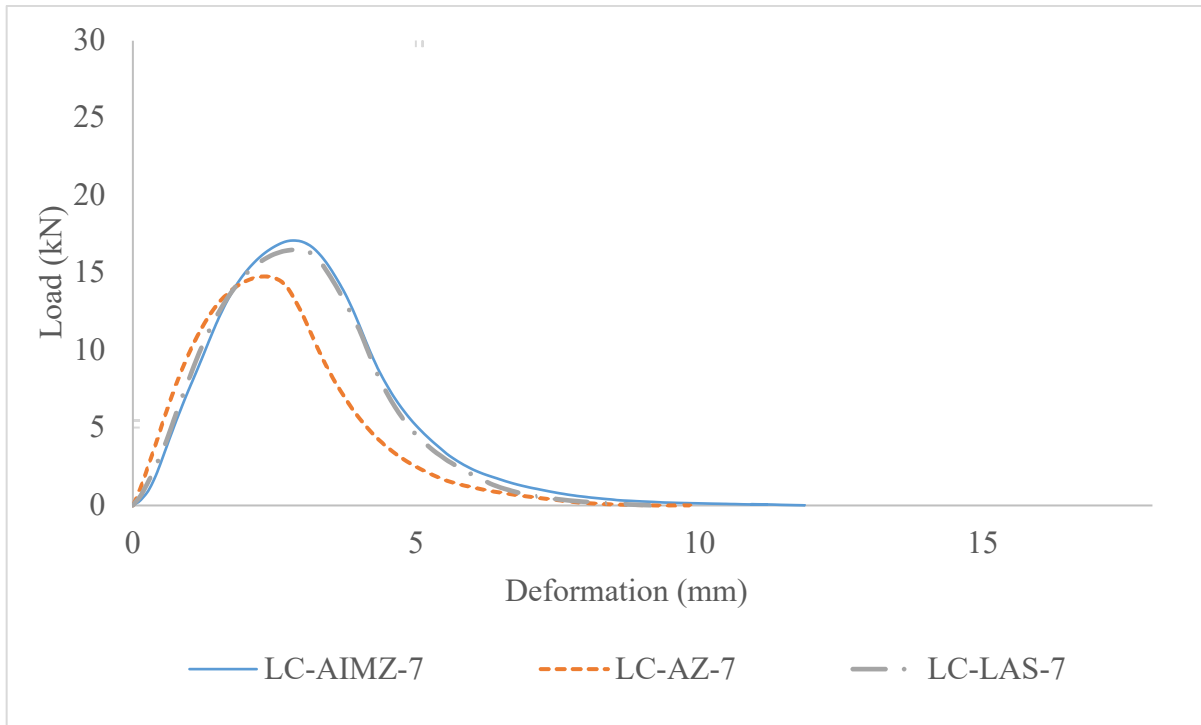
As we have three independent variables, such as binder type, additive, and aging level, the general linear model was run using Minitab to determine if there is significant influence of each variable on the dependent variable, CTindex. The null and alternative hypotheses are H0—there is no significant effect or relationship between the independent variable and the dependent variable— and Ha—there is a significant effect or relationship between the independent variable and the dependent variable. The results of ANOVA from the general linear model are presented in Table 64. As the p-values for binder type and aging level are less than 0.05, this indicates that these variables have a significant effect on the CTindex. But for additive the p-value is 0.865, indicating this variable has no significant effect on the response variable.

Table 64. Results of ANOVA for CT_{index} of All 24 Mixtures

Source	DF	Adj SS	Adj MS	F-Value	P-Value
Binder	1	2303	2303	5.26	0.025
Additive	2	127.1	63.5	0.15	0.865
Aging	3	68007.3	22669.1	51.81	0.000
Error	65	28442.7	437.6		
Lack-of-Fit	17	23328.5	1372.3	12.88	0.000
Pure Error	48	5114.2	106.5		
Total	71	98880.1			

Again, ANOVA was performed to determine if there are differences in the mean values of CTindex among the three mixtures containing AIMZ, AZ, and LAS, respectively, for each binder at each aging level. The null and alternative hypotheses are H0—the mean values are the same for all mixtures and Ha—at least two mean values among the three mixtures differ for individual aging level. The Tukey pairwise comparison test is used to compare the differences between each pair of means.

Tables 65, 66, 67, and 68 tabulate the ANOVA results for CTindex of mixtures with conventional PG 64-16 at the without-aging level and the 3 days, 5 days and 7 days of aging levels, respectively. At the 3 days and 5 days of aging levels, with a p-value of less than 0.05 for each case, the null hypotheses are rejected. This indicates that there is a statistically significant difference between at least two mean values of CTindex among the three mixtures. At the without-aging level and the 7 days of aging levels, no significant difference is observed among the mean CTindex values for the mixtures containing conventional binder.

Table 65. Results of ANOVA for CT_{index} of Mixtures with Conventional PG 64-16 at the Without-Aging Level

Source	DF	Adj SS	Adj MS	F-Value	P-Value
Factor	2	6248	3123.8	4.99	0.053
Error	6	3757	626.2		
Total	8	10005			

Table 66. Results of ANOVA for CT_{index} of Mixtures with Conventional PG 64-16 at the 3 Days of Aging Level

Source	DF	Adj SS	Adj MS	F-Value	P-Value
Factor	2	849	424.49	8.02	0.02
Error	6	317.6	52.93		
Total	8	1166.5			

Table 67. Results of ANOVA for CT_{index} of Mixtures with Conventional PG 64-16 at the 5 Days of Aging Level

Source	DF	Adj SS	Adj MS	F-Value	P-Value
Factor	2	52.08	26.041	8.13	0.02
Error	6	19.23	3.204		
Total	8	71.31			

Table 68. Results of ANOVA for CT_{index} of Mixtures with Conventional PG 64-16 at the 7 Days of Aging Level

Source	DF	Adj SS	Adj MS	F-Value	P-Value
Factor	2	12.12	6.061	3.39	0.104
Error	6	10.73	1.789		
Total	8	22.85			

Tables 69, 70, 71, and 72 show the results derived from Tukey pairwise, illustrating the differences in mean CTindex among the three mixtures with three different additives at different aging levels: without aging, 3 days, 5 days, and 7 days, respectively, for conventional PG 64-16 binder. At the without-aging level and the 7 days of aging level, no significant difference in mean values is observed.

For the 3-day aging level, the only significant difference in mean CTindex is observed between AZ-3 and AIMZ-3. The other two pairwise comparisons yielded a p-value greater than 0.05.

At the 5-day aging level, significant differences in mean values were observed between AZ-5 and AIMZ-5. The other two comparisons indicated insignificant differences.

Table 69. Results of Tukey Pairwise Comparison for CT_{index} of Mixtures with Conventional PG 64-16 at the Without-Aging Level

Difference of Levels	Difference of Means	SE of Difference	95% CI	T-Value	Adjusted P-Value
(AZ-0) - (AIMZ-0)	57	20.4	(-5.7, 119.7)	2.79	0.071
(LAS-0) - (AIMZ-0)	54.8	20.4	(-7.9, 117.5)	2.68	0.081
(LAS-0) - (AZ-0)	-2.2	20.4	(-64.9, 60.5)	-0.11	0.994

*Statistically significant

Table 70. Results of Tukey Pairwise Comparison for CT_{index} of Mixtures with Conventional PG 64-16 at the 3 Days of Aging Level

Difference of Levels	Difference of Means	SE of Difference	95% CI	T-Value	Adjusted P-Value
(AZ-3) - (AIMZ-3)	-22.97	5.94	(-41.20, -4.74)	-3.87	0.019*
(LAS-3) - (AIMZ-3)	-16.86	5.94	(-35.09, 1.37)	-2.84	0.067
(LAS-3) - (AZ-3)	6.11	5.94	(-12.12, 24.34)	1.03	0.588

*Statistically significant

Table 71. Results of Tukey Pairwise Comparison for CT_{index} of Mixtures with Conventional PG 64-16 at the 5 Days of Aging Level

Difference of Levels	Difference of Means	SE of Difference	95% CI	T-Value	Adjusted P-Value
(AZ-5) - (AIMZ-5)	-5.89	1.46	(-10.37, -1.40)	-4.03	0.016*
(LAS-5) - (AIMZ-5)	-2.69	1.46	(-7.17, 1.80)	-1.84	0.236
(LAS-5) - (AZ-5)	3.2	1.46	(-1.29, 7.68)	2.19	0.152

*Statistically significant

Table 72. Results of Tukey Pairwise Comparison for CT_{index} of Mixtures with Conventional PG 64-16 at the 7 Days of Aging Level

Difference of Levels	Difference of Means	SE of Difference	95% CI	T-Value	Adjusted P-Value
(AZ-7) - (AIMZ-7)	1.09	1.09	(-2.26, 4.44)	1	0.603
(LAS-7) - (AIMZ-7)	-1.73	1.09	(-5.08, 1.62)	-1.58	0.323
(LAS-7) - (AZ-7)	-2.82	1.09	(-6.17, 0.53)	-2.58	0.092

*Statistically significant

Tables 72, 73, 74, and 75 tabulate the ANOVA results for CTindex of mixtures with PG 64-16 low carbon at the without-aging level and the 3 days, 5 days, and 7 days of aging levels, respectively. At each aging level, the p-value is greater than 0.05. Thus, no significant difference is observed among the mean CTindex values for the mixtures containing low-carbon binder, and consequently, no significant difference is observed among different additives.

Table 73. Results of ANOVA for CT_{index} of Mixtures with PG 64-16 LC at the Without-Aging Level

Source	DF	Adj SS	Adj MS	F-Value	P-Value
Factor	2	13.97	6.987	0.06	0.943
Error	6	702.08	117.014		
Total	8	716.05			

Table 74. Results of ANOVA for CT_{index} of Mixtures with PG 64-16 LC at the 3 Days of Aging Level

Source	DF	Adj SS	Adj MS	F-Value	P-Value
Factor	2	1.724	0.8618	0.02	0.979
Error	6	237.488	39.5813		
Total	8	239.211			

Table 75. Results of ANOVA for CT_{index} of Mixtures with PG 64-16 LC at the 5 Days of Aging Level

Source	DF	Adj SS	Adj MS	F-Value	P-Value
Factor	2	28.38	14.192	2.31	0.18
Error	6	36.84	6.139		
Total	8	65.22			

Table 76. Results of ANOVA for CT_{index} of Mixtures with PG 64-16 LC at the 7 Days of Aging Level

Source	DF	Adj SS	Adj MS	F-Value	P-Value
Factor	2	51.63	25.814	4.65	0.06
Error	6	33.29	5.548		
Total	8	84.91			

Tables 77, 78, 79, and 80 show the results derived from Tukey pairwise comparison, illustrating the differences in mean CTindex among the three mixtures with three different additives at different aging levels: without aging, 3 days, 5 days, and 7 days, respectively, for PG 64-16 LC binder. No significant differences among the different additives are observed at any aging level for low-carbon binder.

Table 77. Results of Tukey Pairwise Comparison for CT_{index} of Mixtures with PG 64-16 LC at the Without-Aging Level

Difference of Levels	Difference of Means	SE of Difference	95% CI	T-Value	Adjusted P-Value
(LC-AZ-0) - (LC-AIMZ-0)	-0.43	8.83	(-27.53, 26.68)	-0.05	0.999
(LC-LAS-0) - (LC-AIMZ-0)	-2.83	8.83	(-29.94, 24.27)	-0.32	0.945
(LC-LAS-0) - (LC-AZ-0)	-2.4	8.83	(-29.51, 24.70)	-0.27	0.96

*Statistically significant

Table 78. Results of Tukey Pairwise Comparison for CT_{index} of Mixtures with PG 64-16 LC at the 3 Days of Aging Level

Difference of Levels	Difference of Means	SE of Difference	95% CI	T-Value	Adjusted P-Value
(LC-AZ-3) - (LC-AIMZ-3)	0.49	5.14	(-15.27, 16.26)	0.1	0.995
(LC-LAS-3) - (LC-AIMZ-3)	1.07	5.14	(-14.69, 16.84)	0.21	0.976
(LC-LAS-3) - (LC-AZ-3)	0.58	5.14	(-15.18, 16.34)	0.11	0.993

*Statistically significant

Table 79. Results of Tukey Pairwise Comparison for CT_{index} of Mixtures with PG 64-16 LC at the 5 Days of Aging Level

Difference of Levels	Difference of Means	SE of Difference	95% CI	T-Value	Adjusted P-Value
(LC-AZ-5) - (LC-AIMZ-5)	-4.32	2.02	(-10.53, 1.88)	-2.14	0.162
(LC-LAS-5) - (LC-AIMZ-5)	-2.57	2.02	(-8.78, 3.64)	-1.27	0.46
(LC-LAS-5) - (LC-AZ-5)	1.75	2.02	(-4.45, 7.96)	0.87	0.679

*Statistically significant

Table 80. Results of Tukey Pairwise Comparison for CT$_{index}$ of Mixtures with PG 64-16 LC at the 7 Days of Aging Level

Difference of Levels	Difference of Means	SE of Difference	95% CI	T-Value	Adjusted P-Value
(LC-AZ-7) - (LC-AIMZ-7)	-3.23	1.92	(-9.13, 2.67)	-1.68	0.288
(LC-LAS-7) - (LC-AIMZ-7)	-5.86	1.92	(-11.76, 0.05)	-3.05	0.051
(LC-LAS-7) - (LC-AZ-7)	-2.63	1.92	(-8.53, 3.27)	-1.37	0.414

*Statistically significant

Figures 43 and 44 show the average number of gyrations required for compacting IDEAL CT specimens, which showed similar behavior to HWT specimens as the specimen thickness for both tests was nearly the same (60.8 mm and 62 mm).

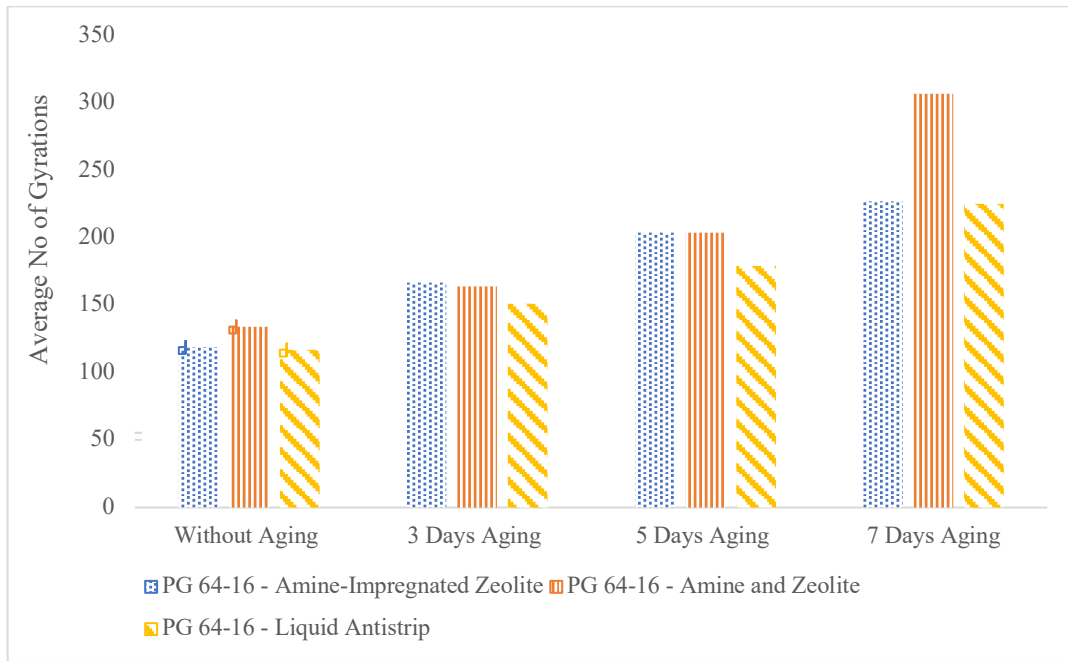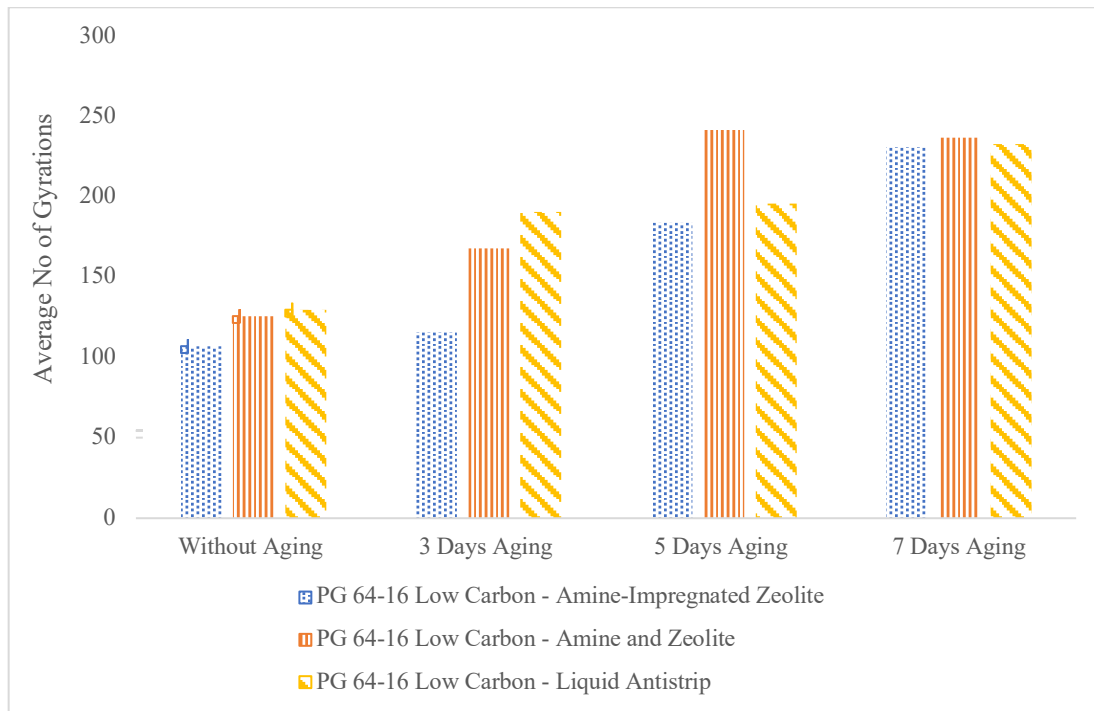Figure 43. Average Number of Gyrations for IDEAL CT Specimens with PG 64-16

Figure 44. Average Number of Gyrations for IDEAL CT Specimens with PG 64-16 LC

6.4 Summary of Statistical Analysis

Table 81 shows the summary of the general linear model analysis for all tests, indicating whether types of binder, types of additives, and aging levels had significant effects on rut depth, wet tensile strength, dry tensile strength, and CTindex, respectively.

Table 81. Summary of General Linear Model Analysis for All Tests

	Binder	Additive (AIMZ, AZ, LAS)	Aging
Rut Depth	NS	NS	S
Wet Tensile Strength	S	S	S
Dry Tensile Strength	S	S	S
CT_{index}	S	NS	S

*S= Significant, NS = Not Significant

Table 82 shows the summary of ANOVA for all tests, indicating whether different additives—including AIMZ, AZ, and LAS—had significant effects on the rut depth, wet tensile strength, dry tensile strength, and CTindex for mixtures containing conventional binder as well as low-carbon binder at each aging level.

Table 82. Summary of ANOVA among AIMZ, AZ, and LAS for All Tests

	Conventional Binder				Low-carbon Binder			
	Without Aging	3 - Days	5- Days	7- Days	Without Aging	3 - Days	5- Days	7- Days
Rut Depth	NS	S	NS	NS	NS	NS	NS	NS
Wet Tensile Strength	NS	S	S	NS	NS	S	S	S
Dry Tensile Strength	NS	NS	NS	NS	NS	NS	NS	NS
CT_{index}	NS	S	S	NS	NS	NS	NS	NS

*S= Significant, NS = Not Significant

Table 83 shows the summary of all Tukey pairwise comparison among AIMZ, AZ, and LAS for all tests and for both binders at each aging level.

Table 83. Summary of Tukey Pairwise Comparison for All Tests

		Conventional Binder				Low-carbon Binder			
		Without Aging	3 - Days	5- Days	7- Days	Without Aging	3 - Days	5- Days	7- Days
Rut Depth	AZ vs AIMZ	NS	S	NS	NS	NS	NS	NS	NS
	LAS vs AIMZ	NS	NS	NS	NS	NS	NS	NS	NS
	LAS vs AZ	NS	S	NS	NS	NS	NS	NS	NS
Wet Tensile Strength	AZ vs AIMZ	NS	NS	S	NS	NS	NS	NS	S
	LAS vs AIMZ	NS	S	S	NS	NS	S	S	S
	LAS vs AZ	NS	NS	NS	NS	NS	S	NS	NS
Dry Tensile Strength	AZ vs AIMZ	NS	NS	NS	NS	NS	NS	NS	NS
	LAS vs AIMZ	NS	NS	NS	NS	NS	NS	NS	NS
	LAS vs AZ	NS	NS	NS	NS	NS	NS	NS	NS
CT_{index}	AZ vs AIMZ	NS	S	S	NS	NS	NS	NS	NS
	LAS vs AIMZ	NS	NS	NS	NS	NS	NS	NS	NS
	LAS vs AZ	NS	NS	NS	NS	NS	NS	NS	NS

*S= Significant, NS = Not Significant

6.5 Moisture-Induced Shear-Thinning Index

Figure 45. MISTI Value of Conventional and Low-carbon Binder
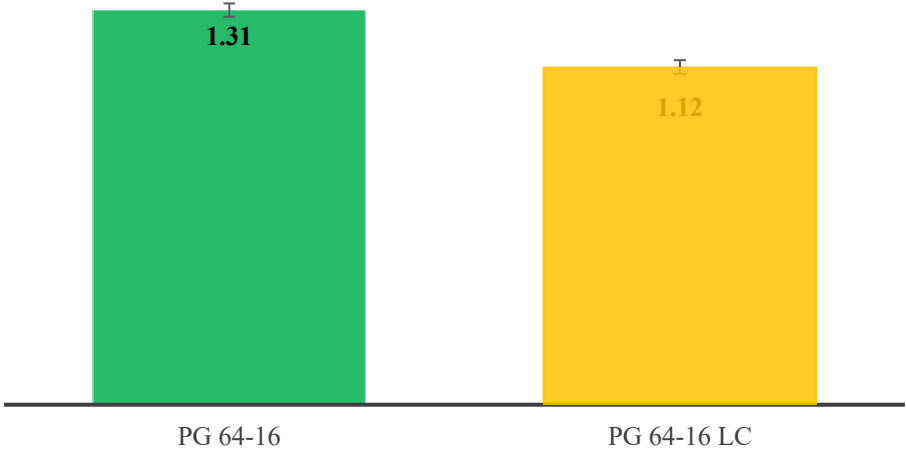
The rheological property of shear-thinning is significantly affected by changes in interfacial bonding. The shear-thinning test can detect any alterations at the interface by manipulating the surface chemistry of siliceous particles and modifying the interfacial connection. The molecular interaction of the bitumen matrix influences the relationship between shear rate and viscosity in the shear-thinning zone. A higher degree of interaction correlates with a more prominent decrease in viscosity with increasing shear rate. A higher shear-thinning value (power-law slope) indicates increased interaction between the bitumen and the glass beads.

The control asphalt binder showed a MISTI reading of 1.31 as shown in Figure 45, surpassing the upper threshold of the acceptable range (0.9 to 1.1). This deviation suggests a heightened interaction between the bitumen and aggregates that, while beneficial in some contexts, may indicate susceptibility to moisture-related damage in this scenario. On the other hand, the low-carbon binder reported a MISTI value of 1.12 as shown in Figure 45, which is slightly above the acceptable limit. This indicates a slightly increased interaction relative to the control but still close to the preferred range. The minor increase in the MISTI value for the low-carbon binder could be indicative of a more robust molecular interaction that does not significantly compromise moisture resistance.

6.6 Multiple Stress Creep Recovery

Figure 46. Percent Recovery of Modified Binder Compared to Control Sample at Two Stress Levels
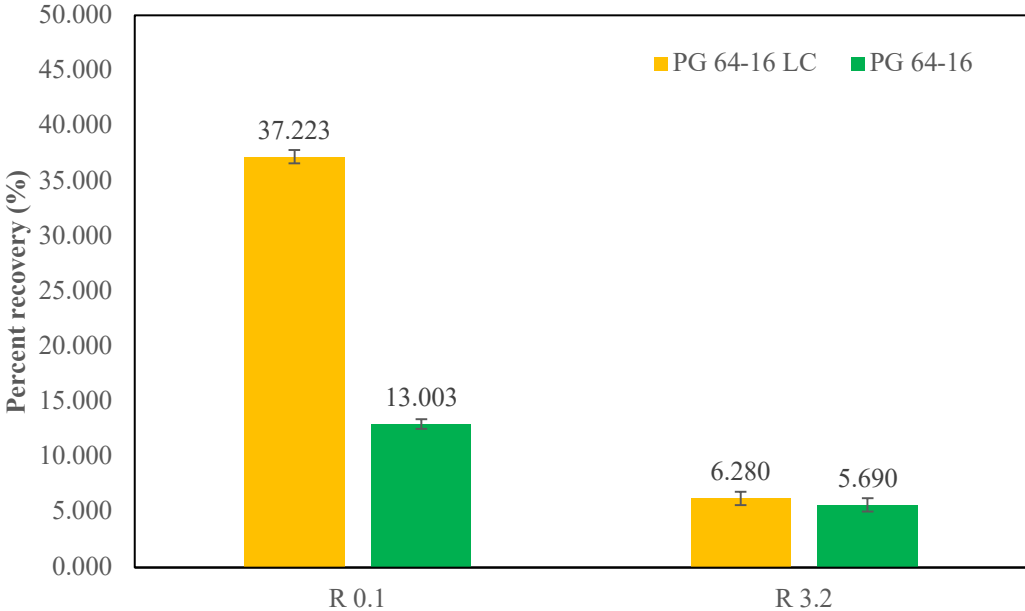
The comparison of the Percent Recovery of both binders at different stress levels is shown in Figure 46. Percent Recovery is a measure of an asphalt binder's ability to return to its original shape after the removal of a load. A higher Percent Recovery indicates better elastic properties, which are important for handling repeated traffic loads without permanent deformation. A lower Percent Recovery, on the other hand, suggests a less elastic binder that may be prone to permanent deformation after load cycles, leading to surface issues, such as rutting and cracking. Increasing this parameter can improve the binder's elastic properties, making the pavement more resilient to traffic stresses, thus reducing the chances of permanent deformation and extending the pavement's service life. However, reducing this parameter could mean decreasing the lifespan of the pavement and increasing the need for repairs.

The results showed that the percent recovery of the low-carbon binder was 37.22% at a stress level of 0.1 KPa, while for the control binder (PG 64-16), it was 13.00%. At a higher stress level of 3.2 KPa, the recovery rates were 6.28% for the low-carbon binder and 5.69% for the control binder. These figures indicate a significant improvement in recovery performance of the low-carbon binder at lower stress levels compared to the control, although this advantage decreases under higher stress conditions.

Figure 47. Non-recoverable Creep Compliance of Modified Binder Compared to Control Sample at Two Stress Levels
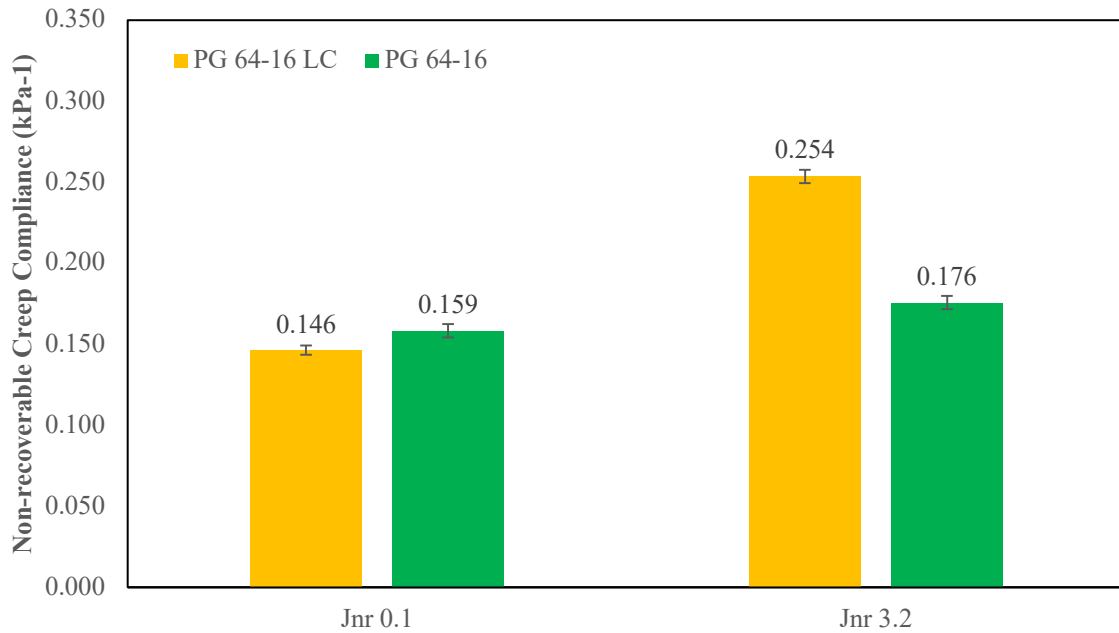

Figure 47 displays a comparison between the Non-recoverable Creep Compliance (Jnr) of modified binder and neat asphalt binder. The Jnr value measures the amount of permanent deformation that stays in the asphalt binder after a load is applied and removed. A lower Jnr value signifies that the binder is more resistant to permanent deformation, which is desirable for pavements that will face heavy loads or high traffic volumes. On the other hand, a higher Jnr value suggests that the binder is more prone to permanent deformation, which could lead to rutting issues when used in similar pavement conditions. A decrease in Jnr values indicates an improvement in the asphalt binder's ability to resist permanent deformation, which results in a more durable pavement that can sustain heavier loads without significant rutting. An increase in Jnr values implies a decline in resistance to permanent deformation, which could lead to more frequent maintenance and early replacement of the pavement.

In terms of Non-recoverable Creep Compliance, the Jnr value for the low-carbon binder at a 0.1 KPa stress level was 0.14, compared to 0.15 for the control binder, indicating a slightly better resistance to permanent deformation under low stress. However, at the 3.2 KPa stress level, the Jnr values increased to 0.25 for the low-carbon binder and 0.17 for the control binder, suggesting that the low-carbon binder is more prone to permanent deformation under higher stress levels.

7. Summary

7.1 Conclusions

This study investigates the mechanical properties of asphalt mixtures containing amine-impregnated zeolite (AIMZ) compared to two other additives: amine and zeolite (AZ) used separately and a commercial liquid antistripping agent (LAS) known as AD-HERE® LOF 65-00. The hypothesis involves the protection of amine from thermal degradation within zeolite pores and its gradual release from the zeolite pores during the pavement's service life. Additionally, the study examines the mechanical properties of HMA incorporating PG 64-16 Low Carbon (LC) binder, which contains 10% waste plastics, offering potential sustainability benefits in addressing global warming and plastic pollution. The investigation also evaluates the impact of long-term aging on the mechanical performance of asphalt mixtures compared to unaged counterparts. The following conclusions can be drawn from the findings:

- Rut depths measured using the Hamburg Wheel Track (HWT) tests showed a gradual decrease from the non-aged level to the 7-day aged level. Regardless of the aging level, the rut depths at 15,000 passes were consistently less than 3.1 mm for all mixtures. We did not observe any significant difference in rut depth between mixtures containing conventional and low-carbon binders. Additionally, the variance in rut depth among mixtures containing different additives was minimal.

- In the general linear model analysis, it was found that the types of binder and additive did not have a significant effect on rut depth. However, aging level did have a significant impact on rut depth. According to the Tukey pairwise comparison, at the 3 days of aging level, mixtures with conventional binder and AZ had significantly lower rut depth compared to mixtures with AIMZ and LAS. There were no other significant differences found among AIMZ, AZ, and LAS for conventional and low-carbon binder at any aging level.

- The wet tensile strength, as measured through the indirect tensile strength (ITS) test, increased with higher aging levels. However, mixtures containing the PG 64-16 LC binder showed lower wet tensile strength compared to those containing the conventional PG 64-16 binder at all aging levels.

- The type of binder, additive, and aging level all had a significant impact on wet tensile strength. According to the Tukey pairwise comparison, for the conventional binder, mixtures incorporating AIMZ had significantly higher wet tensile strength than those with LAS at 3 days of aging. At 5 days, mixtures with AIMZ also had significantly higher wet tensile strength compared to those with LAS and AZ. For the low-carbon binder, mixtures with AIMZ had significantly higher wet tensile strength than those with LAS with 3 days of aging. At 5 days, of aging mixtures with AIMZ had significantly higher wet tensile

strength compared to only those with LAS, while at 7 days of aging, AIMZ mixtures had significantly higher wet tensile strength than both LAS and AZ.

- The dry tensile strength measured through the indirect tensile strength (ITS) test showed an increase with increasing aging levels. However, mixtures containing PG 64-16 LC binder exhibited lower dry tensile strength compared to those containing conventional PG 64-16 binder across all aging levels.

- Based on the general linear model analysis, the type of binder, additive, and aging level significantly impacted the dry tensile strength. However, according to Tukey pairwise comparison, no significant difference was found between additives for any binder at any aging level.

- When comparing the TSR (Tensile Strength Ratio) among mixtures with conventional binder, the TSR for mixtures containing AIMZ increased from 0.74 at the initial stage to 0.86 after 3 days of aging, followed by a slight decrease to 0.83 after 7 days of aging. In contrast, mixtures utilizing LAS exhibited a gradual decline in TSR from 0.84 to 0.77 from the initial stage to 7 days of aging. The TSR values for mixtures with AZ remained consistent across all aging levels.

- For mixtures with a low-carbon binder, the TSR (tensile strength ratio) for LC-AIMZ increased gradually from 0.78 to 0.93, while the TSR for LC-LAS decreased gradually from 0.89 to 0.83 over the 7-day aging period. The TSR values for LC-AZ stayed relatively stable throughout the aging process.

- Mixtures containing AIMZ showed higher TSR values compared to those with AZ and LAS binders at both 5-day and 7-day aging levels, regardless of the type of binder. This indicates that zeolites may offer some protection to amines against thermal degradation and help in their gradual release over time.

- The CT_{index} values obtained from IDEAL CT testing showed a gradual decrease as aging levels increased for all tested mixtures. Mixtures with low-carbon binder initially had lower CT_{index} values compared to those with conventional PG 64-16 at the without aging level. However, by the 3-day aging level, mixtures with PG 64-16 LC demonstrated similar results to those with conventional PG 64-16. Furthermore, at both 5 and 7 days of aging, mixtures using low-carbon binder showed higher CT_{index} values than those using conventional binder. This indicates that low-carbon binder offers improved resistance to cracking over an extended period.

- The type of binder and aging level had a significant effect on CT_{index}. However, different types of additives—AIMZ, AZ, and LAS—had no significant effect on CT_{index}. According to Tukey pairwise comparison, for conventional binder, mixtures with AIMZ had

significantly higher CT_{index} than mixtures with AZ at the 3 days and 5 days of aging levels. Otherwise, all other pairwise comparisons for conventional and low-carbon binder at any aging level showed no significant differences among AIMZ, AZ, and LAS.

- The load vs. deformation curves from IDEAL CT show that aging has a significant impact on the post-peak slope for mixtures with conventional binder. This impact makes them steeper and indicates a more brittle behavior as aging progresses. On the other hand, the slope of mixtures with low-carbon binder is less susceptible to changes caused by aging, suggesting a more consistent performance over time.

- MISTI value indicates that the traditional asphalt binder is more prone to moisture compared to the low-carbon binder. While both readings are higher than the ideal range, the low-carbon binder is closer to the acceptable threshold, suggesting potentially better performance in resisting moisture.

- The MSCR test results show significant differences in the performance of low-carbon and conventional asphalt binders. The low-carbon binder has a higher percent recovery and lower Jnr at 0.1 KPa, indicating better performance under low stress. However, at 3.2 KPa, its performance is less impressive. Under higher stress, its recovery rate is similar to the conventional binder, and it exhibits a significantly higher Jnr, suggesting worse elasticity and higher susceptibility to permanent deformation. In summary, low carbon binders are suitable for low-load conditions, but may not be ideal for high-stress environments.

7.2 Limitations and Recommendations

The findings of this study provide valuable insights but are not exhaustive, indicating the need for broader research to achieve more definitive conclusions. Future investigations could address the following areas for a deeper understanding:

- The study was conducted using a single type of zeolite. Future studies could explore the impact of various synthetic zeolites on the effectiveness of amine-impregnated zeolite.

- This study examined a specific dosage of amine-impregnated zeolite. Evaluating a range of dosages for amine-impregnated zeolite could offer insights into optimal compositions.

- Considering zeolite's widespread use in warm mix asphalt technologies, the potential benefits of lowering mixing and compaction temperatures with amine-impregnated zeolite warrant further investigation.

- The study utilized a low-carbon binder comprised of 10% waste plastics. Assessing the performance of binders with higher percentages of waste plastics could contribute to more

sustainable asphalt pavement solutions. Again, difference in effects of using various types of plastics (e.g., HDPE, PVC, PET, PP, PS, etc.) can also be investigated.

- Reclaimed Asphalt Pavement (RAP) is widely used in practice while constructing roads in California and other states. However, RAP was not incorporated in this study. Use of RAP along with AIMZ and plastics can lead to different results, which can be evaluated.

The results of this study serve as a starting point toward integrating amine-impregnated zeolite into asphalt pavement, prompting further investigations to enhance the reliability of the findings and refine the optimization process. Additionally, these findings contribute to the ongoing efforts aimed at incorporating post-consumer plastics into asphalt pavement, thereby adding value to the existing body of research in this field.

Bibliography

Abdalfattah, I. A., Mogawer, W. S., & Stuart, K. (2022). Recycled polyethylene (RPE) modified asphalt mixtures: Performance predictions using pavement Mechanistic-Empirical design and evaluation of return on investment. *Construction and Building Materials*, *356*, 129164. https://doi.org/10.1016/j.conbuildmat.2022.129164

Ahmadinia, E., Zargar, M., Karim, M. R., Mahrez, A., & Ahmadinia, E. (2012). Performance evaluation of utilization of waste Polyethylene Terephthalate (PET) in stone mastic asphalt. *Construction and Building Materials*, *36*, 984–989. https://doi.org/10.1016/j.conbuildmat.2012.06.015

Al-Hadidy, A. I., Alzeebaree, R., Abdal, J. A., & Niş, A. (2023). Mechanical performance and statistical analysis of natural and synthetic zeolite-warm mix asphalt as a function of compaction efforts. *Journal of Building Engineering*, *75*, 106985. https://doi.org/10.1016/j.jobe.2023.106985

Alhwaige, A. A., Agag, T., Ishida, H. and Qutubuddin, S. (2013), Biobased Chitosan Hybrid Aerogels with Superior Adsorption: Role of Graphene Oxide in CO2 Capture. RSC Adv. 2013, 3, 16011–16020. https://doi.org/10.1039/C3RA42022A

Aksoy, A., Şamlioglu, K., Tayfur, S., & Özen, H. (2005). Effects of various additives on the moisture damage sensitivity of asphalt mixtures. *Construction and Building Materials*, *19*(1), 11–18. https://doi.org/10.1016/j.conbuildmat.2004.05.003

Arabani, M., Pirbasti, Z. R., & Hamedi, G. H. (2021). Investigating the impact of zeolite on reducing the effects of changes in runoff acidity and the moisture sensitivity of asphalt mixtures. *Construction and Building Materials*, *268*, 121071. https://doi.org/10.1016/j.conbuildmat.2020.121071

Badawy, A. E. and Rahim, A (2023). Evaluation of Nanoclay Additives for Improving Resistance to Moisture Damage in Hot Mix. DOI: 10.31979/mti.2022.2151

Caro, S., Masad, E., Bhasin, A. and Little, D., N. Moisture susceptibility of asphalt mixtures, Part 1: Mechanisms, Int. J. Pavement Eng. 9 (2) (2008) 81–98.

Chang, X., Liang, W., Long, Y., Xiao, Y., & Xue, Y. (2023). Optimal zeolite structure design for VOC emission reduction in asphalt materials. *Construction and Building Materials*, *366*, 130227. https://doi.org/10.1016/j.conbuildmat.2022.130227

Chen, W., Zhao, H., Xue, Y., & Chang, X. (2022). Adsorption effect and adsorption mechanism of high content zeolite ceramsite on asphalt VOCs. *Materials*, *15*(17), 6100. https://doi.org/10.3390/ma15176100

Choi, S., Drese, J. and Jones, C. (2009), Adsorbent Materials for Carbon Dioxide Capture from Large Anthropogenic Point Sources. ChemSusChem, 2: 796 854. https://doi.org/10.1002/cssc.200900036

Csanyi, L. H. (1957). FOAMED ASPHALT IN BITUMINOUS PAVING MIXTURES. *Highway Research Board Bulletin*, *160*. https://trid.trb.org/view/101130

Dindi, A., Viet Quang, D. and Abu-Zahra, M.R.M. (2019), CO_2 adsorption testing on fly ash derived cancrinite-type zeolite and its amine-functionalized derivatives. Environ. Prog. Sustainable Energy, 38: 77-88. https://doi.org/10.1002/ep.12940

Esfandabad, A. S., Motevalizadeh, S. M., Sedghi, R., Ayar, P., & Asgharzadeh, S. M. (2020). Fracture and mechanical properties of asphalt mixtures containing granular polyethylene terephthalate (PET). *Construction and Building Materials*, *259*, 120410. https://doi.org/10.1016/j.conbuildmat.2020.120410

Gao, Mengdan, Liyun Yang, Shuangjian Yang, Tong Jiang, Fei Wu, and Tetsuya Nagasaka. (2022). "Simple Aminated Modified Zeolite 4A Synthesized Using Fly Ash and Its Remediation of Mercury Contamination: Characteristics and Mechanism" *Sustainability* 14, no. 23: 15924. https://doi.org/10.3390/su142315924

Ge, L., Wei, J., Geng, L. et al. (2022), Amine-bifunctionalized ZSM-5/SBA-16 composite for CO_2 adsorption. J Porous Mater 29, 19–31. https://doi.org/10.1007/s10934-021-01146-5

Gürü, M., Çubuk, M. K., Arslan, D., Farzanian, S. A., & Bilici, İ. (2014). An approach to the usage of polyethylene terephthalate (PET) waste as roadway pavement material. *Journal of Hazardous Materials*, *279*, 302–310. https://doi.org/10.1016/j.jhazmat.2014.07.018

Hamedi, G. H., & Tahami, S. A. (2018). The effect of using anti-stripping additives on moisture damage of hot mix asphalt. *International Journal of Adhesion and Adhesives*, *81*, 90–97. https://doi.org/10.1016/j.ijadhadh.2017.03.016

Hao, G., He, M., Lim, S. M., Ong, G. B., Zulkati, A., & Kapilan, S. (2024). Recycling of plastic waste in porous asphalt pavement: Engineering, environmental, and economic implications. *Journal of Cleaner Production*, 140865. https://doi.org/10.1016/j.jclepro.2024.140865

Hesami, E., & Mehdizadeh, G. (2017). Study of the amine-based liquid anti-stripping agents by simulating hot mix asphalt plant production process. *Construction and Building Materials*, *157*, 1011–1017. https://doi.org/10.1016/j.conbuildmat.2017.09.168

İskender, E., Aksoy, A., & Özen, H. (2012). Indirect performance comparison for styrene–butadiene–styrene polymer and fatty amine anti-strip modified asphalt mixtures. Construction and Building Materials, 30, 117–124. https://doi.org/10.1016/j.conbuildmat.2011.11.027

J, V. D. T., Harvey, J., Muench, S. T., Smith, K. D., Snyder, M. B., Al-Qadi, I. L., Ozer, H., Meijer, J., Ram, P., Roesler, J. R., & Kendall, A. (2015, January 1). Towards Sustainable Pavement Systems: A reference document. https://rosap.ntl.bts.gov/view/dot/38541

Ji, L. (2013). Study on preparation process and Properties of Polyethylene terephthalate (PET). *Applied Mechanics and Materials*, *312*, 406–410. https://doi.org/10.4028/www.scientific.net/amm.312.406

Jia, W., Li, Q., Zhang, L. et al. (2020), Highly efficient photocatalytic reduction of CO2 on amine-functionalized Ti-MCM-41 zeolite. *J Nanopart Res* 22, 288 https://doi.org/10.1007/s11051-020-05019-x

Joos, L., Swisher, J. A. and Smit, B. (2013). Molecular Simulation Study of the Competitive Adsorption of H2O and CO2 in Zeolite 13X. Langmuir 2013, 29, 15936–15942 https://doi.org/10.1021/la403824g

Kim, Y. R., Castorena, C., Elwardany, M. D., Rad, F. Y., Underwood, B. S., Gundha, A., Gudipudi, P., Farrar, M., & Glaser, R. (2021). Long-Term Aging of asphalt mixtures for performance testing and prediction: Phase III results. In *Transportation Research Board eBooks*. https://doi.org/10.17226/26133

Lee, S.C., Hsieh, C.C., Chen, C.H. and Chen, Y.S. (2013). CO2 Adsorption by Y-Type Zeolite Impregnated with Amines in Indoor Air. *Aerosol Air Qual. Res.* 13: 360-366. https://doi.org/10.4209/aaqr.2012.05.0134

Li, R., Leng, Z., Yang, J., Lü, G., Huang, M., Lan, J., Zhang, H., Bai, Y., & Zhang, D. (2021). Innovative application of waste polyethylene terephthalate (PET) derived additive as an antistripping agent for asphalt mixture: Experimental investigation and molecular dynamics simulation. Fuel, 300, 121015. https://doi.org/10.1016/j.fuel.2021.121015

Lin, Z., Wei, J., Li, G., Mei, D., & Liao, L. (2018). An Amine Double Functionalized Composite Strategy for CO2 Adsorbent Preparation using a ZSM-5/KIT-6 Composite as a Support. *Energy Technology*, *6*(9), 1618–1626. https://doi.org/10.1002/ente.201700780

Liu, X., Gao, F. et al. (2016), Zeolite@Mesoporous silica-supported-amine hybrids for the capture of CO_2 in the presence of water, Microporous and Mesoporous Materials Volume 222, 1 March 2016, Pages 113-119

Mashaan, N. S., Chegenizadeh, A., & Nikraz, H. (2022). Performance of PET and nano-silica modified stone mastic asphalt mixtures. *Case Studies in Construction Materials*, *16*, e01044. https://doi.org/10.1016/j.cscm.2022.e01044

Modarres, A., & Hamedi, H. (2014). Effect of waste plastic bottles on the stiffness and fatigue properties of modified asphalt mixes. *Materials in Engineering*, *61*, 8–15. https://doi.org/10.1016/j.matdes.2014.04.046

Mousavi, M., Aldagari, S., Seo, D. K., & Fini, E. H. (2022b). Reducing the carbon footprint of bituminous composites using Amine-Impregnated zeolite. ACS Sustainable Chemistry & Engineering, 10(39), 13004–13016. https://doi.org/10.1021/acssuschemeng.2c02609

Movilla-Quesada, D., Raposeiras, A. C., & Olavarría, J. (2019). Effects of recycled polyethylene terephthalate (PET) on stiffness of hot asphalt mixtures. *Advances in Civil Engineering*, *2019*, 1–6. https://doi.org/10.1155/2019/6969826

Murge, P., Dinda, S. and Roy, P. (2019), Zeolite-Based Sorbent for CO_2 Capture: Preparation and Performance Evaluation, Langmuir 2019, 35, 46, 14751–14760 Publication Date: October 29, 2019. https://doi.org/10.1021/acs.langmuir.9b02259

Ojuri, O. O., Osagie, P. O., Oluyemi-Ayibiowu, B. D., Fadugba, O. G., Tanimola, M. O., Chauhan, V. B., & Jayejeje, O. O. (2022). Eco-friendly stabilization of highway lateritic soil with cow bone powder admixed lime and plastic granules reinforcement. Cleaner Waste Systems, 2, 100012. https://doi.org/10.1016/j.clwas.2022.100012

Panda, D., Singh, S. K., & Kumar, E. A. (2018). A comparative study of CO_2 capture by amine grafted vs amine impregnated zeolite 4A. *IOP Conference Series: Materials Science and Engineering*, *377*, 012148. https://doi.org/10.1088/1757-899x/377/1/012148

Park, D., Seo, W., Kim, J., & Vo, H. V. (2017). Evaluation of moisture susceptibility of asphalt mixture using liquid anti-stripping agents. *Construction and Building Materials*, 144, 399–405. https://doi.org/10.1016/j.conbuildmat.2017.03.214

Pérez-Botella, E., Martínez-Franco, R., González-Camuñas, N., CantíN, Á., Palomino, M., Moliner, M., Valencia, S., & Rey, F. (2020). Unusually low heat of adsorption of CO_2 on ALPO and SAPO molecular sieves. *Frontiers in Chemistry*, *8*. https://doi.org/10.3389/fchem.2020.588712

Pietro Campo, F., Tua, C., Biganzoli, L., Pantini, S., & Grosso, M. (2021). Natural and enhanced carbonation of lime in its different applications: A review. *Environmental Technology Reviews*, *10*(1), 224–237. https://doi.org/10.1080/21622515.2021.1982023

Quan, C., Jia, X., Zhang, K., Zhang, Y., Naqvi, S. R., Amin, N. a. S., & Gao, N. (2021). Amine-impregnated silica zeolite from microalgae ash at different calcination temperatures for CO 2 capture. *International Journal of Energy Research*, *46*(2), 1220–1233. https://doi.org/10.1002/er.7241

R. Szostak, Handbook of Molecular Sieves: Structures, Springer Science & Business Media, (1992). http://refhub.elsevier.com/S1387-1811(15)00551-X/sref18

Santos, S.C.G., Pedrosa, A.M. Garrido, Souza, M.J.B., Cecilia, J.A. and Rodríguez-Castellón, E (2015, June 12). "Carbon dioxide adsorption on micro-mesoporous composite materials of ZSM-12/MCM-48 type: The role of the contents of zeolite and functionalized amine:" *Materials Research Bulletin*, 70, 663–672. https://doi.org/10.1016/j.materresbull.2015.05.037

Şengül, C. E., Ayyildiz, D., İskender, E., & Aksoy, A. (2022). The effect of hydrated lime mixing forms and ratios on performance in asphalt pavements. *Teknik Dergi*, *33*(4), 12243–12263. https://doi.org/10.18400/tekderg.902668

Singh, D., Showkat, B., Rajan, B., & Shah, A. (2020). Rheological interference of amine and Silane–Based antistripping agents on crumb Rubber–Modified binder. *Journal of Materials in Civil Engineering*, *32*(2). https://doi.org/10.1061/(asce)mt.1943-5533.0003004

Sollazzo, G., Longo, S., Cellura, M., & Celauro, C. (2020). Impact Analysis Using Life Cycle Assessment of Asphalt Production from Primary Data. *Sustainability*, *12*(24), 10171. https://doi.org/10.3390/su122410171

Taherkhani, H., & Arshadi, M. (2017). Investigating the mechanical properties of asphalt concrete containing waste polyethylene terephthalate. *Road Materials and Pavement Design*, *20*(2), 381–398. https://doi.org/10.1080/14680629.2017.1395354

Tarrer, A. R. and Wagh, V. P., "The Effect of the Physical and Chemical Characteristics of the Aggregate on Bonding," Strategic Highway Research Program SHRP Report 91–507, 1991.

Tayebali, A.A., Knappe, D. R. U. and Mandapaka, V. L. (2008). Effect of prolonged heating on the asphalt-aggregate bond strength of HMA containing liquid anti-strip additives. (Report Number: FHWA/NC/2007-08), *North Carolina. Dept. of Transportation. Research*

and Analysis Group; United States. Federal Highway Administration. https://rosap.ntl.bts.gov/view/dot/18682

Wasiuddin, N. M., Fogle, C. M., Zaman, M., & O'Rear, E. A. (2007). Characterization of thermal degradation of liquid amine Anti-Strip additives in asphalt binders due to RTFO and PAV-Aging. *Journal of Testing and Evaluation*, *35*(4), 387–394. https://doi.org/10.1520/jte100660

Xiao, R., Ding, Y., Polaczyk, P., Maa, Y., Jiang, X., and Huang, B. (2022, August). "Moisture damage mechanism and material selection of HMA with amine antistripping agent." *Materials & Design*, 220, 110797. https://doi.org/10.1016/j.matdes.2022.110797

Xu, S., Xiao, F., Amirkhanian, S., & Singh, D. (2017). Moisture characteristics of mixtures with warm mix asphalt technologies – A review. *Construction and Building Materials*, *142*, 148–161. https://doi.org/10.1016/j.conbuildmat.2017.03.069

Yang, W., Du, T. et al. (2017), Amine-functionalized mesoporous ZSM-5 zeolite adsorbents for carbon dioxide capture, *Solid State Sciences*, *73*, 27–35

Yuan, Y., Wei, J. et al. (2020), An amine-bifunctionalization strategy with Beta/KIT-6 composite as a support for CO2adsorbent preparation, *RSC Advances*, *10*(56), 34187–34196. https://doi.org/10.1039/D0RA05044J

Zou, F., Leng, Z., Cao, R., Li, G., Zhang, Y., & Sreeram, A. (2022). Performance of zeolite synthesized from sewage sludge ash as a warm mix asphalt additive. *Resources, Conservation and Recycling*, *181*, 106254. https://doi.org/10.1016/j.resconrec.2022.106254

About the Authors

Shadi Saadeh, PhD

Dr. Shadi Saadeh joined the California State University, Long Beach (CSULB) Civil Engineering and Construction Engineering Management Department in 2007. Dr Saadeh worked for the Texas Transportation Institute (TTI) from 2003–2005 and the Louisiana Transportation Research Center (LTRC) from 2006–2007. He received his BSc in civil engineering from University of Jordan (1997), MSc in Civil Engineering from Washington State University (2002), and PhD in Civil Engineering from Texas A & M University (2005). Dr. Saadeh's research focuses on granular materials, including asphalt mixes and its constituents. His main areas of research are experimental characterization of highway materials, constitutive modeling of highway materials at the microstructural level, performance evaluation of highway infrastructure, flexible pavement design and analysis, and experimental characterization of highway materials using X-ray computed tomography (CT), image analysis techniques, and mechanical testing. Dr. Saadeh has authored research papers in high-quality engineering and scientific journals such as Journal of Transportation Research Board (TRB), American Society for Testing and Materials (ASTM), Journal of the American Society for Civil Engineers (ASCE), Journal of the Association of Asphalt Paving Technologists (AAPT), and Journal of Computational Materials Science.

Unmona Aditi

Unmona Aditi is currently a Master's student in Civil Engineering at CSULB with a specialization in transportation engineering. She holds a Bachelor's Degree in Civil Engineering from Bangladesh University of Engineering and Technology. Her research interests include flexible pavement materials.

Mohammad Javad Kazemi

Mohammad Javad Kazemi is a PhD student in Civil Engineering at Arizona State University.

Elham Fini, PhD

Dr. Ellie Fini is an Associate Professor at Arizona State University, an Invention Ambassador at the American Association for the Advancement of Science, a Fulbright Scholar of Aalborg University of Denmark, a Senior Sustainability Scientist at the Global Institute of Sustainability and Innovation, and Director of the Innovation Network for Materials, Methods and Management. Her research focuses on the production, characterization and atomistic modelling of sustainable novel materials for use in construction. In addition to more than 200 scholarly publications and numerous invited talks, her research has been featured by BBC Women in STEM, Science Nation, Wired Magazine, and CNBC. She is editor of the ASCE Journal of Materials and the Journal of Resources, Conservation & Recycling. She has served as the president

of ASCE's North Carolina Northern Branch and a program director of the National Science Foundation. Her achievements have been recognized via multiple awards including an NSF CAREER award, ASEE Gerald Seeley award, BEYA Emerald STEM Innovation award, NC BioTech Research Excellence award, and WTS Innovative Transportation Solution award, to name a few.

Roger Khoudessian

Roger Khoudessian is an Instructor at the Joint Training and Certification Program at CSULB.